



The
University
Of
Sheffield.

Phosphoinositides in ciliary transport and ciliopathies

By:

Xiaoming Fang

A thesis submitted in partial fulfilment of the requirements for the degree
of Doctor of Philosophy

The University of Sheffield

Faculty of Science

Department of Biomedical Science

2017.09.04

Acknowledgments

First, I would like to thank my supervisor Jarema Malicki for his patience and continuous support. I appreciate his time and intellectual support. He has been always available to discuss my project in detail. I also would like to thank my advisors Tanya Whitfield and Albert Ong. They offered me an opportunity to talk about my science and gave valuable feedback. I am grateful for their critical thinking and kind advice.

For providing me with insight and technical expertise, I would like to thank Christopher Hill for assistance in Electron Microscopy experiments and Darren Robinson for help with Light Microscopy. A big thank you to staff in the Aquarium of the University of Sheffield. They have been doing a great job taking care of my fish. I would also like to thank the Malicki Lab members, Niedharsan Pooranachandran for his technical support, Eleni Leventea for her critical reading of my writing and lending me a hand when I need it. Finally, Stone Elworthy provided invaluable advice on many occasions.

I would like to thank National Institutes of Health (USA) and the Department of Biomedical Science for funding without which this project would not be possible.

Last but not the least, I am grateful for the support from my friends and family. Practically, I would like to thank Xian Zhang for encouraging me to do my PhD project and Karen Hung for always being available when I need.

Abstract

Cilia are finger-like protrusions that function in the detection and processing of a wide variety of signals. In vertebrates, they are intimately involved in early embryonic patterning, the differentiation and function of sensory neurons, morphogenesis and physiology of duct epithelia, cell motility and metabolism. Lipid composition of the ciliary membrane and its contribution to cilia function is one of the least studied areas of cilia biology. Here I use a collection of transgenic lines to determine the phosphoinositide content of the ciliary membrane and to test the role of phosphoinositides in cilia morphogenesis and function. My studies reveal that specific types of phosphoinositides are found in the ciliary membrane and that their content plays an important role in cilia morphology and function. Moreover, I generated a zebrafish model of a human ciliopathy to test whether some aspects of its mutant phenotype can be alleviated by manipulating the phosphoinositide content in the ciliary membrane. Finally, my studies developed a method that is generally applicable to the manipulation of ciliary content of other PIs in a living vertebrate using other enzymes.

Key words: Cilia, Phosphoinositide, Zebrafish

Abbreviations

4EBP-1	4E-binding protein 1
BBS5	Bardet-Biedl syndrome 5
cKO	conditional knock out
CSF	cerebrospinal fluid
DAG	diacylglycerol
dpf	days post fertilization
Fgf	fibroblast growth factor
FRAP	fluorescent recovery after photobleaching
FYVE	Fab1, YotB, Vac1, EEA1
gRNA	guide-RNA
hpf	hours post fertilization
HPLC	high-performance liquid chromatography
IFT	intraflagellar transport
JSRD	Joubert syndrome and related disorders
MEFs	mouse embryonic fibroblasts
MOPDII	Majewski Osteodysplastic Primordial Dwarfism Type II
mTOR	mammalian target of rapamycin
PBD	phosphoinositide binding domain
PH	plecstrin homology
PI	phosphoinositide
PI3K	phosphatidylinositol 3-kinase
PI(3,4)P ₂	phosphatidylinositol 3,4-bisphosphate
PI(3,4,5)P ₃	Phosphatidylinositol-3,4,5-triphosphate
PI(4,5)P ₂	phosphatidylinositol 4,5-bisphosphate
PTEN	Phosphatase and TENsin homolog
PX	phox-homology
RPE-hTERT	immortalized retinal pigment epithelium
SARA	mad anchor for receptor activation
SEM	scanning electron microscopy
SHH	sonic hedgehog
SSTR	somatostatin receptor
TEM	transmission electron microscopy
TLC	thin layer chromatography
TRPP	transient receptor potential polycystin
TULP3	tubby-like protein 3
TZ	transition zone

Table of Contents

Chapter 1 Introduction	11
1.1 Cilia	12
1.1.1 Discover history of cilia and flagella	12
1.1.2 Cilia structure	13
1.1.3 Ciliary function	15
1.1.4 Ciliopathies	17
1.2 Phosphoinositides (PIs)	19
1.2.1 The basic structure of PIs	19
1.2.2 The research history of PI in vertebrates	19
1.2.2 The role of PI in biological processes	21
1.2.3 PIs in cilia	22
1.3 Zebrafish as a vertebrate model of developmental biology	23
1.4 Overall hypothesis	24
1.5 Aims	25
1.5.1 Detection of PI content in the ciliary and periciliary membrane	25
1.5.2 Determination of PI function in the ciliary membrane	26
Chapter 2 PI contents identification in vertebrate cilium	29
2.1 Introduction	30
2.1.1 Detection and identification of PIs	30
2.2 Results	34
2.2.1 PI content detection in the ciliary and periciliary membrane	34
2.3 Discussion	48
2.4 Summary	52
Chapter 3 PIs function in the cilium	53
3.1 Introduction	54
3.1.1 General strategies for the study of PI function	54
3.2 Experimental design	54
3.2.1 Ciliary PIs function study approach	54
3.2.2 Functional analysis of the ciliary PI(3,4,5)P ₃ and PI(4,5)P ₂	55
3.3 Results	57
3.3.1 Transient expression of effectors	57
3.3.2 Effector expression in stable transgenic lines	57
3.3.3 Phenotypic analysis of effector lines	61
3.4 Discussion	70
3.5 Summary	76
Chapter 4 INPP5E function study in zebrafish	78
4.1 Introduction	79
4.1.1 5-phosphatases	79
4.1.2 <i>In vitro</i> studies of INPP5E function	80
4.1.3 INPP5E and human diseases	81
4.2 Results	83

Characterization of INPP5E function in zebrafish	83
4.2.1 Using the CRISPR-Cas9 to generate a zebrafish mutant of INPP5E.....	84
4.2.2 Phenotype analysis of <i>Inpp5e</i> zebrafish mutant	84
4.2.3 A novel genetic system to monitor Opsin transport in zebrafish.....	89
4.3 Discussion	93
4.4 Summary.....	95
Chapter 5 Discussion and Future Plans	96
5.1 The use of transgenic lines.....	97
5.2 The use of Heatshock promoter.....	98
5.3 Identification of Ciliary PIs	99
5.4 PI function in cilia	102
5.4.1 The role of PI(4,5)P ₂	102
5.4.2 PI(3,4,5)P ₃ function.....	103
5.4.3 PI(4)P	104
5.5 Potential clinical benefits of this work	104
5.6 Future plans	105
Chapter 6 Materials and methods	108
References	134

Chapter 1

Chapter 1

Introduction

1.1 Cilia

1.1.1 Discover history of cilia and flagella

Cilia and flagella are amongst the oldest known organelles. They are highly conserved hair-like structures that project from almost all types of cells. In early years of light microscopy, cilia and flagella were simply distinguished by number, length, and motility. Around 1674-5, a Dutch scientist Antony van Leewenhoek was the first to be able to distinguish motile cilia by observing the moving organisms using light microscopy (Van Leewenhoek). Later in 1889, the improvement of bright field light microscopy by the Carl Zeiss Jena company made the observation of the primary cilium in vertebrate cells possible (Bloodgood, 2009). The basic organization of cilia and flagella was uncovered in 1950' by using transmission electron microscopy (TEM) (Bloodgood, 2009).

The golden age of cilia and flagella research started from 1990's when a graduate student from Rosenbaums' lab, Keith Kozminski, discovered the intraflagellar transport (IFT) in *Chlamydomonas* flagella (KozMINSKI et al., 1993). Afterwards, IFT was shown to be crucial for cilia assembly in *Chlamydomonas*, *C. elegans*, mice and human (Pazour and Rosenbaum, 2002; Tsujikawa et al., 2007). The discovery of IFT revolutionized the field by switching from simple microscopy observation to functional analysis.

In the beginning of the 21th century, cilia stimulated a new level of research interest after scientists became aware of their roles in developmental biology, cell signaling and medical research. One key contribution to cilia research

was the direct demonstration of a sensory receptor role of kidney primary cilia (Pazour et al., 2002), their central role in left-right asymmetry in vertebrates (Taulman et al., 2001) and the realization that membrane receptors involved in sonic hedgehog signaling pathway localize to cilia (Huangfu et al., 2003; Pazour and Bloodgood, 2008).

In the following sections, I will give a brief structural and functional introduction about cilia.

1.1.2 Cilia structure

1.1.2.1 Basic structure

Cilia can be structurally divided into the basal body, the transition zone, microtubule based axoneme, the ciliary membrane and ciliary tip. At the base of the cilium is the basal body, which is a microtubule-organizing center derived from the mother centriole, the older one from the centriole pair. Microtubule doublets of the ciliary axoneme emerge from the basal body. The junction between the distal end of the basal body and the axoneme functions as a ciliary gate, and is referred to as the transition zone (TZ) (Reiter et al., 2012). Transition zone proteins act as modular components of a filter that regulates transport into or out of cilia. A large number of human genetic diseases (so called ciliopathies) are caused by transition zone protein mutations. The whole cilium is covered by the ciliary membrane, which extends from the plasma membrane.

1.1.2.2 Photoreceptor cilia

Vertebrate photoreceptor cells consist of the outer segment, the connecting cilium, the cell body and the synaptic terminal (Kennedy and Malicki, 2009; Rodieck, 1973). The photoreceptor outer segment is a specialized sensory

cilium that extends from the connecting cilium. To adapt to its light-sensing function, the surface area of the ciliary membrane dramatically increases and folds into compact disks during the elongation and formation of the outer segment (Salinas et al., 2017; Steinberg et al., 1980).

1.1.2.3 The ciliary membrane

The ciliary membrane extends from and is a continuation of the cell membrane. Although it is not a membrane-enclosed organelle, the cilium has a distinct membrane composition of both lipid and protein content. Early biochemical study of cilia from *Paramecium tetraurelia* revealed that the lipid and protein composition in isolated cilia fraction differs from the deciliated cell body (Adoutte et al., 1980) (Kaneshiro, 1987). However, for a long period of time, little was known about the exact lipid composition due to the technical difficulty of isolating mammalian primary cilia. Recently, distinct PI composition of cilia was characterized by lipid antibody staining and protein biosensors (Chávez et al., 2015; Garcia-Gonzalo et al., 2015). The ciliary membrane, proteins and their interactions have been extensively studied for the last decade, classic examples include hedgehog pathway components (Rohatgi et al., 2007), GPCRs such as opsin or Sstrs (Daza et al., 2012; Schou et al., 2015) and Polycystins (Nauli et al., 2003; Yoder et al., 2002).

One hypothesis about the reason why the cilium is a unique compartment is based on the fact that the diffusion barrier localized at the cilia base maintains the unique ciliary composition. Evidence indicates that the diffusion barrier exists and excludes the ciliary membrane proteins from the plasma membrane. For example, glucophosphatidylinositol anchored protein fused to a fluorescent protein (YFP-GL-GPI) is excluded from the surrounding area of the apical membrane around the primary cilia outgrowth (Vieira et al., 2006). In addition, applying fluorescent recovery after photobleaching (FRAP) in the ciliary and plasma membrane at the apical surface reveals that diffusion to cilia

is limited by protein size, which indicates the existence of the physical diffusion barrier (Kee et al., 2012).

1.1.3 Ciliary function

The two main functions of cilia are sensory and hydrodynamic. The primary cilium mediates a variety of signal transduction processes in vision, olfaction, mechano-transduction and developmental signalling (Malicki and Johnson, 2017). The outer segment of the photoreceptor cell, for example, detects photons, and olfactory cilia detect small molecules (Pugh and Lamb, 2000). The hedgehog pathway, on the other hand, functions in cilia to mediate limb and spinal canal patterning during morphogenesis (Huangfu et al., 2003). Similarly, motile cilia display a variety of functions. They keep lung airways clean from contaminants, such as dirt and bacteria. They also facilitate sperm cell movements and determine left-right asymmetry of the vertebrate body plan in early embryogenesis (Essner et al., 2005).

1.1.3.1 The intraflagellar transport (IFT)

Cilia do not synthesize their own proteins; all proteins required for ciliogenesis and ciliary function are transported to cilia from the cell body. How are key components, such as tubulin, radial spokes and dynein arms, transported along microtubules during cilia assembly? Cells facilitate this transport by intraflagellar transport (IFT) machinery (Rosenbaum JL1, 2002). Tubulin and other cargo proteins are transported from the base to the tip of the cilium through the anterograde transport. This transport is mediated by the kinesin-2 motor family, which carries both the IFT-B and IFT-A complex. On the way back, the dynein motor drives the IFT-A and the IFT-B complex from the tip back to the cilia base through the retrograde transport.

IFT proteins are highly conserved across species from *C. elegans* to human (Pedersen and Rosenbaum, 2008). The function of IFT particles was studied through genetic methods in a wide range of organisms (Han et al., 2003b; Lunt et al., 2009; Ocbina and Anderson, 2008). The presence and function of IFT is essential for both the construction and maintenance of cilia structure in all species.

1.1.3.2 Cilia and signaling pathways

Cilia are believed to mediate multiple signaling pathways during vertebrate development. One of the most well studied signaling pathways that is mediated by the primary cilium during development is the Sonic Hedgehog (Shh) signaling pathway. The first demonstration that Shh pathway is cilia dependent was in mice mutants. In these mutant mice, which lacked ventral neural tube cell types and displayed other SHH phenotypic defects, both IFT172 and IFT 88 were disrupted (Huangfu et al., 2003). Similar in zebrafish, maternal zygotic IFT88 mutant fish displayed Shh signaling defects in the neural tube, however, different defect pattern was shown (Huang and Schier, 2009). In contrast to mouse mutants, zebrafish mutant displayed a dampened but expanded pattern of Shh in the neural tube. Moreover, basal body proteins are required for Shh signaling in both chicken and mice (Davey et al., 2007; Delous et al., 2007; Ferrante et al., 2006). Hedgehog pathway key components, such as PTCH, SMO, GLI2 and GLI3, are also known to be enriched in cilia (Corbit et al., 2005; Haycraft et al., 2005; Rohatgi et al., 2007).

Apart from Shh, the role of cilia in Wnt signaling pathway received a lot of attention. The Wnt pathway is divided into the canonical (Wnt/ β -catenin) and non-canonical (Wnt/PCP) signaling pathway based on its dependence on β -catenin (Klaus and Birchmeier, 2008). The early connection between cilia and the Wnt pathway came from the studies of Inversin, which localizes in cilia and interacts with Dishevelled, a component of both Wnt/ β -catenin and

Wnt/PCP pathway (Otto et al., 2003; Shiba et al., 2009). Later, efforts focused on finding direct evidence indicating that cilia loss affects Wnt pathway, however, data from *in vivo* models was controversial. In Wnt/ β -catenin pathway, on one hand, the key Wnt component was not affected in mouse and zebrafish IFT88 mutants (Huang and Schier, 2009). On the other hand, in Kif3a mutant mice, Dishevelled was constitutively phosphorylated (Corbit et al., 2008). In Wnt/PCP, polarity defects were observed in the organ of Corti from IFT88 conditional knockout mice, however, the distribution of core PCP components, such as *Vangl2* was normal (Jones et al., 2008). In addition, PCP signaling control of cell division was considered as a possible cause for kidney cysts suggesting a connection to ciliogenesis. Fat4 is known as a key role in vertebrate PCP. In *fat4*^{-/-} mice, kidney cysts were reported (Saburi et al., 2008). However, the connection between Fat4 and cilia has not been further established.

Other pathways are also related to cilia. Fibroblast growth factor (Fgf) signaling was shown to regulate cilia length in zebrafish morphants (Hong and Dawid, 2009; Neugebauer et al., 2009). Notch signaling pathway regulates left-right asymmetry through cilia length control, which was demonstrated in the zebrafish DeltaD mutant (Lopes et al., 2010a). Notch signaling component, Notch3, is cilia enriched in wild-type epidermis. The inhibition of Notch reporter activity was demonstrated in IFT74 shRNA treated cells indicating a role of cilia in Notch pathway (Ezratty et al., 2011). To firmly establish the role of cilia in Notch signaling, it will be important to have some *in vivo* data from both cilia mutants demonstrating Notch defects and classic Notch mutants showing ciliary dysfunction.

1.1.4 Ciliopathies

Functional defects in many intracellular organelles may cause human diseases, and the same applies to cilia. Ciliopathies are human genetic disorders

resulting from mutations in gene products that localize in the cilium or the centrosome (Hildebrandt et al., 2011). Due to its diverse biological roles, including whole-cell locomotion; movement of fluid; chemo-, mechano-, and photo-sensation; and the regulation of metabolism (Malicki and Johnson, 2017; Satir and Christensen, 2007), defects in the cilium are associated with a range of human diseases, such as primary ciliary dyskinesia, hydrocephalus, polycystic liver and kidney disease, retinitis pigmentosa, obesity, LRA defects, polydactyl and even psychiatric disorders (Eley et al., 2005). Ciliary defects are found to lead to an ever growing set of developmental and adult diseases. As a result from mutations in ciliary proteins, several phenotypes arise, like nephronophthisis, Bardet-Biedl syndrome, Alstrom syndrome, and Meckel-Gruber syndrome (Fliegauf et al., 2007).

Centrosomopathies, which result from centrosome dysfunctions, also cause rare syndromes including Majewski Osteodysplastic Primordial Dwarfism Type II (MOPDII)(Rauch et al., 2008) and primary microcephaly (Thornton and Woods, 2009). Centrosomopathies occur as a result of mutations in proteins that interact with or localize to the centrosome (Kodani et al., 2015).

The criteria for separating centrosomopathies from ciliopathies are not clear, due to the fact that many centrosomal proteins participate in cilia formation and function. Consequently, many defects in centrosomes are well known causes of ciliopathies. Mutations in proteins, which localize in the subdistal appendage of the mother centriole, for instance, affect the initiation of ciliogenesis and consequently result in ciliopathies. Examples of such proteins are SDCCAG8 (Otto et al., 2010), which when defective causes renal-retina ciliopathy, and CC2D2A (Veleri et al., 2014), mutations of which cause Meckel and Joubert syndrome. In addition, lack of some centrosomal proteins phenotypically overlaps with ciliopathies. For example, defects in PLK4, a kinase that regulates centrosome biogenesis, were reported to have ciliopathy phenotypes: photoreceptor and left-right asymmetry defects were

observed in *plk4* morphants (Martin et al., 2014).

1.2 Phosphoinositides (PIs)

1.2.1 The basic structure of PIs

PIs are phosphorylated derivatives of phosphatidylinositol. They are generated by kinases and phosphatases that act upon their membrane-bound lipid substrates. Phosphorylation occurs in one of the -OH group of the inositol ring that is linked to the diacylglycerol (DAG) backbone (Figure 1). Only positions -3, -4, and -5 are actually phosphorylated in natural PIs. These phosphorylation events give rise to seven well-known PIs (Di Paolo and De Camilli, 2006; Frew et al., 2008).

1.2.2 The research history of PI in vertebrates

In the 1940s, Jordi Folch identified inositol in the ethanol-insoluble phospholipid fraction from bovine brain and determined that it contains phosphates and inositol in a molar ratio of 2:1 (Balla, 2005). Fifteen years later, the observation of the turnover of membrane phospholipids in the brain cortex, give researchers glimpse of their importance in cell biology (Hokin and Hokin, 1955).

Another important breakthrough in the understanding of PIs came when inositol triphosphate (IP3) became known as the source of second messengers in transducing signals from cell surface receptors (Hokin, 1985). Cell biologists developed interest in PIs due to their importance in shaping membranes and controlling vesicular trafficking and organelle physiology (Ferguson et al., 2000). The attention of scientists who study ion channels also turned towards PIs as it became obvious that many channels or transporters require PIs for their activity or control.

Phosphatidylinositol (PI)

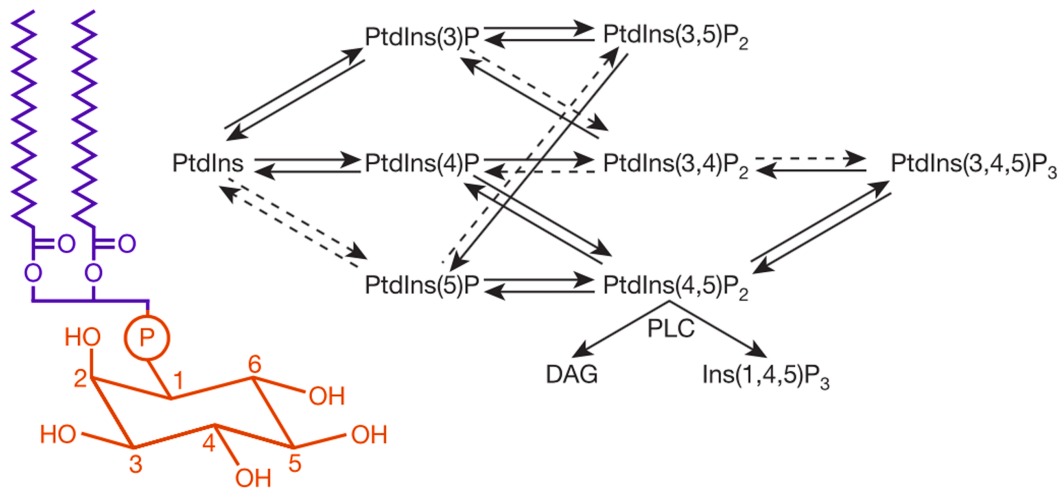


Figure 1. The PI structure and metabolic reactions of seven PIs.

Phosphatidylinositol consists of phosphatidic acid which contains glycerol and two fatty acid tails (purple) and an inositol head (orange). Modified from (Di Paolo and De Camilli, 2006).

The discovery of phosphatidylinositol 3-kinases (PI3Ks) is another milestone in PIs studies. PI3K and PTEN are two key regulators of the PI3K pathway that regulates cell proliferation, growth and survival (Fruman et al., 2017; Worby and Dixon, 2014). These two proteins are among the most frequently mutated in human cancers (Chalhoub and Baker, 2009). PI3K pathway is activated by growth factors bind to receptor tyrosine kinase (RTK). The activation of PI3K increases the level of PIP₃ and is followed by the phosphorylation of AKT, which results in the activation of mammalian target of rapamycin (mTOR) pathway. mTOR then phosphorylates p70S6 and 4E-binding protein 1 (4EBP-1), which initiates the translation of cell cycle regulators. As a negative regulator, PTEN inhibits PI3K/AKT/mTOR pathway by decreasing the level of PIP₃ and consequently downregulates AKT's phosphorylation. Mis-regulation of PI3K signalling is considered a marker of human cancer.

The association with PI3K made PIs gain attention of cancer biologists (Okkenhaug, 2013). Could this be cilia related? This may be the case

because TOR complex 1 (TORC1) was shown to regulate cilia size and function in zebrafish development (Yuan et al., 2012). Ciliation defects, which are a hallmark for cancer cells (Toftgård, 2009), may be due to the mis-regulation of the cell cycle. To date, a classic example of a ciliopathy, polycystic kidney disease, involves excessive cell proliferation and a loss of cell polarity, which are also major features of cancer cells.

In addition, immunologists noted that many pathogenic organisms produce PI-enzymes to invade or reprogram host cells to produce the pathogen (Katso et al., 2001). Neuroscientists also discovered that synaptic vesicle exocytosis and recycling requires PIs at multiple steps during brain development (Cremona et al., 1999). This incomplete list of PI functions is still increasing as more and more cellular processes are linked to these universal lipid regulators.

1.2.2 The role of PI in biological processes

PIs participate in almost all aspects of cell functions in variety of ways (Di Paolo and De Camilli, 2006). PIs are important regulators of many intracellular processes, including vesicle transport, signal transduction and cytoskeletal dynamics (Czech, 2000; Di Paolo and De Camilli, 2006; Gamper and Shapiro, 2007). PIs are highly involved in organelle biology through the regulating vesicular trafficking (Mayinger, 2012). They also modulate lipid distribution and metabolism via the interaction with lipid transfer proteins (Falkenburger et al., 2010). PIs regulate ion channels, pumps, and transporters and mediate both endocytic and exocytic processes (Hille et al., 2015). PIs are also photo-sensing and signal transduction dependent in the invertebrate organisms (Balla, 2010). Increasing number of biological processes have become known to require PIs in the last 20 years. Gradually, these phospholipids are turning into one of the most universal categories of signaling molecules in eukaryotic cells.

Multiple regulators are involved in PIs metabolism. This, as expected, is associated with a number of human diseases, from rare genetic disorders such as Lowe syndrome and Dent disease to the most common ones such as cancer, obesity, and diabetes (McCrea and De Camilli, 2009; Suchy et al., 1995). Many of these PI related disorders result from defects in phospholipid metabolizing enzymes. It turns out that the enzyme not only catalyzes a specific reaction but also acts as a related PI pool. As a result, PI metabolizing enzymes began to be noticed by pharmaceutical companies as potential therapeutic targets.

1.2.3 PIs in cilia

At least two lines of evidence reveal that PIs have a prominent role in cilia. First, several ciliary proteins feature PI binding domains (Nachury et al., 2007). TULP3 was shown to interact with PI(4,5)P₂ and bridge the IFT-A complexes with ciliary and/or periciliary membrane (Mukhopadhyay et al., 2010). BBS5, a Bardet-Biedl syndrome protein family member, was also revealed to display the affinity towards PIs due to the existence of two tandem PH domains in the N-terminus (Jin et al., 2010). Moreover, smad anchor for receptor activation (SARA) features another PI binding domain, the FYVE domain, and interacts with PI(3)P in photoreceptor outer segment (Chuang et al., 2007). Second, ciliary proteins encoded by Joubert/MORM ciliopathy syndrome locus, INPP5E, and the Lowe's syndrome related protein, OCRL, are PI phosphatases (Bielas et al., 2009). In animal models and humans alike defects in ciliary PI binding proteins have dramatic consequences. For example, mutations in the Tubby-like 3 gene cause embryonic-lethality and neural tube defects (Norman et al., 2009). Defects in other ciliary PI-interacting proteins cause kidney defects, blindness, mental retardation and obesity (Ishikawa and Marshall, 2011b)

The restricted spatial distribution of PIs forms a membrane signature that

defines the identity of cellular organelles. A given membrane has a predominant PI signature. For example, the plasma membrane is PI(4,5)P₂ rich while Golgi membranes are PI(4)P rich (Di Paolo and De Camilli, 2006). As the ciliary membrane is continuous with the cell membrane, a unique PI identity is essential for the ciliary membrane to be distinguished from the surroundings. Moreover, the specialized membrane composition is not only characterized by unique lipid content but also by organelle-specific protein components. The PI signature of intracellular membranes including the ciliary membrane facilitates the accumulation of specific proteins.

Many signal transduction components are membrane associated. A specialized PI content in the ciliary membrane may be associated with cilia specific signalling pathways. As mentioned above, potential cilia related PI binding proteins include TULP3, BBS5 and SARA. TULP3 is a negative regulator of Hh signalling pathway (Chávez et al., 2015; Garcia-Gonzalo et al., 2015). BBS5 is a member of the BBSome core component, which involves vesicular transport of membrane proteins to the primary cilia (Jin et al., 2010). Therefore, we may speculate that PIs might be involved in the regulation of ciliary transport (potentially through the BBSome) and signalling pathways such as Hh signalling. In particular, regulation of the ciliary transport or function of signalling components through ciliary PIs could be potentially critical for body weight regulation and photoreceptor function.

1.3 Zebrafish as a vertebrate model of developmental biology

Zebrafish has emerged as a significant experimental organism for developmental biology research (Grunwald and Eisen, 2002; Link and Megason, 2008). It was first selected by George Streisinger in the 1980s and later, in 1990s, promoted as a vertebrate model for genetic screening by

Christiane Nüsslein-Volhard's group in Tübingen and Wolfgang Driver's group in Boston. Two large-scale screens were conducted and identified hundreds of mutants that related to a wide variety of developmental processes, including ciliogenesis (Malicki et al., 1996; Schier et al., 1996; Thisse and Zon, 2002; Van Eeden et al., 1996; Whitfield et al., 1996). Through the 'big screen', zebrafish has been pushed to the forefront of developmental biology research. The genetic analysis of development and physiology established on *Drosophila* was extended to a vertebrate, the zebrafish.

Zebrafish is a freshwater tropical fish. It is relatively small, which makes it easy to maintain tens of thousands of animals in aquaria. Mature fish have high fertility and can produce over 100 eggs at weekly intervals with well feeding. Zebrafish biology allows ready access to all developmental stages. As zebrafish embryos and larvae are transparent, they can be easily imaged real time using live specimens. They can be used in vertebrate genetics for screening cilia mutants, which are particularly easy to identify in this model (Sun et al., 2004). Recently, they can be efficiently mutagenized using TALENs and CRISPRs to generate heritable mutant alleles of chosen loci. Zebrafish is a vertebrate, which displays many similarities to human anatomy, physiology and cell biology (Link and Megason, 2008). The fish retina, for example, has the same major cell classes: photoreceptor cells, bipolar cells, Müller cells, ganglion cells, horizontal cells and amacrine cells as the human retina. All of this makes zebrafish one of the most broadly useful and cost-effective animal models of human genetic disorders.

1.4 Overall hypothesis

The main idea is that ciliary dysfunctions including human ciliopathies may not result from cilia absence, which presumably causes embryonic lethality, but from defects in cilia-mediated or associated signal transduction defects. These defects could happen at the stage of phospholipid-mediated initiation of

signal transduction in cilia, similar to PI(3,4,5)P₃-mediated PI3K pathway activation, or during transport of specialized ciliary signaling proteins.

Transport of transmembrane signaling proteins to cilia, such as Opsin (a GPCR), or Polycystin (a TRP channel), requires a series of closely interconnected steps: vesicle transport to the base of cilia, crossing the selective diffusion barrier at the transition zone, and finally intraflagellar transport along the ciliary axoneme. These transport steps are selectively enhanced or attenuated by a number of mechanisms including membrane modifications. Membrane phospholipids in particular are likely to function at each step of ciliary transport mechanisms.

Despite their importance that I mentioned in other sections, the content of PIs in the ciliary membrane has not yet been well investigated. We hypothesize that ciliary and periciliary cell membranes, periciliary vesicles and perhaps even sub-compartment of the ciliary membrane feature unique PI composition.

Furthermore, we postulate that specific PI content is required for cilia function. Through interacting with PI binding proteins such as TULP3 or SARA, certain ciliary PIs may indirectly participate in ciliary transport such as IFT or function in signaling pathways such as sHH pathway or Wnt pathway.

Using living vertebrate embryo, we are able to monitor PI composition across developmental stages and directly test the developmental and physiological roles of ciliary phosphoinositides in an intact organism.

1.5 Aims

1.5.1 Detection of PI content in the ciliary and periciliary membrane

Despite several recent studies, the content of PIs in the ciliary membrane

remains relatively poorly understood. Using a zebrafish model, I will determine the PI content in the ciliary and periciliary membrane and test PI functions in the context of an intact living animal.

Cilia are unique subcellular compartments. In this project, I hypothesize that the ciliary and/or periciliary membrane contains a unique PI composition just as the Golgi and early endosome (Figure 2). Nearly two decades of research have identified numerous PI-binding domains, many of which have been used as sensors of membrane PI content in tissue culture (Lemmon, 2003; Lemmon et al., 1996). I will apply knowledge obtained through these studies to living vertebrate embryos. Plecstrin homology (PH) domain based sensors are very well established in mammalian tissue culture for PI detection (Lemmon et al., 1996). In order to apply them in zebrafish, I will construct vectors to express PH domain based sensors with well-established binding specificity: PH-PLC delta, which recognizes PI(4,5)P₂; PH-TAPP1, which binds PI(3,4)P₂; PH-BTK, which recognizes PI(3,4,5)P₃; and PH-AKT, which interacts with both PI(3,4,5)P₃ and PI(4,5)P₂.

I will use the above sensors to detect PI composition in cilia of different tissues during several developmental stages. I hypothesize that ciliary PI content varies during specific physiological status such as cell differentiation. The ciliary PI content change could indicate signalling events within the cell.

1.5.2 Determination of PI function in the ciliary membrane

I hypothesize that ciliary PIs are required for cilia function. Although many studies indicated that PI function in cilia assembly and maintenance, this has not been directly demonstrated. To test the role of PI in cilia directly, I will target the PI specific kinases or phosphatase to the ciliary membrane. Arl13b was used as the targeting signal. I will focus on the ciliary function of

PI(4,5)P₂ and PI(3,4,5)P₃ first. Based on publications of ciliary PI related proteins, I believe that these two PIs are particularly relevant to cilia function.

1.5.2.1 Examination of phenotypes after disruption of PI contents in the ciliary membrane

I hypothesize that PI(3,4,5)P₃ or PI(4,5)P₂ content changes (either increases or decreases) in cilia would cause ciliopathy-related phenotypes, such as cystic kidneys, photoreceptor degeneration, hedgehog-related phenotypes and so on. To change ciliary PI content, I will do the following:

- a. Overexpress cilia targeted phosphatase Inp54p, which dephosphorylates PI(4,5)P₂ and generates PI(4)P.
- b. Overexpress cilia targeted phosphatase Ptena, which dephosphorylates PI(3,4,5)P₃ and generates PI(4,5)P₂.
- c. Overexpress cilia targeted kinase PI3K, which phosphorylates PI(4,5)P₂ and generates PI(3,4,5)P₃.
- d. Generate a loss of function zebrafish mutant of ciliary phosphatase INPP5E

1.5.2.2 Generation of a genetic system to monitor opsin transport in the photoreceptor

I will apply standard histology methods to evaluate photoreceptor loss in ciliary mutants. To monitor more subtle changes in photoreceptors, opsin transport will be monitored using the opsin-GFP assay. To investigate the mechanism of photoreceptor degeneration in cilia mutants, in chapters that follow I will describe a genetic system that I constructed to monitor opsin transport in zebrafish photoreceptors. These analyses revealed morphological abnormalities of cilia and functional defects, which point to unidentified

functions of PI(3,4,5)P₃ or PI(4,5)P₂ in cilia.

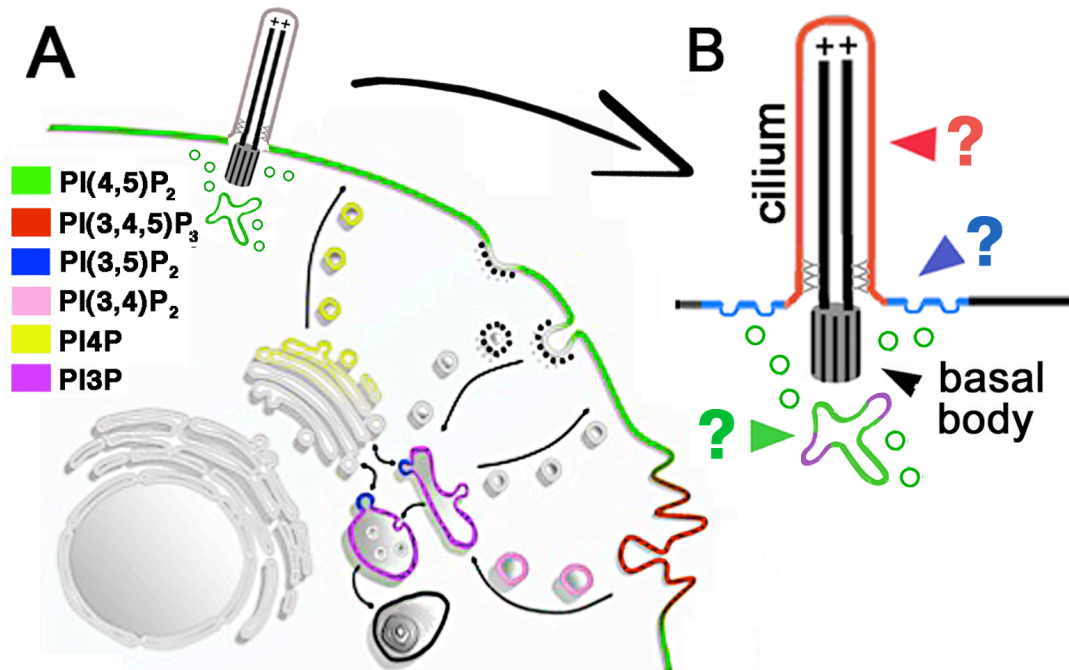


Figure 2. PIs in subcellular membranes.

(A) Colour coded PI content in the plasma membrane and subcellular membranes. (B) The PI content in the ciliary membrane and periciliary membrane remains largely unknown. Modified from Di Paolo & De Camilli (2006) and Yale/Keck website.

Chapter 2

Chapter 2

PI contents identification in vertebrate cilium

2.1 Introduction

2.1.1 Detection and identification of PIs

Owing to their crucial functions in cellular processing, it is important that the levels of PI in the cell can be measured accurately. Briefly, PI detection methods can be divided into biochemistry methods, antibody detection and PI binding motif based detection (Idevall-Hagren and De Camilli, 2015).

2.1.1.1 Biochemical methods

Biochemistry methods such as thin layer chromatography (TLC) and ion-exchange high-performance liquid chromatography (HPLC) are used to identify or quantify lipids from cell or tissue extracts (Várnai and Balla, 1998). Metabolic labelling with [³H] inositol or [³²P] inorganic phosphate is required beforehand. Both TLC and ion-exchange HPLC are able to detect monophosphate and bi-phosphate without further distinguishing which position of the inositol ring is phosphorylated. Mass spectrometry is also an effective method for lipid identification. Distinguishing between different fatty acid chains can be achieved without radioactive labelling. Biochemistry methods can be used in combination to measure phospholipid composition *in vivo*. This was done in *Paramecium tetraurelia* to show that the composition of the ciliary membrane is different from the deciliated body (Andrews and Nelson, 1979; Kaneshiro, 1987).

One major disadvantage of biochemistry methods is the poor temporal and spatial resolution of lipid identification. Biochemistry data can reveal PI

species or an overall PI level from the whole organism that is analysed. However, it is difficult to know how PIs are distributed in the plasma membrane or in other subcellular membranes at any given stage. Moreover, for a given membrane, the dynamics of PI levels or species are also poorly detected using biochemistry methods.

To analyse PIs *in situ*, which most cell biology and developmental studies require, fluorescent detection based methods are widely used.

2.1.1.2 Antibody based PI detection

Many PI antibodies are commercially available. The distribution pattern of PIs in the plasma membrane or intercellular membranes can be visualized through antibody staining. Semi-quantitative detection is also achievable by estimating signal intensity. However, due to the need of fixation and permeabilization for antibody staining, natural lipid distributions are easily affected by detergents (Hammond et al., 2009). Moreover, the antibodies cannot detect PIs that are bound by interacting proteins. Competitive protein binding and detergents affect the precision of PI detection. Another weakness of antibody detection is the limit of antibodies to monitor dynamic changes in PIs during biological processes.

2.1.1.3 PIs binding domains for PIs detection

Enzymes or effector proteins bind a target PI through specific PI-binding domain and those domains have become valuable tools at *in situ* PIs analysis (Itoh and Takenawa, 2002). A PI biosensor, which was constructed by fusing a PI binding domain to a fluorescent protein, can yield information regarding intracellular distribution and translocation of PIs after stimulation in living or fixed cells or in whole organisms. Numerous protein domains have been identified to monitor PI levels and changes, such as pleckstrin homology (PH)

domain, phox-homology (PX) domain and Fab1, YotB, Vac1, EEA1 (FYVE) domain (Lemmon, 2008). The FYVE domain and P4M domain are used to detect phosphatidylinositol monophosphate PI(3)P and PI(4)P respectively (Chuang et al., 2007). PI(4,5)P₂, with the highest abundance among all PIs, can be detected by both PH domain and PX domain. PH domains are also commonly used to detect PI(3,4)P₂, and PI(3,4,5)P₃. There is no well-studied protein domain that can be applied to detect PI(5)P or PI(3,5)P₂ (Takenawa and Itoh, 2006).

2.1.1.3.1 PH domains

Nearly two decades of research have identified numerous PI-binding domains, many of which have been used as biosensors for the membrane PI detection. One of the best-characterized PI binding motifs is the pleckstrin homology domain, referred to as the PH domain.

The PH domain was first characterized in pleckstrin, a protein kinase C substrate that is expressed in platelets (Mayer et al., 1993). The binding affinity towards PI(4,5)P₂ was first reported by Harlan in 1994 (Harlan et al., 1994). They indicated that the lipid-binding site was located at the lip of the β-barrel. After this initial finding, many other PH domain proteins with different PI binding affinities and specificities were identified. These new PH domain proteins include the AKT PH domain that specifically binds both PI(3,4)P₂ and PI(3,4,5)P₃ and the TAPP1 PH domain that specifically recognizes PI(3,4)P₂ (Lemmon et al., 1996).

PH domains are highly conserved modules of approximately 120 amino acids (Lemmon and Ferguson, 2000). All PH domains share a common core structure that consists of a 7-strand-sandwich formed from two nearly orthogonal sheets (Figure 3). These two antiparallel sheets, consisting of 4 and 3 strands, form a pocket-like space for PIs binding. PH domains are also

electrostatically polarized, with their positively charged face directed towards with the PI negatively charged hydrophilic head (Ferguson et al., 1995a; Ferguson et al., 1995b). Notably, not all PH domains bind PIs. The PH domains in OCRL and INPP5B, both of which function as inositol 5-phosphatases, fail to bind PIs according to Mao's data from PI strips based binding and liposome pull-down assays (Mao et al., 2009). A lack of the positively charged pocket in OCRL and INPP5B results in the PI binding deficiency of their PH domains, which is in agreement with the electrostatic potential binding model.

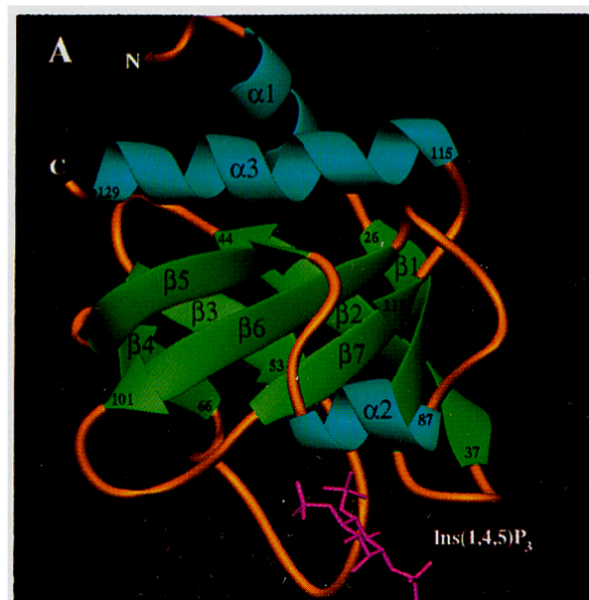


Figure 3. A model of the PH-PLC δ -Ins(1,4,5)P₃ complex. Ribbons represent PH-PLC δ 12-130 amino acids in complex with Ins(1,4,5)P₃ (Ferguson et al., 1995a).

2.1.1.3.2 PH domains based PI detection

Fused with fluorescent proteins, PH domain based biosensors became one of the most valuable tools for PI *in vivo* studies. They can be used as direct reporters, which usually consist of a PH domain and a fluorescent protein, for the analysis of PIs distribution, concentration and translocation. Moreover, they can be applied to FRET (fluorescence resonance energy transfer)-based

strategies (Idevall-Hagren and De Camilli, 2015). In one approach, a PI binding domain (PBD) is fused to a couple fluorophores, CFP and YFP for example. FRET occurs between a PBD-CFP and a PBD-YFP when these two PI-binding proteins accumulated at high concentration at the membrane. In another approach, the PI sensor is comprised by a PBD fused to two fluorophores N- and C-terminus at the same time, such as CFP-PBD-YFP. FRET occurs due to a conformational change when PBD binds PIs (Sato et al., 2003). FRET based approaches have advantage as tools to monitor the PI level changes as the fluorescent signal serves as a direct readout; however the low signal-to-noise ratio can be a technically challenging in such experiments.

PH domain-based direct reporters are applied to monitor classic biological processes, such as endocytosis (Posor et al., 2013), the basolateral plasma membrane formation in epithelial cells (Gassama-Diagne et al., 2006) and membrane phospholipids level during flagella biogenesis (Wei et al., 2008). In Wei's et al. study, the authors showed that PI(4,5)P₂ was a key regulator of axoneme growth in *Drosophila* spermatogenesis. The plasma membrane PI(4,5)P₂ depletion through the overexpression of SigD, a enzyme that hydrolyses PI(4,5)P₂ and generates PI(4)P, affects basal body docking and flagella axoneme structure. PH-PLC δ was used to monitor the level of PI(4,5)P₂ in the plasma membrane, however, there were no further comments in regard to the PI composition of the sperm flagella membrane.

2.2 Results

2.2.1 PI content detection in the ciliary and periciliary membrane

To evaluate PI content in the ciliary membrane, I used PH domain-based

sensors that display distinct PI binding specificities: PH-PLC delta, which recognizes PIP(4,5)₂ (Várnai et al., 2002); PH-TAPP1, which binds PIP(3,4)₂ (Manna et al., 2007); PH-Btk, which recognizes PIP(3,4,5)₃ (Manna et al., 2007); and PH-AKT, which interacts with both PIP(3,4,5)₃ and PIP(4,5)₂ (Yang et al., 2002). Binding specificities of these domains are documented by multiple studies. Experiments were performed in zebrafish model because it allows me to look at different types of cilia at one developmental stage and one type of cilia at many developmental stages.

To prevent PH-sensors from constantly binding to PIs, which could sequester PIs and affect zebrafish development, all sensors were expressed from the heatshock promoter (Figure 4). These experiments were performed in Arl13b-GFP transgenic line Tg(*βact:Arl13b-EGFP*) (Borovina et al., 2010), a commonly used transgenic line to visualize cilia. This approach allowed us to visualize PI contents in the cilium and related membranes at the cilia base in the intact zebrafish embryo. PI sensors have already been used in elegant studies to visualize membrane polarity in migrating cells in living zebrafish embryos (Yoo et al., 2010).



Figure 4. Schematic of the PH domain-based PI biosensor. The PH domain is fused to mcherry and expression driven by the heatshock promoter, which makes it possible to control in time.

2.2.1.1 PH sensors transient expression assays

First, transient expression of PH sensors was carried out in zebrafish embryos. The heatshock treatment was applied at 2 days post fertilization (dpf) to induce expression. The expression and distribution patterns were analysed 5 hours

post heatshock in living embryos using confocal microscopy.

2.2.1.1.1 The binding affinity was from PH domain binding pocket

To validate the binding specificity, I made the control construct for PH-PLC, PH-PLC^{K30L,K32L,R40L}, which included 3 point-mutations (Lys30>Leu, Lys32>Leu, Arg40>Leu) in key amino acids in the binding pocket (Stauffer et al., 1998; Várnai and Balla, 1998). These mutations were shown to abolish PH-PLC binding to PI(4,5)P₂ (Raucher et al., 2000). Sensors were transiently expressed in Tg(β act:Arl13b-EGFP) zebrafish embryos through DNA injection and heatshock induction. Mcherry-positive cells were analysed. PH-PLC clearly labelled plasma membrane (Figure 5 upper panel), which is known to be PI(4,5)P₂-rich. In some cells, it also colocalized with GFP labelled Arl13b, a ciliary marker. In the mutated PH-PLC control (Figure 5 lower panel), PH-PLC^{K30L,K32L,R40L}, mcherry signal was evenly distributed across the entire cell. There was no obvious enrichment or colocalization of PH-PLC^{K30L,K32L,R40L} with the plasma membrane or with Arl13b. These data indicated that I was able to induce PH-PLC sensor expression in zebrafish embryos. This PH sensor was able to function as a specific PI detector as indicated by its ability to label the plasma membrane. The binding was mediated by PH domain binding pocket and it was abolished by mutating key amino acid in this pocket. Moreover, I observed colocalization between PH-PLC and a cilia marker Arl13b.

2.2.1.1.2 Summary of PH sensor analysis in transient expression experiments

All five sensors listed in Table 1 were used through transient expression in Tg(β act:Arl13b-EGFP) zebrafish embryos to determine ciliary PI content. A co-localization between PH-PLC and a cilia marker, Arl13b, was observed in some cells. PI(4,5)P₂ either appeared at the proximal end (Figure 6B) or

along the entire length of the cilium (Figure 6C). Occasionally, the PH-AKT sensor also marked PI(3,4)P₂ and/or PI(3,4,5)P₃ pool at the proximal end of cilium (Figure 6D). Because this was transient overexpression experiment, the fluorescent intensity of PH sensors varied from sample to sample. Given high variability and low sample size, I did not quantify these results. A systematic analysis was required for a better understanding of the distribution pattern of PIs in the ciliary and periciliary membrane. To this end, I generated stable zebrafish transgenic lines, which express PH sensors (listed in Table 1), for further studies.

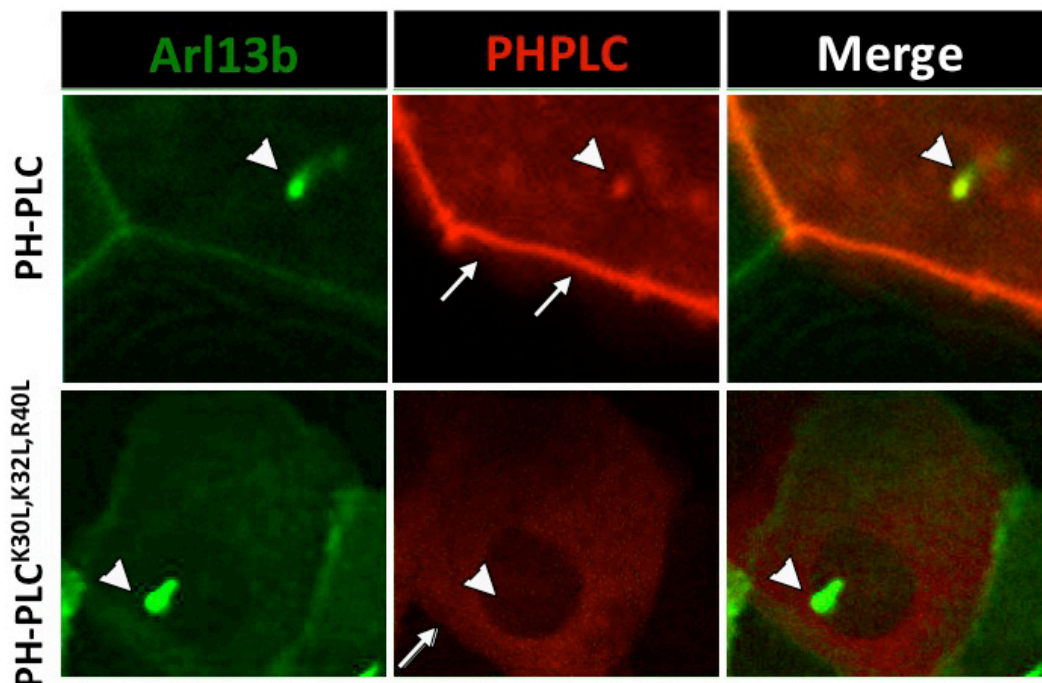


Figure 5. PH-PLC sensor is able to detect PI(4,5)P₂ in Tg(β act:Arl13b-EGFP) zebrafish embryos. Confocal images of skin epithelium expressing PH-PLC sensor and a binding-deficient control PH-PLC^{K30L,K32L,R40L}. PH-PLC sensor signal (red) clearly labels the plasma membrane (white arrow) and co-localizes with the cilia marker Arl13b. The PH domain mutant PH-PLC^{K30L,K32L,R40L} is distributed evenly across the entire cell cytoplasm, with no obvious enrichment in the membrane or in the cilium.

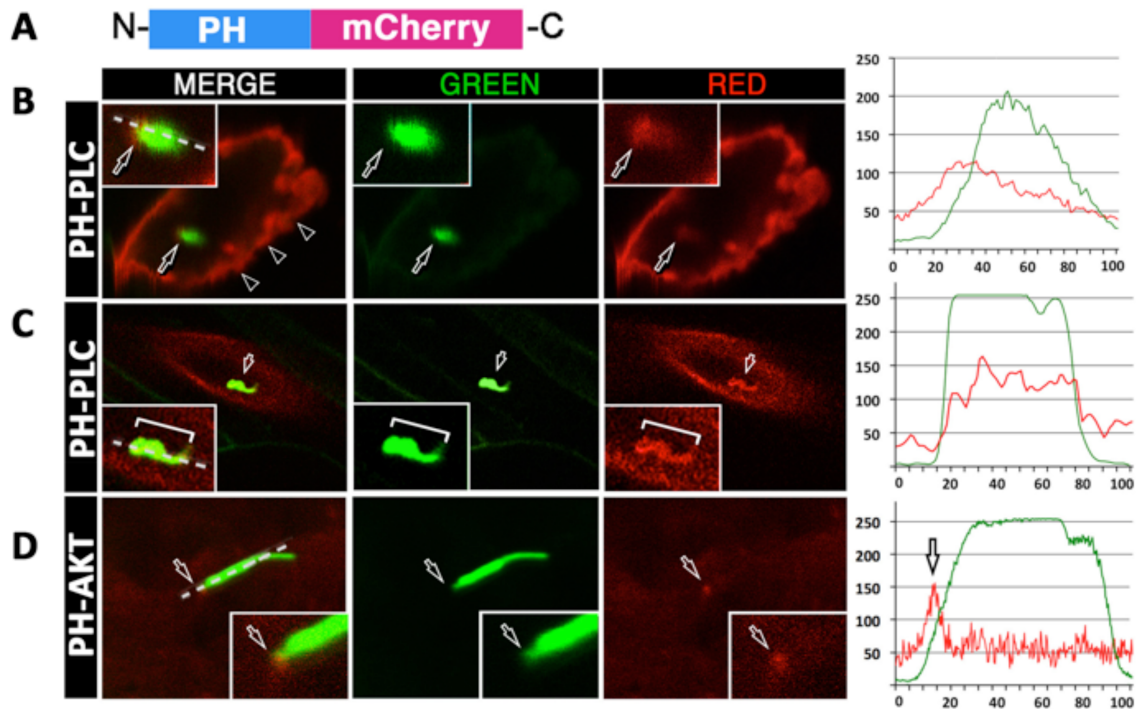


Figure 6. $PI(4,5)P_2$ is present at the base of cilia or along the entire cilia length in some cells.

(A) Schematic of a PH-domain sensor used to visualize PIs in the ciliary membrane.

(B-D) Confocal images of sensor localization (red) in cilia of living zebrafish embryos visualized with *Arl13b-GFP* transgene (green) at 2 dpf. Graphs to the right show the intensity of red (PH domain sensor) and green (the ciliary membrane visualized with *Arl13b-GFP*) signal along the dashed lines that transect the image in the far-left panels. Insets show enlarged images of cilia.

(B, C) PH-PLC sensor enriched at the base of the cilium (arrow) and to a lesser extent in the cilium itself.

(D) PH-AKT sensor is enriched at the cilia base (arrows in the images and graph to the right).

In all graphs, the horizontal axis shows the percentage length of the transect line.

Table 1. Sensors applied for transient and stable expression

Name	Specificity
PH-PLC	PI(4,5)P ₂
PH-PLC ^{K30L, K32L, R40L}	no binding
PH-TAPP1	PI(3,4)P ₂
PH-BTK	PI(3,4,5)P ₃
PH-AKT	PI(3,4)P ₂ and PI(3,4,5)P ₃

2.2.1.2 Using stable transgenic lines to analyze PIs in ciliary membranes

The generation of transgenic sensor lines is described in Material and Methods chapter. Briefly, transgene-positive adult G0s were out crossed with wild-type fish and the progeny with transgene was selected and raised to adulthood (F1 generation). This step was repeated in F1, F2... generation until the transgene displayed mendelian segregation ratio (50%). All four PH sensors used in my studies were mendelian lines.

2.2.1.2.1 PH-PLC is effective at detecting PI(4,5)P₂

To make sure PH sensors function as PI detectors, I first looked at a well characterized PI(4,5)P₂-rich structure, the stereocilia. Stereocilia are actin-filled structures which form at the apical surface of hair cells. PI(4,5)P₂ was shown to localize to the hair bundle in frog saccular hair cells by antibody staining (Hirono et al., 2004).

As expected, I observed PH-PLC labelled stereocilia in the developing otic vesicle of 32 hours post fertilization (hpf) embryos (Figure 7A). The PH-PLC sensor specifically targets PI(4,5)P₂ compared with the PH-AKT sensor (see lack of specific signal in Figure 7B compared to 7A).

PI(3,4,5)P₃ has a central role in the polarization of neuron and epithelial cells.

In epithelial cells, PI(3,4,5)P₃ is excluded from the apical surface of the plasma membrane and regulates the basolateral membrane formation (Gassama-Diagne et al., 2006). As anticipated, the PH-AKT sensor revealed the basolateral localization of PI(3,4,5)P₃ in the otic vesicle lumen (Figure 7B).

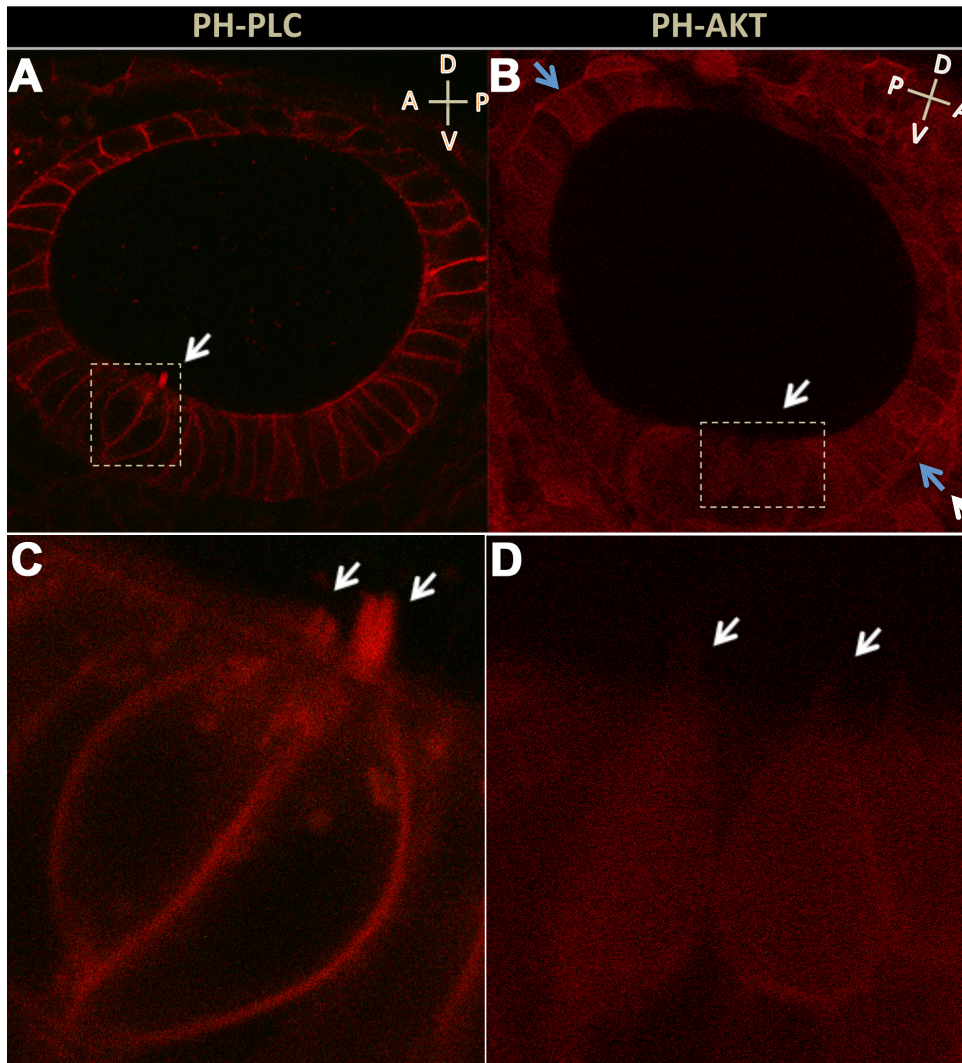


Figure 7. PH-PLC sensor is effective at detecting PI(4,5)P₂

Confocal images of otic vesicles from *Tg(hsp70:PH-PLC-mcherry)* and *Tg(hsp70: PH-AKT-mcherry)* transgenic zebrafish embryos at 32hpf (5 hours post heatshock). PH-PLC is highly enriched in the stereocilia (A) (white arrows), which cannot be observed in the PH-AKT sensor line (B). In contrast to PHPLC, the PH-AKT sensor reveals PI(3,4,5)P₃ labelled basolateral plasma membrane (blue arrows). (C-D) Higher magnification images of the boxed areas in A and B respectively.

2.2.1.2.2 PIs distribution at early stages in zebrafish retina

I compared PI composition in cilia of different tissues. I hypothesize that ciliary PI content varies during cell differentiation and in different developmental stages. To test this, I first looked at zebrafish photoreceptors, which contain a highly specialized cilium. I applied PH-PLC, PH-TAPP1 and PH-BTK sensors in transgenic zebrafish lines and analysed PI distribution patterns throughout development. Transgenic zebrafish larvae from early stages were fixed and sectioned through the entire retina.

At 3 dpf, there was no clear distribution pattern for any of the three PIs (Figure 8A-A', C-C', E-E'). At 5 dpf, the PH-PLC sensor appeared in the outer segment, cell membrane and in the synaptic layers predominantly. At the same stage, the PH-TAPP1 revealed puncta in photoreceptor cells (Figure 8D'). These puncta followed a "one punctum per cell" pattern.

This suggested that $PI(3,4)P_2$ puncta correlate with the location of connecting cilia. To test that, further analysis was carried out on Tg(*hsp70*:PH-TAPP1-mcherry) transgenic embryos (Figure 9). Acetylated tubulin was used as a marker to label the connecting cilium. Upon closer inspection, the PH-TAPP1 puncta were observed as early as 3 dpf and most of them localized at the apical surface of the cell. Later, at 5 dpf, some PH-TAPP1 positive puncta seemed to localize around the connecting cilium. In other cells, however, these puncta were observed in other areas of the cytoplasm. Thus, it remains unclear which structure is visualized by the PH-TAPP1 sensor.

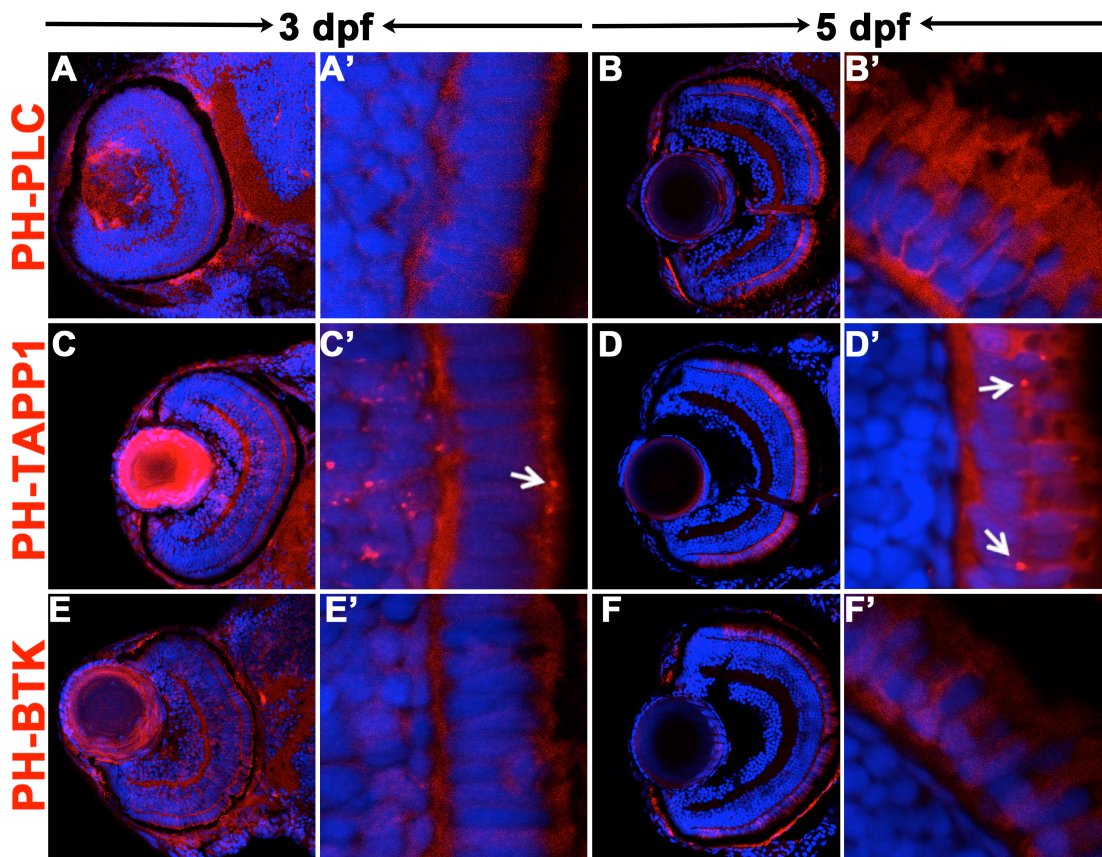


Figure 8. PI distribution studies in zebrafish photoreceptors.

Confocal images of retina sections of *Tg(hsp70:PH-PLC-mCherry)*, *Tg(hsp70:PH-TAPP1-mCherry)* and *Tg(hsp70:PH-BTK-mCherry)* transgenic larvae at 3 and 5 dpf.

(A-B') PH-PLC revealed that $PI(4,5)P_2$ is present at the cell membrane at 3 dpf. It also accumulates in the synaptic layer, the cell membrane and the outer segment at 5 dpf. (C-D') PH-TAPP1 revealed puncta (white arrows) at the apical ends of photoreceptor cells at 3 dpf (C-C') and "one punctum per cell" pattern at 5 dpf (D-D'). (E-F') PH-BTK expression did not reveal any specific distribution pattern of $PI(3,4,5)P_3$ at both 3 (E-E') and 5 (F-F') dpf. Nuclei are counterstained with DAPI (blue).

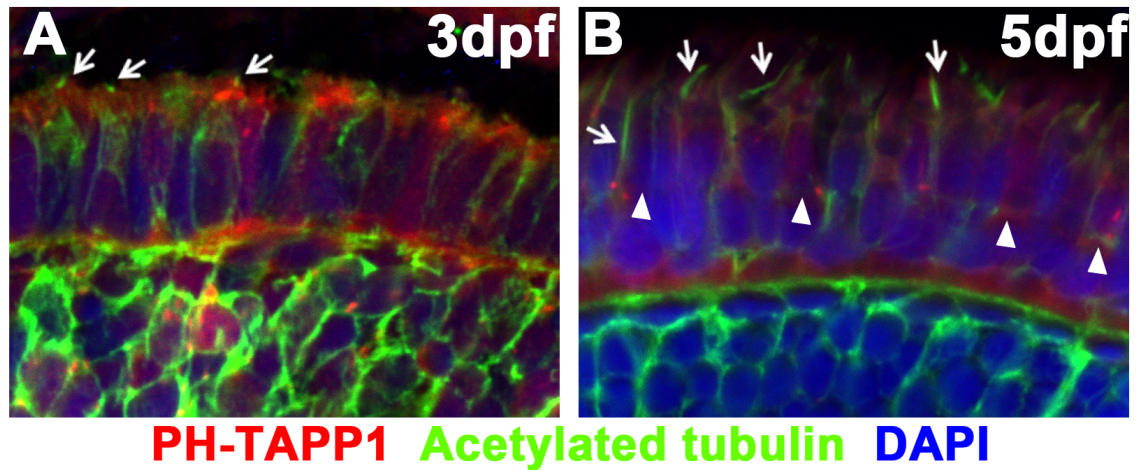


Figure 9. Confocal images of a cryosection through the retina of *Tg(hsp70:PH-TAPP1-mCherry)* transgenic line. Acetylated tubulin staining was applied to mark the connecting cilia. Nuclei were counterstained with DAPI. PH-TAPP1-labelled puncta were observed at both 3 (A) and 5dpf (B) and most localise near to the outer limiting membrane (white arrowhead).

2.2.2.2 Analysis of PIs distribution in primary cilia

I hypothesized that ciliary PI content varies during cell differentiation and in different developmental states. To test this, I applied PH-AKT and PH-PLC sensors in transgenic zebrafish lines and compared PI composition in cilia from different tissues (Table 2 and Table 3). Through live imaging of embryos at 1, 2 and 3 dpf, I observed that PI(4,5)P₂ and PI(3,4,5)P₃ localise to cilia in some muscle and epithelial cells with variable frequency (Figure 10). Examples of cilia colocalized, semi-colocalized with sensor signal was shown in Figure 11.

Epithelial and muscle cells were analysed first as their morphologies are relatively easy to recognize. Over a hundred cells were analysed from both PH-AKT and PH-PLC transgenic lines. 32% of primary cilia from muscle cells displayed PH-PLC sensor signal (19 out of 59 cilia analysed). Apart from that, 9 cilia showed semi-colocalization with PH-PLC sensor signal. In contrast, epithelial cell cilia did not contain PH-PLC frequently. Only 2 out of the 79

cilia (3%) analysed displayed with PH-PLC signal. In parallel, I used PH-AKT sensor, which labels both PI(3,4)P₂ and PI(3,4,5)P₃. Thirteen cilia were found displaying PH-AKT signal out of 157 that were analysed. Thus, although colocalization was detectable, the majority of primary cilia were not PI(3,4)P₂ or PI(3,4,5)P₃ enriched in epithelial or muscle cells in zebrafish embryos based on PH-AKT sensor assays. However, PH-PLC is detectable in over 50% of cilia, which speaks to a potential importance of PI signalling in cilia of muscle cells.

Table2: PH-AKT sensor assays

	Epithelial cells		Muscle cells	
	colocalized	semi-colocalized	colocalized	semi-colocalized
1 dpf	3/27 (11%)	1/27 (4%)	3/16 (19%)	3/16 (19%)
2 dpf	0/43 (0%)	2/43 (5%)	1/31 (3%)	1/31 (3%)
3 dpf	6/36 (17%)	3/36 (8%)	0/4 (0%)	2/4 (50%)
Total	9/106 (8%)	6/106 (6%)	4/51 (8%)	6/51 (18%)

Table3: PH-PLC sensor assays

	Epithelial cells		Muscle cells	
	colocalized	semi-colocalized	colocalized	semi-colocalized
1 dpf	1/29 (3%)	4/29 (14%)	4/24 (17%)	4/24 (17%)
2 dpf	1/50 (2%)	8/50 (16%)	15/35 (43%)	5/35 (14%)
Total	2/79 (3%)	12/79 (15%)	19/59 (32%)	9/59 (15%)

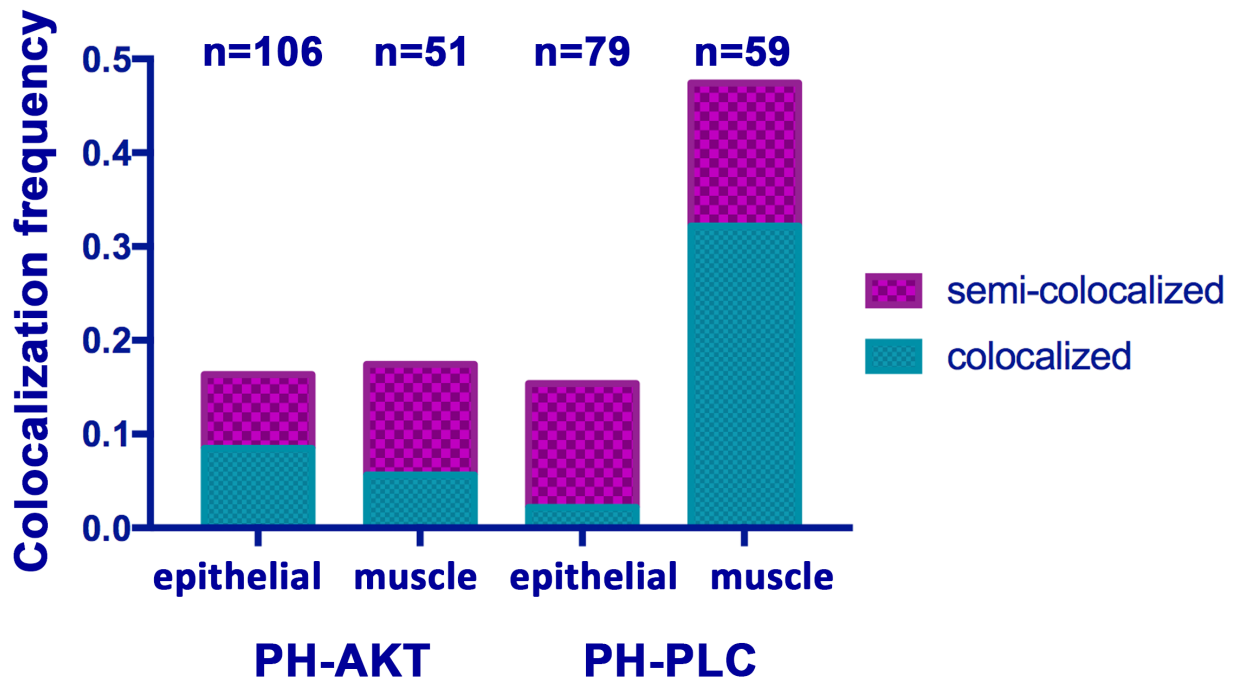


Figure 10. Quantification of the colocalization between sensor signal and cilia in epithelial and muscle cells.

PI(4,5)P₂ was most enriched in the primary cilium of muscle cells. 32% of cilia analysed showed colocalization with PH-PLC signal. 15% primary cilia were found to have weaker PH-PLC signal or signal only at the base or tip of the cilium. However, the same sensor labelled much fewer cilia from epithelial cells: 2% of cilia display convincing colocalization and 13% possible colocalization. PH-AKT displayed 8% colocalization and 12% semi-colocalization in muscle cells, 8% colocalization and 7% semi-colocalization in epithelial cells. Colocalization frequency is shown in green and semi-colocalized frequency is shown in purple, n=cell number.

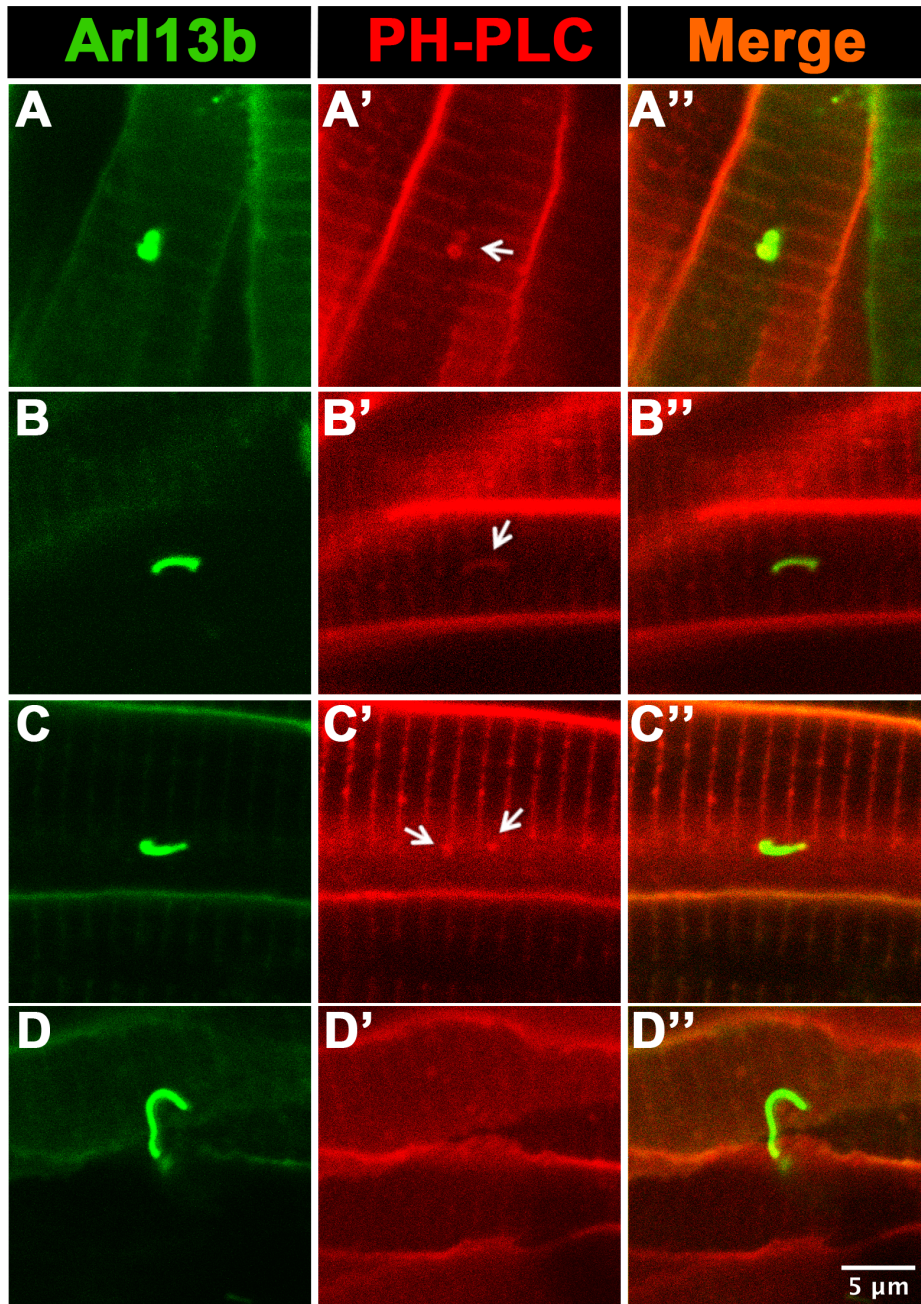


Figure 11. Examples of colocalization, semi-colocalization and no colocalization for PH-PLC sensor and the cilia signal.

Confocal images of zebrafish muscle cells. 2 dpf embryos generated by *Tg(hsp70: PH-PLC-mCherry)* outcrossing with *Tg(βact:Arl13b-EGFP)* line were analysed 5 hours after heatshock. (A-B'') Convincing colocalization, primary cilia shape can be observed in PH-PLC sensor channel (red signal). (C-C'') Semi-colocalization and (D-D'') no colocalization examples. White arrow indicates PH-PLC sensor signal. Scale bar: 5 μm

Table 4: Summary of PI sensors location

One line was analysed for each PH sensor. All lines segregated in a mendelian fashion as described previously.

Transgenic lines	PI specificity	Analysis results
PH-PLC	PI(4,5)P ₂	<p>a. Labelled plasma membrane and actin-rich stereocilia.</p> <p>b. Localized at the synapse layer, the cell membrane and the outer segment in photoreceptor cells.</p> <p>c. Poorly labelled cilia from skin cells (about 2% colocalization frequency)</p> <p>d. More frequently labelled the primary cilia in muscle cells (about 32% colocalization frequency)</p>
PH-PLC ^{K30L} , K32L, R40L	no binding affinity	No enrichment
PH-TAPP1	PI(3,4)P ₂	<p>a. Poorly labelled cilia</p> <p>b. Formed puncta in the photoreceptor cytoplasm.</p>
PH-AKT	PI(3,4)P ₂ and PI(3,4,5)P ₃	<p>a. As expected labelled the basolateral membrane in the epithelium cells from the otic vesicles.</p> <p>b. Around 8% primary cilia were PH-AKT enriched in skin and muscle cells.</p>
PH-BTK	PI(3,4,5)P ₃	<p>a. Poorly labelled cilia</p> <p>b. No certain distribution pattern was observed</p>

2.3 Discussion

2.3.1 Can PH-sensors function as detectors of PIs in the ciliary membrane?

The PH domain based PI sensors have been used for decades and their specificities are well characterized. The feasibility of using PH sensors in zebrafish has been demonstrated in study of neutrophils (Deng et al., 2011).

Since PH domains are around 150 amino acids, PI sensors overall are small. The PH domains used in AKT, PLC delta, TAPP1 and Btk sensors are 157, 175, 123 and 170 amino acids respectively. Fusions with mCherry yield sensors that are less than 420 amino acids in length. Previous studies have shown that Protein A (430 aa) is able to diffuse into cilia (Kee et al., 2012). I thus anticipate that all sensor proteins will freely diffuse in and out of cilia. Regardless of their ability to enter cilia, they allow us to monitor PI content in periciliary vesicles and cell membranes. In fact, sensor-positive cilia were largely seen using the PH-PLC sensor, which is the largest of all the sensors. Consequently, sensor size should not limit PI detection in cilia.

In future experiments, I would like to investigate PH-PLC and PH-BTK sensor localization in the *inpp5e*^{-/-} mutant (see Chapter 4). INPP5E is thought to dephosphorylates PI(4,5)P₂ and/or PI(3,4,5)P₃. Through these experiments, I may be able to distinguish the ciliary substrates of INPP5E, which could vary during development and in different cell types.

2.3.2 Will the sensor overexpression cause phenotypes?

One concern when applying PH sensors in zebrafish is that the constant interaction between sensors and PIs may affect PI-regulated pathways

through competitive binding. The *hsp70* promoter was used to temporally limit the expression level of the sensors. The heatshock time was adjusted so that the shortest possible duration was used to keep sensor levels at their lowest informative levels. No obvious phenotype has been observed from embryos with sensor expression after heatshock treatment. Those embryos went on to reach adulthood with no phenotypical defects. This indicates that heatshock induced PH sensor expression allows us to study the PI distribution, *in vivo*, without adverse side effects.

2.3.3 PIs in the photoreceptor

I applied PH sensors to look at photoreceptor cells that contain specialized cilium known as the outer segment. Sensor expression was induced at 4 dpf and analysed at 5 dpf. PH-PLC sensor localized to the outer segment, the synapse layer and the cell membrane. This finding is in agreement with the zebrafish data from Brockerhoff *et al.* using the same approach (Brockerhoff, 2011). Rajala *et al.* (Rajala *et al.*, 2014) also showed the high abundance of PI(4,5)P₂ in the outer segment in mouse photoreceptors through antibody staining against PI(4,5)P₂. Moreover, PI 5-phosphatase INPP5E localizes to the photoreceptor inner segment in mice (Bielas *et al.*, 2009), which is in agreement with the low PI(4,5)P₂ abundance in the cell body. Overall, different strategies were applied in zebrafish and mice with the similar results indicating that PI(4,5)P₂ localizes to the outer segment.

I tried to investigate the correlation between PH-TAPP1 labelled puncta and the connecting cilia. The data revealed a one-punctum-one-cell pattern, however, further analysis needs to be done. It will be interesting to identify exactly what the puncta are. There was no clear membrane enrichment of PH-BTK indicating that PI(3,4,5)P₃, if present in cilia at all, is present at low levels and may be transient. It may appear at a higher level in developmental stages that were not investigated thus far. There was no clear trend for

PI(3,4)P₂ and PI(3,4,5)P₃ localization in the otic vesicle.

2.3.4 Why are the colocalization rates of cilia and PH-sensor low?

The data presented here demonstrate that the PH-sensors are able to detect PIs in the membrane of cilia. However, the colocalization rates of different PH sensors with cilia are relatively low. One reason for this could be that the bi-phosphate or tri-phosphate that I looked at is not the main ciliary membrane PIs. An exception is the PH-PLC sensor, which detects signal in 32% of cilia of muscle cells.

While my experiments were in progress, the PI composition of the ciliary membrane was described by papers from Schiffmann's (Chávez et al., 2015) and Reiter's groups (Garcia-Gonzalo et al., 2015). Both visualized PI(4)P in the ciliary membrane using antibody staining or PI biosensor (EGFP-2xP4M) in cultured mammalian cells. In addition, Reiter's group revealed PI(4,5)P₂ at the proximal end of cilia using PHPLC-EYFP sensor. I did not test PI(4)P in the ciliary membrane so this discussion will focus on the PI(4,5)P₂ results. Both my results and published data revealed the existence of PI(4,5)P₂ in the ciliary membrane. However, PI(4,5)P₂ localizes in around 30% according to my *in vivo* data (Figure 10). There were no comments in the paper about the frequency of PI(4,5)P₂ - the ciliary membrane colocalization so I assume that the rule is generally applied to all primary cilia at least.

Why were there fewer PI(4,5)P₂ - positive according to my work? First, this can be simply due to cell type differences. NIH3T3 (mouse fibroblasts) and IMCD3 (epithelia cells, polarized) cells are used to perform the PI antibody staining and the PI biosensor imaging after transfection. My work was mainly focused on muscle and epithelium cells due to the large population of the cell number and distinguishable morphology. Second, the ciliary PI composition

could be the developmental stage or cell cycle depended. I examined zebrafish embryos at 2dpf, which is an early developmental stage with massive biological events on going. In general, most of the ciliated cells are in G0 phase of the cell cycle. In cells exiting the cell cycle, cilia need to be resorbed (Plotnikova et al., 2009). Cilia are still present in G1, start to resorb in G2/S phase and are fully resorbed before mitotic entry. In this case, a ciliated cell could be in G0, G1 or G2/S phase. It is possible that PI compositions in the ciliary membrane vary depending on cell cycle stages. In cultured cells, cilia were induced through serum starvation after confluence. After this treatment, the majority of cells were in the G0 phase. Whereas for a 2dpf living zebrafish embryo, which phase a ciliated cell is in is uncertain. Third, ciliary PI compositions may be varying due to species differences. This possibility could be considered as a consequence of the cell type difference. Cultured cells that have been used for experiments mentioned above include NIH3T3, IMCD3, mouse embryos fibroblast or neural stem cells, all of which are derived from mice. It is unlikely that the ciliary PI composition varies between mouse and zebrafish but still can be considered as a possibility.

The transgenic PI biosensor lines that have been generated in this study are effective tools that are able to globally monitor PI composition across developmental stages and cell cycles. These tools are not limited to ciliary membrane. With proper markers, these tools can be applied to intracellular and plasma membranes. In figure 7, for example, I observed that PI(3,4,5)P₃ is absent from the apical surface and enriched at the basolateral plasma membrane in the otic vesicle of PH-AKT transgenic embryos. This finding is in agreement with Gassama-Diagne *et. al's* work indicating that PI(3,4,5)P₃ regulates basolateral surface formation (Gassama-Diagne et al., 2006).

As I do not have the sensor for PI(4)P at this moment, it is difficult to confirm those results in zebrafish. Also, it is possible that the ciliary membrane PI content is highly dynamic. Other PIs may have a transient function, but have

not been detected due to their low abundance. If it is difficult to visualize the PI with low abundance in the ciliary membrane, loss of function phenotype study could be an indirect way to show the existence of low abundance PIs. In the next chapter, I described work that I carried out on ciliary PI function.

2.3.5 How to interpret the PH sensor results in the muscle and skin cells?

I would expect that PI content is differing in different cells. The ciliary PI(4,5)P₂ were higher in the muscle cells than epithelial cells, whereas PI(3,4,5)P₃ level was the same in epithelial and muscle cells. The data supports the idea that the PI content of cilia varies depending on cell type, or varies in response to the cell environment.

2.4 Summary

In this chapter, I established a group of zebrafish transgenic lines that stably expressed PH domain based sensors for PI *in vivo* detection. PI(4,5)P₂ was observed in the ciliary membrane from the muscle cell and occasionally observed in the ciliary membrane from the epithelial cell. PI(3,4,5)P₂ was also found in the ciliary membrane with low frequency. Thus PH sensors function as PI detectors *in vivo* and revealed that PI content in ciliary membrane differs depending on cell types and developmental stages. In the future, these tools can be applied to study phosphatase or kinase mutants as PI monitors.

Chapter 3

Chapter 3

PIs function in the cilium

3.1 Introduction

3.1.1 General strategies for the study of PI function

An effective way to test PI function is loss-of-function studies of PI kinases or phosphatases. For example, knocking-out of *pten* gene results in embryonic development defects in zebrafish (Faucherre et al., 2008). However, this strategy cannot modify PI content in specific tissues or organelles. Alternatively, PI composition can be modified by overexpression of the PI kinases or phosphatases in target subcellular membranes. The ectopically expressed enzyme is usually membrane attached through membrane localization signal such as CAAX (Kurokawa et al., 2012). In a more complex approach, the chemical dimerization strategy relies on the heterodimerization of protein domains from FK506 (FKBP) and mTOR (FRB). This strategy can achieve a quick membrane translocation between FKBP fusion and FRB fusion induced by rapamycin or its analog iRap. For example, PI(4,5)P₂ can be depleted by inducible membrane translocation of Inp54p, a yeast inositol polyphosphate 5-phosphatase that specifically dephosphorylates at 5-position of PI(4,5)P₂. Using this strategy, the function of PI(4,5)P₂ was assessed in ion channels (Suh et al., 2006) and plasma membrane (Hammond et al., 2012).

3.2 Experimental design

3.2.1 Ciliary PIs function study approach

Phenotypes associated with defects in ciliary PI phosphatases (such as

INPP5E and OCRL) and cilia-related PI binding proteins suggest that PI content is essential for cilia function. To test this directly, I manipulated PI content in the ciliary membrane by targeting PI specific phosphatases or kinases into the cilium. As the first step, I focused on PI(3,4,5)P₃ and PI(4,5)P₂ for several reasons. First, they were both detected using our approach in the ciliary membrane, albeit at low frequency. Second, these two PIs are particularly easy to manipulate because they are only metabolized into two other main PIs (Di Paolo and De Camilli, 2006). Their metabolism is catalysed by well-characterized phosphatases or kinases (such as PTEN and PI3K). Finally, these phosphatases and kinases are also clinically relevant.

3.2.2 Functional analysis of the ciliary PI(3,4,5)P₃ and PI(4,5)P₂

For reasons mentioned above, I started by manipulating PI(3,4,5)P₃ and PI(4,5)P₂ content. To deplete PI(3,4,5)P₃, I targeted the PI(3,4,5)P₃ 3-phosphatase PTEN, which dephosphorylates positions 3, to the cilium. To deplete PI(4,5)P₂, 4,5-biphosphate 5-phosphatase Inp54p and 4,5-biphosphate 3-kinase PI3K were applied.

To target them to cilia, I fused catalytic domains of PTEN, Inp54p and PI3K to Arl13b, which efficiently targets GFP to cilia and its overexpression does not affect zebrafish viability or ciliogenesis (Duldulao et al., 2009). In addition, Arl13b has been used to target calcium sensors to cilia (Delling et al., 2016). To monitor the level of expression and localization of these fusion polypeptides *in vivo*, I also attached Arl13b to GFP (Figure 12). Arl13b tagged at its C-terminus with EGFP has been extensively used, and both C- and N-terminal PTEN fusions are functional (Furnari et al., 1998) (Liu et al., 2005). I anticipated that such fusion proteins would change membrane PI content. I followed the same approach for PI3K and Inp54p. As ciliary targeting of

those enzymes would cause PI composition change and consequently induce ciliary phenotypes, I called those enzymes effectors.

PI3K and PTEN are closely relevant to tumorigenesis and cancer in human (Okkenhaug, 2013; Worby and Dixon, 2014). Using ubiquitous promoter to express Arl13b-EGFP-Enzyme fusions in stable transgenic lines could result in strong embryonic phenotypes. To prevent this from happening, I used a heatshock promoter to drive expression of transgenes in stable lines. As time passes by, expressed fusion proteins may be degraded. A disadvantage of this method is that it provides only transient expression, which means only a limited amounts of enzymes are expressed at a certain time. This can be overcome by applying multiple heatshocks or applying longer heatshocks.

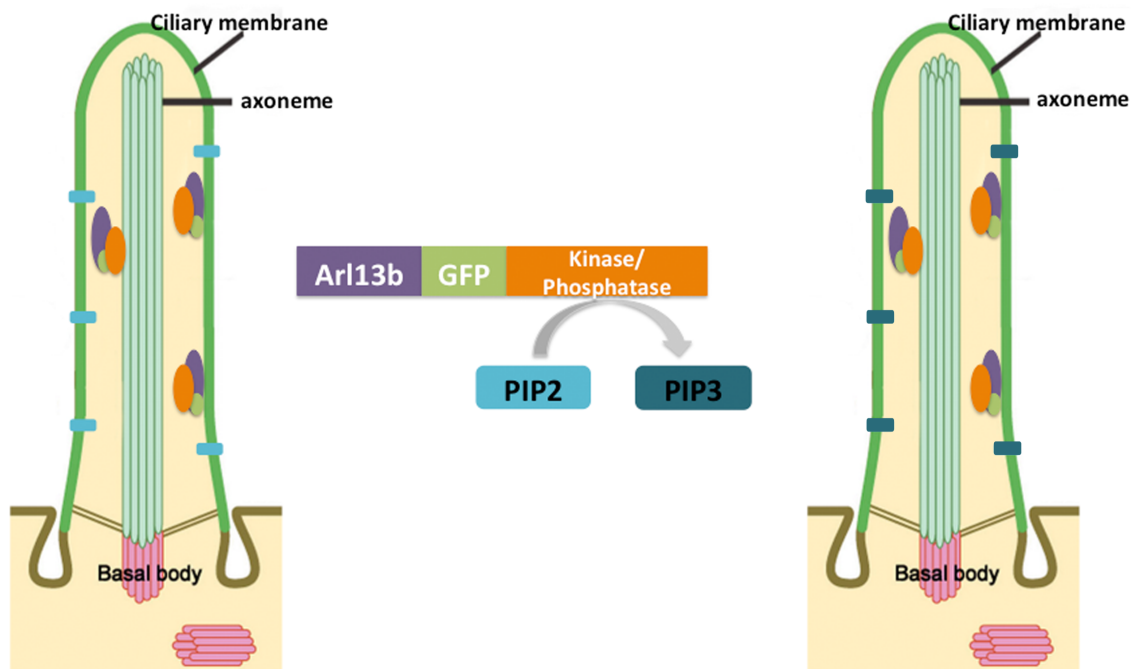


Figure 12. Schematic of the effector strategy.

PI phosphatases or kinases were targeted to cilia through Arl13b, a ciliary protein. To visualize their localization, EGFP was also attached to the fusion protein. After targeting, the PI composition of the ciliary membrane was changed due to the catalytic activity of a kinase or a phosphatase.

3.3 Results

3.3.1 Transient expression of effectors

As the first step, I transiently expressed effectors and their inactive control constructs in zebrafish embryos through DNA microinjection. Constructs were expressed after heatshock induction. The GFP signal could be observed through fluorescent microscopy as early as 2 hours after heatshock. To improve signal-to-noise ratio, embryos were analysed 4 hours after heatshock using confocal microscopy. Following heatshock, I observed cilia labelling with Arl13b-EGFP-enzyme fusion in multiple organs and various cell types, such as olfactory sensory neurons, hair cells, and muscle (Figure 13). Cytoplasmic expression was present in some cells with different brightness. I thought this might be due to the inconsistent DNA amount, which differs from cell to cell following DNA construct injections into embryos.

3.3.2 Effector expression in stable transgenic lines

The focus of my interest was PI function in cilia, which exist on most vertebrate cells. Transient expression could not satisfy the need for phenotypic study of zebrafish development or global cilia dysfunction. To this end, I made stable transgenic lines, which ubiquitously express Arl13b fused to a kinase or phosphatase effector driven by a heatshock promoter. As above, EGFP was inserted to monitor expression and localization.

After the final cloning step of the destination constructs, microinjection was carried out in AB wild-type zebrafish background. GFP positive embryos were raised to adulthood. Multiple G0 founders were identified by out crossing. Specifically, G0 individuals were out crossed with wild-type fish and the progeny was checked for GFP fluorescence. Owing to the *cm1c2*:EGFP cassette from the Tol2 vector backbone (destination vector) that I used in my

experiments, the green heart was used as a indicator for successful insertion of the transgene.

Positive F1 embryos were raised to adulthood. As a general issue of the transgenic expression, different insertions would give different expression patterns depending on their location in the genome. To validate our transgenic lines and demonstrate their utility in studying cilia, I analysed GFP expression in these lines using confocal microscopy. Lines used in these experiments are listed in Table 5. Representative images are shown from the otic vesicle, the midbrain-hindbrain boundary, the trunk and the spinal cord (Figure 14).

Table 5 Transgenic lines that has been analysed

NAME	SPECIFICITY	TRANSIENT ¹	Number of MENDELIAN LINES
PTENa	(3,4,5)>(4,5)	YES	Stable but non-mendelian
PTENa ^{C124GG129E}	Inactive mutation	YES	1
Inp54p	(4,5)>(4)	YES	2
Inp54p ^{D281A}	Inactive mutation	YES	1
PI3K	(4,5)>(3,4,5)	YES	2
PI3K ^{K802R}	Inactive mutation	YES	1

¹ Transient expression;

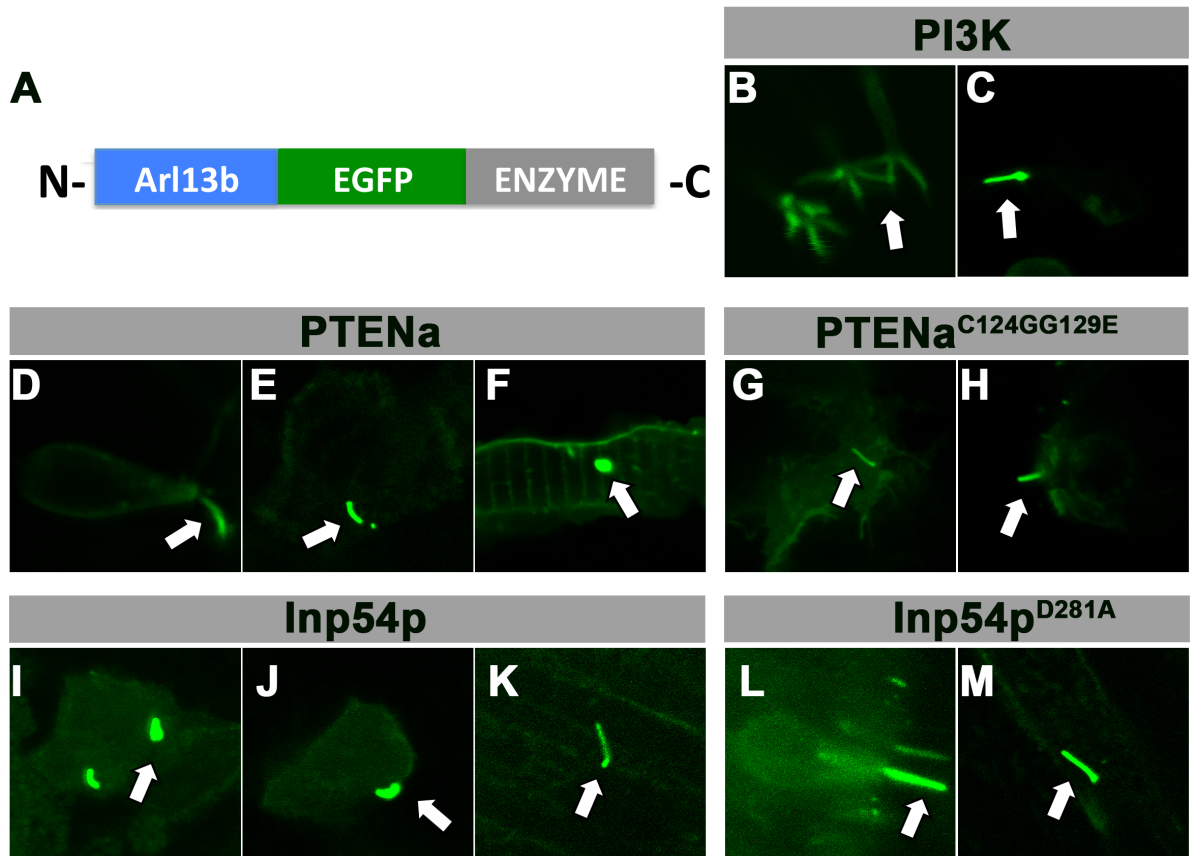


Figure 13. Transient expression of the effector constructs in zebrafish embryos.

(A) Schematic representation of the effector construct. (B-M) Confocal images of Arl13b-EGFP-enzyme effector expression induced by heatshock. Cilia were labelled in various types of cells. (B-C) Arl13b-EGFP-PI3K expressed in cilia of olfactory sensory neurons (B) and a hair cell (C). (D-F) Arl13b-EGFP-PTENa expressed in the cilium of an olfactory sensory cell (D), a skin epithelium cell (E) and a muscle cell (F). (G-H) Arl13b-EGFP-PTENa^{C124GG129E}, the inactive control for PTENa, expressed in the cilium of a skin epithelium cell (G) and a hair cell (H). (I-K) Arl13b-EGFP-Inp54p expressed in the cilium of a skin epithelium cell (Han et al.) and a muscle cell (K). (L-M) Inp54p^{D281A}, the inactive control for Inp54p, expressed in the cilium of a hair cell (L) and a skin epithelium cell (M).

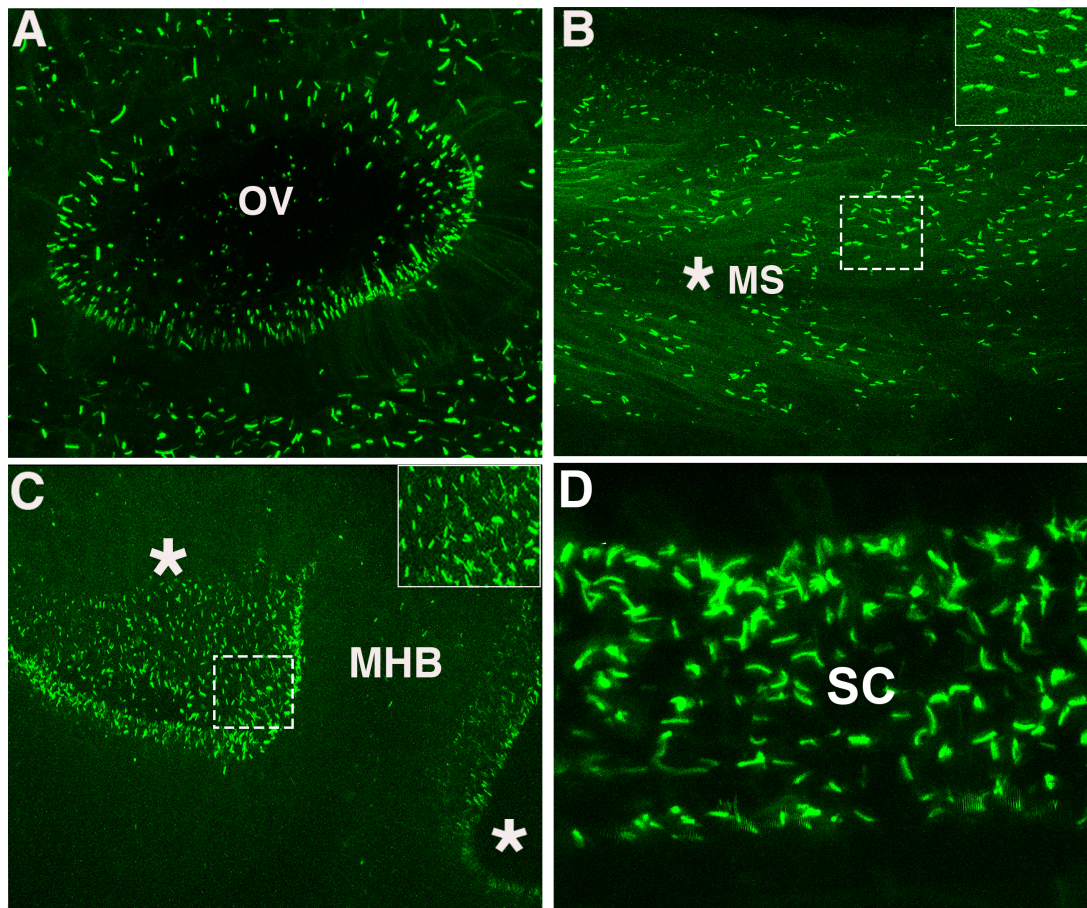


Figure 14. Examples of cilia expression from different organs of living zebrafish embryos.

Confocal images of *Tg(hsp70:Arl13b-EGFP-Ptena)* and *Tg(hsp70:Arl13b-EGFP-Inp54p^{D281A})* transgenic embryos at 30 hpf. (A) Image of cilia from the otic vesicle and surrounding tissues. (B) The same transgene labelled cilia in muscle cells. The myoseptum (MS) is indicated by a asterisk. Inset displays cilia in muscle fibers at higher magnification. (C) Brain ventricle cilia were visualized using the same line. Asterisks indicate the midbrain and hindbrain ventricle at higher magnification. Inset displays cilia from the midbrain ventricle. (D) Cilia from the spinal cord in the same line (higher magnification). OV, otic vesicle. MHB, midbrain-hindbrain boundary.

3.3.3 Phenotypic analysis of effector lines

3.3.3.1 Depletion of PI(4,5)P₂ by Inp54p overexpression

To study the role of PI(4,5)P₂ at the ciliary membrane, as the first step, I overexpressed Inp54p, a yeast 5-phosphatase that hydrolyses PI(4,5)P₂ at 5 position of the inositol ring and generates PI(4)P (Wiradjaja et al., 2001). To monitor the level of expression and localization of the fusion polypeptide *in vivo*, GFP was used as a marker (Figure 13 A). Kinase and phosphatase fusions were overexpressed using a heatshock promoter in stable transgenic lines.

I first induced expression at 26 hours post fertilization (hpf) and analysed the embryos at 30-32 hpf. At those stages, ciliated organs have relatively simple morphology and cells are easy to image.

3.3.3.1.1 Cilia length and morphology defects

I first looked at the otic vesicle and the spinal canal. At 32 hpf, cilia of epithelial cells project into the ear lumen and become elongated. Inp54p ciliary overexpression resulted in a longer cilia phenotype in the early otic vesicle (Fig 15 A-A'). Cilia length was measured on a single plane image through the center of the otic vesicle (Figure 15 C). Compared to the Inp54p^{D281A} inactive control transgenics, the average cilia length significantly increased, which indicated that PI(4,5)P₂ plays a role in cilia elongation.

After Inp54p overexpression, longer cilia were similarly observed in the spinal canal of the same stage embryos. However, length quantification was not carried out due to the irregular shape of cilia from the spinal canal. In addition, bulges were frequently observed on cilia tips or occasionally on the ciliary shaft (Figure 15 B-B'). The bulge frequency was measured in both Inp54p and control group. A significant difference was observed (Figure 15 D).

Due to irregular orientation of spinal canal cilia, cilia viewed along their axis could be mistaken as bulges. To further analyse cilia morphology, scanning electron microscopy (SEM) analysis was carried out. Zebrafish embryos were heatshocked at 26 hpf for 30min. Fluorescent embryos were selected and fixed at 32 hpf.

The depletion of PI(4,5)P₂ caused by Inp54p overexpression resulted in bulge formation at cilia tips (Figure 16 B-B') of the skin epithelial cells. In contrast, regular cilia morphology was observed in zebrafish embryos overexpressing Inp54p^{D281A} (Figure 16 A-A'). Results of SEM from the epithelial skin cilia were consistent with findings from confocal imaging of spinal canal cilia (Figure 15 B-B').

3.3.3.1.2 Analysis of the ciliary microtubules

What is the nature of these bulges? To further understand the cilia morphology change, I applied acetylated-tubulin antibody staining on Inp54p and Inp54p^{D281A} overexpression background respectively. Transgenic zebrafish embryos from outcross of transgenic lines were heatshocked at 26 hpf and selected for fluorescence at 32 hpf. Fixation and whole mount staining followed. Cilia morphology was analysed using confocal microscopy.

No obvious microtubule defect in the distribution of acetylated tubulin was observed in cilia of transgenic animals. Staining appeared normal in both Inp54p and control group (Figure 17 A-C''). Ciliary bulges were labelled by EGFP from the transgene rather than the anti-acetylated tubulin antibody. The same results were obtained from skin epithelium cells (Figure 17 B-B'') and hair cells (Figure 17 C-C''). Based on these findings, the morphology defect appears to result from the accumulation of membranes or IFT cargo proteins rather than ciliary axoneme defect.

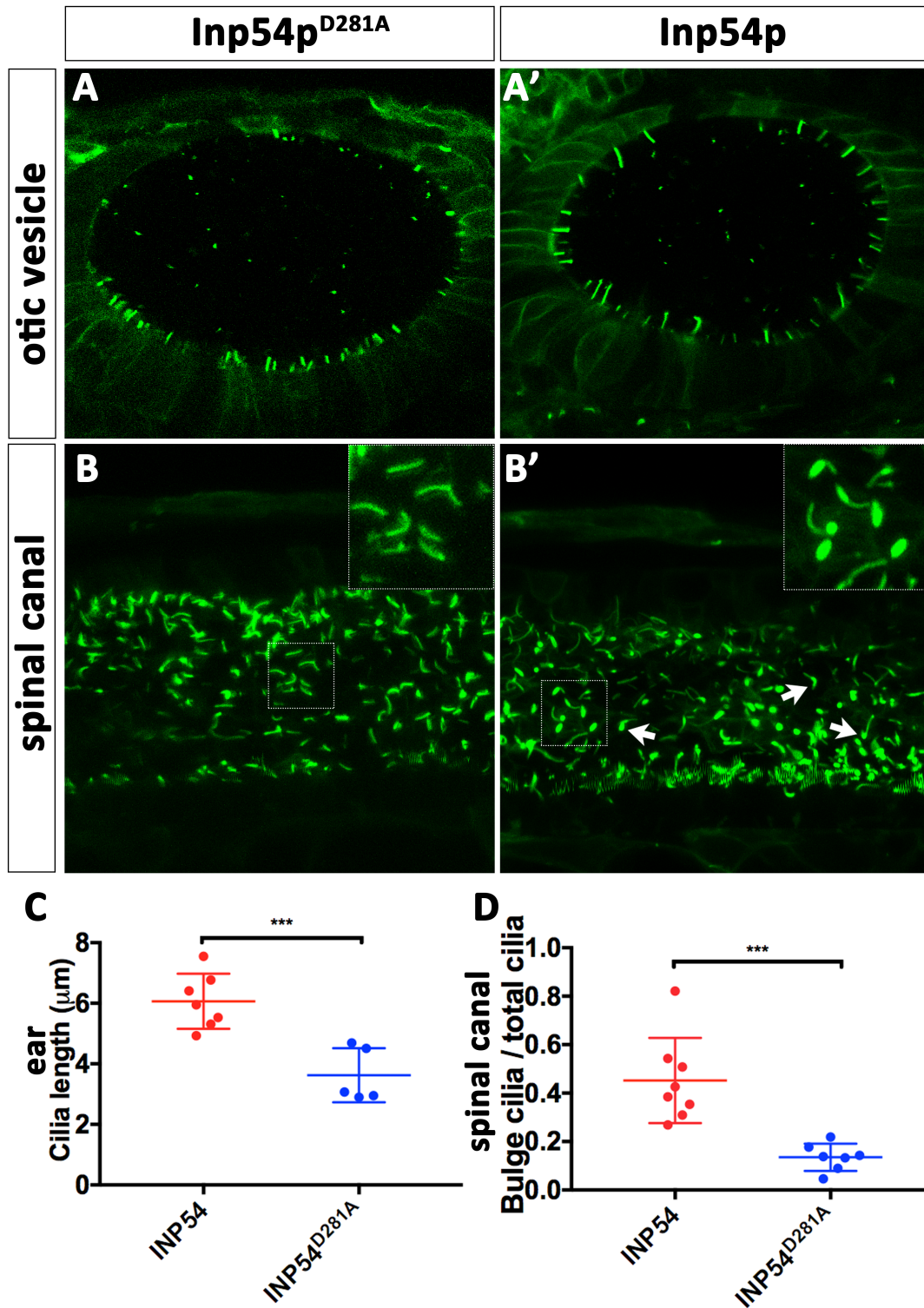


Figure 15. Depletion of PI(4,5)P₂ in cilia affects their length and morphology.

(A - B') Confocal images of the otic vesicle (A - A'') and the spinal canal (B - B'') of zebrafish embryos at 32 hpf (5 hours after heat shock). Shown are Tg(hsp70: Arl13b-EGFP-Inp54p^{D281A}) inactive enzyme control line (A and B)

and *Tg(hsp70: Arl13b-EGFP-Inp54p)* (A' and B'). The depletion of $PI(4,5)P_2$ in cilia results in their elongation, compared to the control (A, A'). Bulges frequently form on spinal canal cilia in *Inp54p* overexpressing animals (B, B'). Insets show higher magnification of boxed areas.

(C) Quantification of cilia length in the otic vesicle of two transgenic lines. $P < 0.001$ in unpaired *t* test. (D) Quantification of cilia morphology defects (bulges) in the spinal canal as the percentage of total number of cilia. $P < 0.0005$ in unpaired *t* test. In (C, D), means and SD are shown.

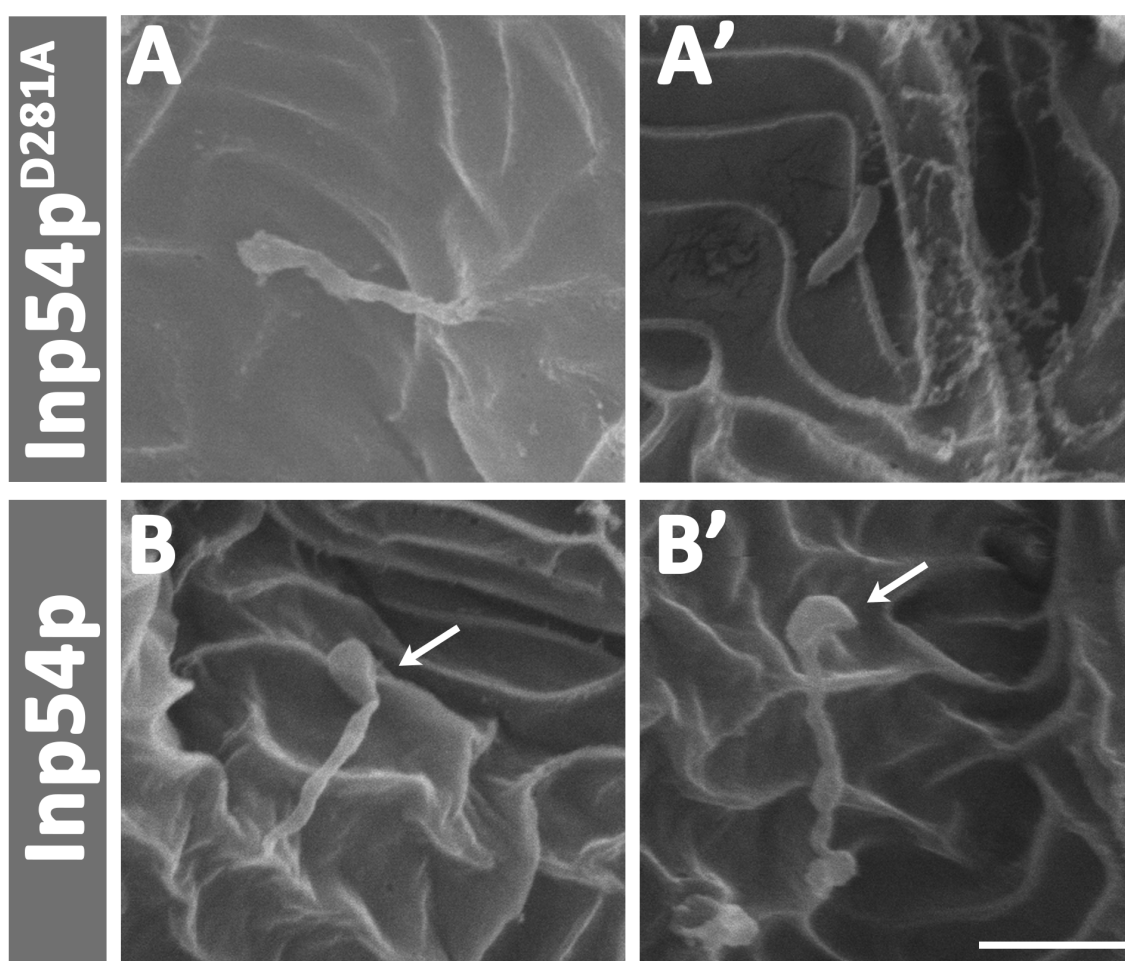


Figure 16. Bulges form on cilia tips after *Inp54p* overexpression

Representative images of cilia from skin epithelium cells of *Tg(hsp70:Arl13b-EGFP-Inp54p^{D281A})* embryo (A-A') and *Tg(hsp70:Arl13b-EGFP-Inp54p)* embryo (B-B'). The depletion of $PI(4,5)P_2$ caused by *Inp54p* overexpression resulted in bulge formation at tips of cilia. Arrow indicates a bulge at cilium tip. Scale bar: 2 μ m.

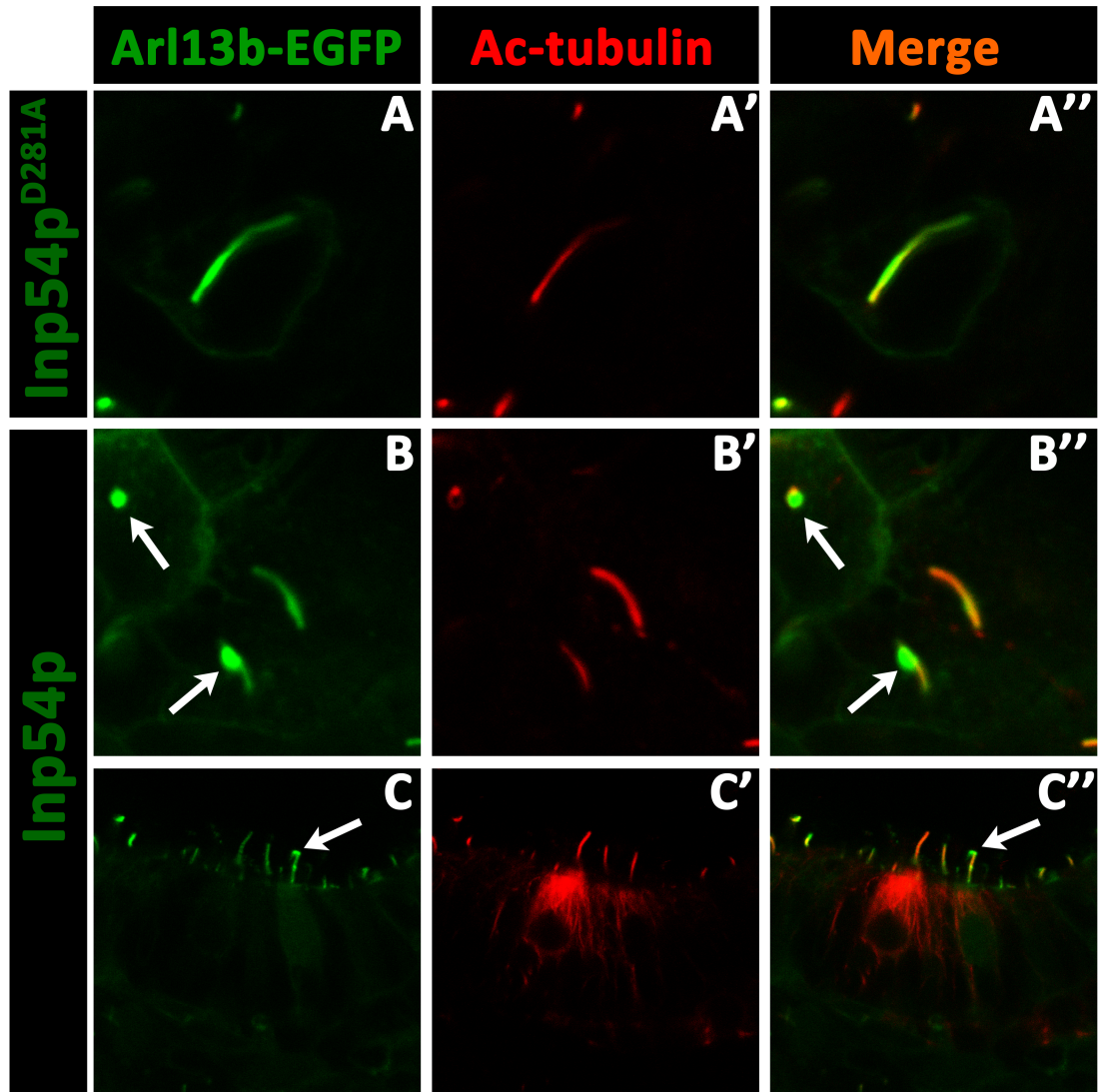


Figure 17. Ciliary bulges does not contain microtubules.

Representative confocal images from antibody staining for acetylated tubulin in *Tg(hsp70:Arl13b-EGFP-Inp54p^{D281A})* (A-A'') and *Tg(hsp70:Arl13b-EGFP-Inp54p)* (B-C'') transgenic zebrafish embryos. *Inp54p* and *Inp54p^{D281A}* GFP fusions are shown in green and acetylated tubulin is shown in red. EGFP labelled bulges (white arrow) were found in *Inp54p* transgenic background but not the control group.

3.3.3.2 Depletion of ciliary PI(4,5)P₂ by PI3K overexpression

Phosphoinositide 3-kinase is a lipid kinase capable of phosphorylating PIs at the 3-position of the inositol ring (Stephens et al., 1993). There are eight catalytic PI3K subunits expressed in vertebrates. They are divided into three classes (class I, class II and class III) based on sequence alignment and domain structures (Vanhaesebroeck et al., 2010). Class I PI3Ks, which are best understood, include p110 α (PIK3CA), p110 β (PIK3CB), p110 γ (PIK3CG) and p110 δ (PIK3CD). Class I PI3Ks use PI(4,5)P₂ as their substrate.

To study the role of PI(4,5)P₂ in the ciliary membrane, as the second step, I induced ciliary overexpression of the catalytic subunit of p110 α . Similar to Inp54p, PI3K was fused to Arl13b-EGFP and heatshock promoter was used to drive transgenic expression. P110 α ^{K802R} (referred to as PI3K^{K802R} in this thesis), which contains a single amino acid substitution that abolishes its catalytic activity, was used as control for p110 α (referred to as PI3K). Stable transgenic lines were made for functional analysis.

I induced transgene expression at 26 hpf by heatshocking and analysed embryos at 30-32 hpf. At 32 hpf, the overexpression of PI3K, which phosphorylated PI(4,5)P₂ to PI(3,4,5)P₃, caused the disappearance or disorganization of cilia from the spinal canal (Figure 18 C-D). Cilia number and length were measured (Figure 18 E-F). As a result, hydrocephalus phenotype was visible at 48 hpf (Figure 18 A-B') and became much more obvious at later stages. No obvious difference was observed in the cilia appearance in the otic vesicle (Figure 18 F-G).

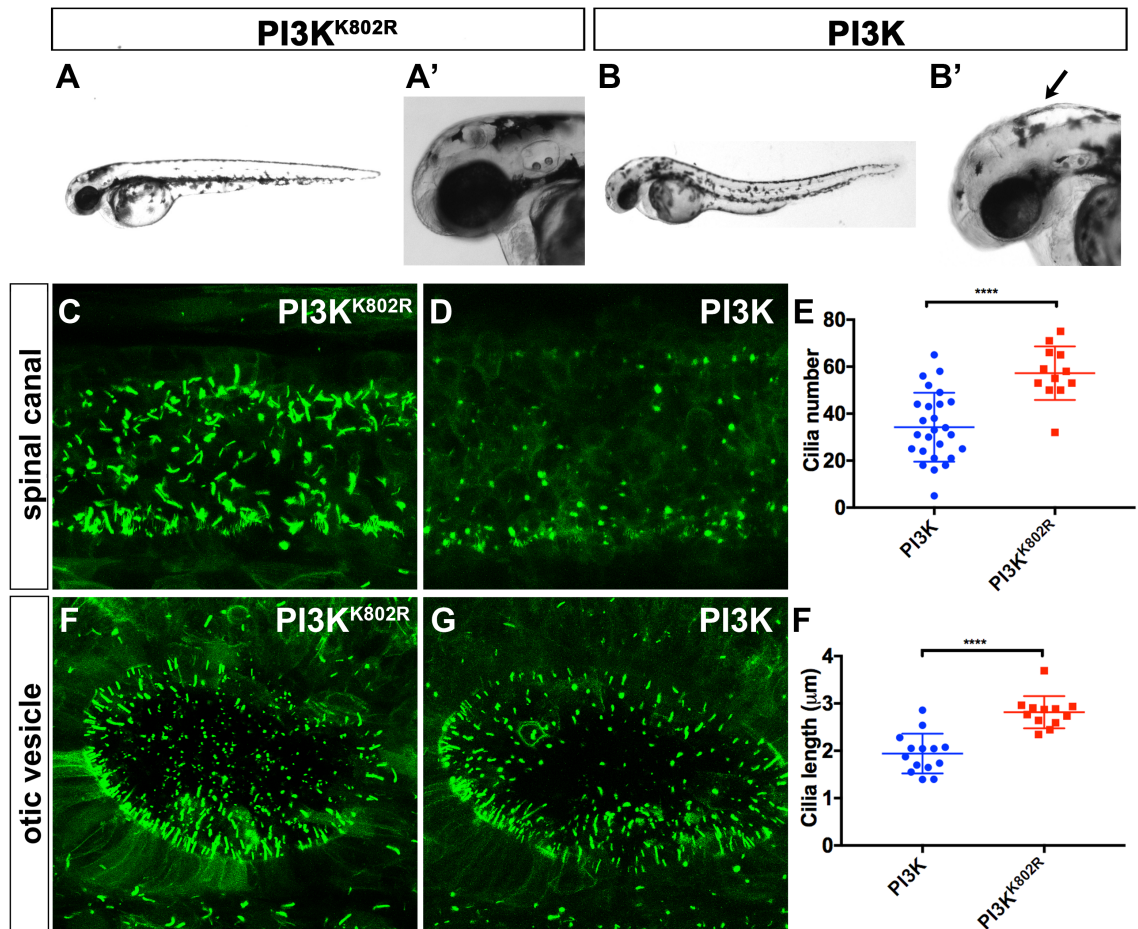


Figure 18. The overexpression of PI3K results in disassembly of spinal canal cilia.

(A-B') Lateral view of embryos expressing a *Tg(hsp70:Ar113b-EGFP-PI3K^{K802R})* inactive enzyme control transgene (A, A') and *Tg(hsp70:Ar113b-EGFP-PI3K)* transgene (B, B') at 54 hpf, 28 hours after heatshock induced expression. PI3K embryo displays upwardly curled tail phenotype and hydrocephalus (black arrow).

(C-G) Confocal images of the spinal canal (C, D) and the otic vesicle (F, G) in 32 hpf embryos. Heatshock was applied at 26 hpf. The spinal canal cilia disassemble after PI3K overexpression (D), however, no obvious cilia defect observed in the otic vesicle (G). The cilia number in a defined region was quantified and the results are shown in (E). (F) Measurement of cilia length from the spinal canal. In (E, F), each dot represents one transgenic embryo. $P < 0.0001$ in unpaired *t* test. Means and SD are provided.

3.3.3.3 Depletion of PI(3,4,5)P₃ by PTEN overexpression

PTEN (Phosphatase and TENsin homolog) belongs to the protein-tyrosine phosphatase superfamily and has lipid phosphatase activity (Worby and Dixon, 2014). It is a human tumour suppressor (Worby and Dixon, 2014). Zebrafish genome encodes two *pten* genes, *ptena* and *ptenb*. The products of these two genes specifically dephosphorylate PI(3,4,5)P₃ at the 3-position of the inositol ring (Faucherre et al., 2007).

I tested the ciliary function of PI(3,4,5)P₃ through PTENa overexpression. The overexpression of PTENa dephosphorylates PI(3,4,5)P₃ and generates PI(4,5)P₂. Same as Inp54p and PI3K, PTENa was attached to Arl13b-EGFP protein and heatshock promoter was used to drive its expression. Stable transgenic lines were made for functional analysis.

I expected that PTENa overexpression would give a phenotype opposite to the one observed in PI3K. Interestingly and in contrast to other PIs effectors, overexpression of PTENa did not produce any obvious phenotype. On the contrary, the enzyme dead control PTENa^{C124GG129E} embryos displayed lateral body curvature at 2 dpf (Figure 19 A-B). Typical cilia morphology was not observed on confocal images taken from the otic vesicle and spinal canal of PTENa^{C124GG129E} overexpression embryos (Figure 19 D, F). EGFP accumulation was observed in the cytoplasm of this transgenic line. On the other hand, Tg(*hsp70:Arl13b-EGFP-PTENa*) displayed normal cilia morphology (Figure 19 C, E).

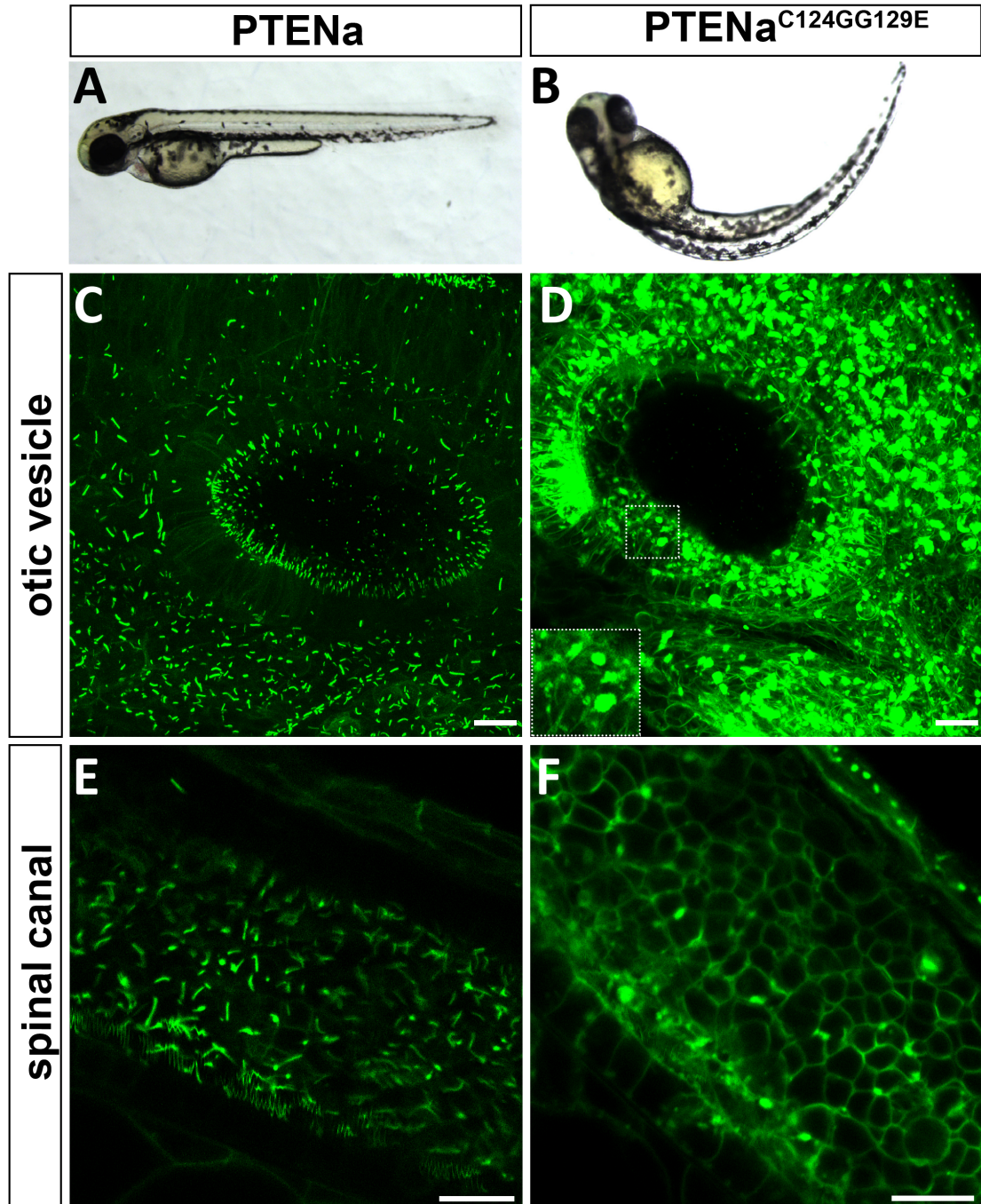


Figure 19. Phenotype of PTENa overexpression in cilia

(A-B) Lateral view of zebrafish embryos from *Tg(hsp70: Arl13b-EGFP-PTENa)* (A) and *Tg(hsp70:Arl13b-EGFP-PTENa^{C124GG129E})* (B) at 48 hpf (22 hours post heat-shock). A lateral body curvature was observed following *Ptena^{C124GG129E}* but not *PTENa* overexpression. (C-F) Confocal images of cilia from the otic vesicle (C-D) and spinal canal (E-F) of 30 hpf embryos (4 hours postheat-shock). Inset shows the box area at a higher magnification. Scale bar 15 μ m.

3.4 Discussion

3.4.1 The use of heatshock promoter

Phosphatase or kinase fusions could be expressed using several approaches. I could use a ubiquitous promoter (such as actin) to express Arl13b-EGFP-enzyme fusions in stable transgenic lines. This, however, could result in strong and potentially lethal embryonic phenotypes. To prevent this from happening, I used a heatshock promoter to drive expression in stable transgenic lines. A disadvantage of this method is that it provides only transient expression, which means that an effector is expressed for a limited time only. As time passes by, the effector protein may be degraded. Multiple heatshocks could be applied to induce stronger and longer expression. The duration and temperature of heatshock could also be varied to adjust the expression to an effective level.

3.4.2 Evaluation of transgenic lines

In transgenic studies, the level of transgene expression is essential. Before phenotypic analysis, transgenes were selected for strength and specificity of expression. Specifically, the percentage of cells expressing the transgene and efficiency of cilia targeting are the two criteria for my transgene selection. Tg(β act:Arl13b-EGFP) line was obtained from Brian Ciruna's lab and used as a reference for selection. Additionally, comparison with cilia specific antibody staining can be applied to evaluate transgenic lines.

3.4.3 Evaluation of enzyme efficiency

How could I evaluate whether the effectors that I applied were sufficient to eliminate given PIs? Changes in PI content will be monitored using sensors (described in Chapter 2) expressed via DNA injections into embryos. This

generates mosaic expression, which makes it easier to visualize sensors in single cells and their cilia. For example, I could use the PI(3,4,5)P₃ specific PH-Btk sensor to monitor the PTENa substrate and dephosphorylation products; PH-TAPP1 for PI(3,4)P₂ and PH-PLC for PI(4,5)P₂. The best but also the most laborious approach is to use a two-transgene system, which provides a temporal control to monitor the ciliary PI composition.

3.4.4 Bulge formation on cilia tips

The depletion of PI(4,5)P₂ by *Inp54p* at 24 hpf did not affect ciliogenesis but it did appear to affect ciliary transport. Since phenotype from *Tg(hsp70:Arl13b-EGFP-Inp54p)* embryos was similar to phenotypes described in IFT-A mutants (Boubakri et al., 2016; Liem et al., 2012), I hypothesized that the bulge formation at cilia tips or in the ciliary shaft may be due to a dysfunction of retrograde transport. One hypothesis is that PI(4,5)P₂ directly or indirectly interacts with the IFT-A complex, which mediates the retrograde transport (Figure 20). As a consequence, PI(4,5)P₂ depletion affects retrograde transport. PI(4,5)P₂ related IFT-A dysfunction may come about in at least two ways: 1. PI(4,5)P₂ could play a role in the assembly of IFT-A and IFT-B complex at the base of cilia. Consequently, the depletion of PI(4,5)P₂ would result in the absence of IFT-A complex from the IFT train; 2. At the cilia tip, PI(4,5)P₂ could work as a signal for the IFT train, to switch from IFT-B kinesin mediated transport mode to IFT-A dynein mode. In this scenario, the absence of PI(4,5)P₂ from the cilia tip would result in retrograde transport defect and IFT train accumulation in cilia tips (Figure 20 C).

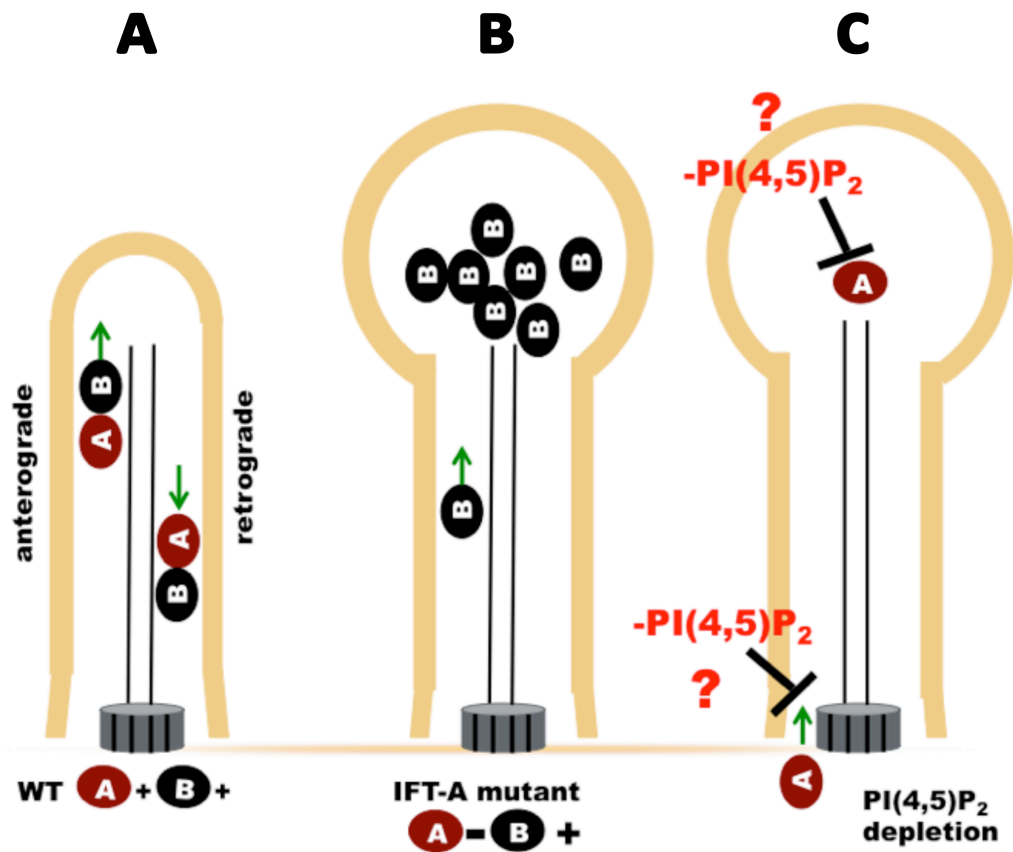


Figure 20. A model of how $PI(4,5)P_2$ affects cilia morphology. (A) In wild-type cilia, anterograde and retrograde transport are carried out by IFT-B and IFT-A complex, respectively. (B) Bulge formation in cilia of IFT-A mutants in mouse and zebrafish has been documented in prior studies (Boubakri et al., 2016; Liem et al., 2012). (C) A hypothetical model demonstrates two possible ways in which the depletion of $PI(4,5)P_2$ could result in bulge formation at the ciliary tip. One possibility is that the depletion of $PI(4,5)P_2$ from the proximal end of cilia prevents IFT-A complex from entering cilia. Second possibility is that the depletion of $PI(4,5)P_2$ results in the failure of IFT train switching to retrograde transport at the tip. Both of these scenarios would result in the accumulation of IFT and IFT cargo proteins at cilia tips and the bulge formation.

3.4.5 The mechanism of cilia disassembly following PI3K overexpression

PI(3,4,5)P₃ regulates the formation of the basolateral plasma membrane in epithelial cells (Gassama-Diagne et al., 2006). In polarized epithelial cells, PI(3,4,5)P₃ localizes at the basolateral plasma membrane in a stable manner and is excluded from the apical plasma membrane. The ectopic overexpression of PI3K increases the amount of PI(3,4,5)P₃ at the apical surface. As a consequence, PI(3,4,5)P₃ binding proteins re-distribute from the basolateral to the apical side. This, in thus, may cause cilia absence in Tg(*hsp70:Arl13b-EGFP-PI3K*) embryos. The excess of basolateral proteins disrupts the apical environment, which could result in cilia disassembly in quiescent cells or a failure of basal body docking following cell division.

Another possible mechanism is that the ciliary expression of PI3K generates higher level of PI(3,4,5)P₃ in the ciliary shaft, which acts as an activator of signalling pathways. Misregulation of signalling pathway could result in cilia disassembly. Although the up-regulation of PI(3,4,5)P₃ accompanies PI(4,5)P₂ depletion, it is unlikely that the disappearance of cilia is caused by loss of PI(4,5)P₂. This is because in *Inp54p* overexpression experiments, which also result in the loss of ciliary PI(4,5)P₂, cilia disassembly was not observed.

The two possible reasons mentioned above might result in the absence or disorganization of cilia from the spinal canal in Tg(*hsp70:Arl13b-EGFP-PI3K*) embryos. The lack of cilia may be a consequence of apical surface disruption by excess of basolateral proteins and the interruption of basal body docking to the apical membrane. Alternatively, it maybe caused by different signalling in the ciliary shaft. Why is this phenotype limited to the spinal canal? One possible reason is spinal canal cells proliferate rapidly, which makes them

sensitive to defects in basal body docking.

3.4.6 Possible pathogenesis of hydrocephalus due to PI3K overexpression

There is a clear fluid in the brain and spinal cord called the cerebrospinal fluid (CSF). Blocking or abnormalities of CSF-flow may lead to the accumulation of CSF and are followed by the widening of brain ventricles, called the hydrocephalus (Orešković and Klarica, 2011). Hydrocephalus is classified as communicating or non-communicating type depending on where the blockade is. If the blockade happens after the exit of CSF-flow to the ventricles, it is communicating hydrocephalus as the flow may still occur in between the ventricles. Communicating hydrocephalus refers to the accumulation of CSF due to the impairment of CSF absorption. The non-communicating hydrocephalus, also called obstructive hydrocephalus, results from the obstruction within the ventricular system (Erickson et al., 2001).

The overexpression of PI3K in cilia caused the up-regulation of PI(3,4,5)P₃ and consequently resulted in the disassembly of cilia. In a 30 hpf zebrafish embryo, cilia that form on the ventral side of the spinal canal are motile, suggesting that a regular fluid flow is required. The disruption of cilia motility and/or structure causes hydrocephalus in the zebrafish brain (Kramer-Zucker et al., 2005). A possible pathology could be that the loss of cilia and cilia motility results in the disruption of fluid flow in the spinal canal and consequently leads to the accumulation of fluid in the brain, which manifests itself as hydrocephalus phenotype. As the flow obstruction in PI3K overexpressing zebrafish occurs in the spinal canal, it might be classified as a non-communicating hydrocephalus.

It is reported that a depletion of primary cilia in radial glia cells resulted in the impairment of cell proliferation through the misregulation of mTORC1 pathway

in *kif3a cKO* mice mutants with the hydrocephalus phenotype (Foerster et al., 2017). I have not done systematic analyses to check if there is any over-proliferation initiated by PI3K overexpression in the spinal canal cilia. The flow-block hypothesis and proliferation-defect hypothesis are both interesting and require further studies.

3.4.7 The mechanism of PTENa^{C124GG129E} phenotype

It is surprising that the control line but not the effector PTENa line displays a phenotype. This result was confirmed by genotyping. The phenotype of PTENa^{C124GG129E} overexpression might be a result of a dominant negative effect. PTENa dephosphorylates PI(3,4,5)P₃ and generates PI(4,5)P₂. A dominant negative effect of PTENa^{C124GG129E} should result in an increase of PI(3,4,5)P₃ level, which is similar to PI3K overexpression. In fact, similar phenotypes were observed in Tg(*hsp70:Arl13b-EGFP-PI3K*) embryos and Tg(*hsp70:Arl13b-EGFP-PTENa^{C124GG129E}*) embryos in the spinal canal. These results support the idea that cilia phenotype resulting from PI3K overexpression is due to the increase of PI(3,4,5)P₃. Moreover, these results suggest a role for PI(3,4,5)P₃ in cilia.

3.4.8 Interpretation of effector phenotypes

Is depletion of the substrate or increase of the product concentration the cause of cilia phenotypes? For example, Inp54p dephosphorylates PI(4,5)P₂ and generates PI(4)P. The ciliary overexpression of Inp54p resulted in the increase of cilia length and bulge formation at the cilia tip. Are these phenotypes caused by the increase of PI(4)P concentration or the depletion of PI(4,5)P₂? Transgenic sensor lines can be used to monitor PI levels before and after effector overexpression. The distribution of PI interacting proteins could also be an indicator. Another way to distinguish which PI species is responsible for a phenotype is to compare phenotypes of enzymes having the

same effect on PI content. For example, both PTEN and Inp54p deplete PI(4,5)P₂. If loss of PI(4,5)P₂ causes cilia phenotype, their overexpression should result in similar phenotype.

3.4.9 Additional controls

Do effector phenotypes result from ciliary PI composition change or from a cytoplasmic effect of enzyme overexpression? To answer this question, non-cilia targeted control is needed. In a non-targeted control construct Arl13b is replaced by its mutated version, Arl13b⁽¹⁻³⁰⁷⁾, which is incapable of cilia localization (Duldulao et al., 2009). If neither the inactive enzyme nor the non-targeted control results in a cilia phenotype, one can conclude that the phenotype is due to a ciliary PI loss of function. The analysis of non-targeted lines is in progress. The full set of control and effector lines are listed in Table 6.

3.5 Summary

We studied the function of ciliary PIs by overexpressing PI kinases or phosphatases in cilia. Depleting PI(4,5)P₂ by overexpression of Inp54p resulted in increased length of cilia the otic vesicle and spinal canal and bulge formation at cilia tips. On the other hand, depleting PI(4,5)P₂ by PI3K overexpression resulted in a disassembly of cilia in the spinal canal. Depleting PI(3,4,5)P₃ by PTENa produces no obvious cilia phenotype. However, cilia disassembly was observed following PTENa inactive control expression

Table 6. The full set of effector and control transgenic lines to be used for phenotypic analysis

NAME	SPECIFICITY	TRANSIENT ¹	STABLE ²
PTENa	(3,4,5)>(4,5)	YES	YES
PTENa ^{C124GG129E}	Inactive mutation	YES	YES
Arl13b (1-307)-EGFP-PTENa ^{C124GG129E}	Non-targeting	In progress	In progress
Inp54p	(4,5)>(4)	YES	YES
Inp54p ^{D281A}	Inactive mutation	YES	YES
Arl13b ⁽¹⁻³⁰⁷⁾ -EGFP-Inp54p	Non-targeting	In progress	YES
PI3K	(4,5)>(3,4,5)	YES	YES
PI3K ^{K802R}	Inactive mutation	YES	YES
Arl13b ⁽¹⁻³⁰⁷⁾ -EGFP-PI3K	Non-targeting	In progress	YES

¹ Transient expression; ² Stable transgenic lines

Chapter 4

Chapter 4

INPP5E function study in zebrafish

4.1 Introduction

4.1.1 5-phosphatases

Inositol polyphosphate 5-phosphatases (5-phosphatases) comprise a family of enzymes that hydrolyze the 5 position phosphate including $PI(3,4,5)P_3$ and $PI(4,5)P_2$. Based on the substrate specificity, mammalian 5-phosphatases have been previously classified into four groups (Majerus et al., 1999). A brief summary of these groups is in table 7. Group I hydrolyzes the water soluble inositol phosphate substrates, such as $Ins(1,4,5)P_3$ and $Ins(1,3,4,5)P_4$, these enzymes are membrane associated and function in calcium signaling. Group II hydrolyzes all four known 5-phosphatase substrates. Group III was previously characterized as only dephosphorylating in the D-3 position. SHIP1 and SHIP2 are members of this group. Group IV, a poorly characterized group, was reported as having an activity that was specific for hydrolysis $PI(4,5)P_2$ and $PI(3,4,5)P_3$. INPP5E is an example of group IV 5-phosphatases. The deletion or deficiency of 5-phosphatases in animal models such as mice or zebrafish suggests that these enzymes serve non-redundant functions in signaling pathways. The deletion of SHIP, a 5-phosphatase expressed mainly in hematopoietic cells, causes severe myeloid proliferation and infiltration of the lung (Helgason et al., 1998). Deficiency of Lowe syndrome causing gene OCRL, results in increased apoptosis and reduced proliferation in the neural tissue of zebrafish (Ramirez et al., 2012).

In regard to cilia, all three known phosphatases that localize in cilia are

5-phosphatases. INPP5E is the first identified ciliary phosphatase that dephosphorylates both PI(4,5)P₂ and PI(3,4,5)P₃. Further details about INPP5E will be introduced in section 4.1.2 and 4.1.3 of this chapter. In addition, two group II 5-phosphatase members, OCRL and INPP5B, are known to localize at primary cilia and play roles in cilia differentiation (Luo et al., 2013). OCRL is a X-chromosome gene product and also known as Lowe syndrome protein. The ciliary localization of OCRL suggests a role of cilia in the Lowe syndrome (Luo et al., 2014). INPP5B is a member of Inositol polyphosphate-5-phosphatase (INPP5) family. It dephosphorylates PI(4,5)P₂ and Ins(1,4,5)P₃. Down-regulation of INPP5B results in cilia defect in cultured cells and zebrafish morphants (Luo et al., 2013). How are these three 5-phosphatases, OCRL, INPP5B and INPP5E, regulated in cilia is unclear. Whether they are functionally compensatory or functionally redundant still requires further studies.

Table 7. Summary of 5-phosphatases (Majerus and York, 2009)

	Substrate		Membrane associated	Examples
	Water soluble	Lipids		
Group I	✓		✓	
Group II	✓	✓	✓	OCRL, INPP5B
Group III		Mainly		SHIP1, SHIP2
Group IV		PIP ₃ and PI((4,5)P ₂		INPP5E

4.1.2 *In vitro* studies of INPP5E function

The *INPP5E* gene is located on human chromosome 9q34.3 and encodes INPP5E, which is also known as 5-phosphatase IV. INPP5E from men and mice were cloned and characterized by several groups (Kisseleva et al., 2000; Kong et al., 2000). It is widely expressed and has the highest expression in the brain and testis as detected by *in situ* hybridization (Kong et al., 2000). INPP5E consist of a proline-rich domain, a catalytic domain and a CAAX motif. In Kong *et al.* study, INPP5E displayed cytoplasmic distribution in cell culture

and was recruited to the TGN through the N-terminal proline-rich domain. In ciliated cell, the C-terminus CAAX motif was shown to be crucial for INPP5E ciliary localization (Humbert et al., 2012).

INPP5E was demonstrated to be involved in the autophagosome-lysosome fusion process. In neuronal cells, the autophagy was inhibited due to the impairment of the autophagy fusion step by INPP5E knockdown. A fraction of INPP5E localized to lysosomes and dephosphorylated lysosomal PI(3,5)P₂, which is also an INPP5E substrate that was proposed by an *in vitro* study (Hasegawa et al., 2016). Furthermore, INPP5E was reported to function as a regulator of the PI3K/Akt pathway. INPP5E overexpression suppressed cell growth and led to FAS induced apoptosis due to the inhibition of AKT phosphorylation in response to the stimulation from insulin-like growth factor (IGF-1) and platelet-derived growth factor (PDGF) (Kisseleva et al., 2002).

4.1.3 INPP5E and human diseases

4.1.3.1 The subcellular localization of INPP5E

INPP5E predominantly localizes to cilia in major organs such as the kidney and retina. This was confirmed by coimmunostaining of INPP5E with ciliary markers or pericentriolar markers. In RPE-hTERT (immortalized retinal pigment epithelium) cell line, INPP5E was tightly colocalized with Arl13b and acetylated tubulin and adjacent to the ciliary base indicated by pericentrin. In GFP-INPP5E transfected IMCD3 cells, cytoplasmic localization was observed in mitotic stages (after the cilium withdrawal). In the kidney, INPP5E positive cilia were observed projecting into the lumen in the renal connecting tubule. In retinal photoreceptor cells, INPP5E localized to the region near the basal body and connecting cilium (Bielas et al., 2009).

4.1.3.2 INPP5E function study *in vivo*

Various INPP5E mutant mice are well characterized *in vivo* models. The first reported *inpp5e*^{-/-} mouse exhibited embryonic and postnatal death (Jacoby et al., 2009). *Inpp5e*^{-/-} early stage embryos displayed multiple phenotypes including bilateral anophthalmia, polydactyly, polycystic kidneys and skeletal defects. No liver alterations, respiratory cilia defects or laterality defects were observed. INPP5E conditional knock-out mutant adult mice were used for later stage phenotypic analysis. No survival defects observed at 6 months. However, ciliopathy features were observed such as retinal degeneration, cystic kidneys and obesity.

Mutations in *inpp5e* have been linked to human ciliopathies such as Joubert syndrome and MORM syndrome (Bielas et al., 2009; Jacoby et al., 2009; Travaglini et al., 2013). Joubert syndrome and related disorders (JSRD) are genetically heterogeneous ciliopathies, which are characterized by midbrain-hindbrain malformation (known as the 'molar tooth sign'), polydactyly, retinal degeneration, nephronophthisis, liver fibrosis and cognitive impairment (Joubert et al., 1969). Nineteen causative genes were identified to date and all those genes encode primary ciliary proteins. MORM syndrome is characterized by mental retardation, retinal dystrophy, truncal obesity and micropenis (Hampshire et al., 2006). MORM syndrome displays similar phenotypes to Bardet-Biedl syndrome and Cohen syndrome; however, it can be distinguished by specific clinical features. To date, all INPP5E related Joubert syndrome mutations were reported to affect the 5-phosphatase catalytic domain. These mutations affect INPP5E phosphatase activity to different extent. Each of the JBTS1 missense mutations significantly affect the phosphatase activity towards PI(3,4,5)P₃. However, phosphatase activity towards the other substrate PI(4,5)P₂ is less severely disrupted (Bielas et al., 2009). This finding suggested that PI(3,4,5)P₃ might be the major substrate

in Joubert syndrome. In contrast, the MORM syndrome mutations cause the deletion of the CAAX motif, which locates at the C-terminus of INPP5E. The CAAX motif is outside the catalytic domain region and is crucial for INPP5E cilia targeting. Consequently, MORM syndrome mutations do not impair catalytic activities towards PI(3,4,5)P₃ or PI(4,5)P₂ (Jacoby et al., 2009).

Apart from rare human ciliopathies, INPP5E is involved in human cancer. In human cervical cancer specimens, *inpp5e* is the fifth highest overexpressed gene compared to non-cancerous samples (Han et al., 2003a). In leiomyosarcoma, INPP5E is 5.7 times overexpressed (Quade et al., 2004). In contrast, compared to non-tumor mucosa samples, gastric cancer cells display INPP5E downregulation (Kim et al., 2003). Primary cilia are implicated in tumorigenesis through the regulation of the cell cycle (Nigg and Raff, 2009). However, a relationship between INPP5E related tumorigenesis and cilia has not been established and requires further investigation.

4.2 Results

Characterization of INPP5E function in zebrafish

Due to the fact that INPP5E mutant mice display embryonic lethality, it is difficult to further investigate the function of INPP5E in mammals. Owing to the external development of zebrafish, it is easy to observe developmental changes and phenotypical defects in this model. To take advantage of this, I generated INPP5E zebrafish mutants using the CRISPR technique. *Inpp5e* gene is highly conserved across species especially at the 5-phosphatase domain. Two consensus motifs, named Domain I and Domain II, indicate that INPP5E function as an inositol polyphosphate 5-phosphatase (Majerus et al., 1999). Missense mutations located at the catalytic domain of *Inpp5e* are linked to the *JBTS1* locus (Figure 21).

4.2.1 Using the CRISPR-Cas9 to generate a zebrafish mutant of INPP5E

Five guide-RNAs (gRNA) were designed and tested. Due to lack of the restriction enzyme digestion site, T7 assay was applied for the gRNA efficiency test. One out of five gRNAs worked. This gRNA, which binds to the middle region of the catalytic domain, was injected together with Cas9 mRNA to one-cell stage zebrafish embryos. 2.4µg/µl gRNA with 0.5 µg/µl of Cas9 mRNA were used.

Healthy looking injected embryos were raised to adulthood. Adult G0s carriers of mutant alleles were selected based on the T7 assay for further studies. Positive G0s were out-crossed with wild-type fish and healthy looking progeny (F1) was raised to adulthood. F1s were genotyped through fin-clipping and different mutant alleles were maintained separately. Experiments that follow were carried out on the *Inpp5e* mutant, which contains a T insertion resulting in a premature stop codon after 423 amino acids of the full-length protein (Figure 21 and Figure 22A).

4.2.2 Phenotype analysis of *Inpp5e* zebrafish mutant

Inpp5e^{-/-} zebrafish larvae displayed several abnormalities including upward body curvature, kidney cysts, ear and liver defects and photoreceptor degeneration.

```

Danio      MSEHGDSIVPFNPTDLRSGEPATKTDIT-VLS-----VDLRTEKSHNEELR
Homo      -----MPSKAENLRPSEPAPQPPEGRTLQGQLPGAPPAQR--AGS--PPDAPGS--E
Mus       -----MPSKSAACLHRTE-APGQLEGRMLGQPPNTEKKLIPTPGFPLPASDSQGSE-T
                : * :  * * * *      * ,                    . : ..

Danio      DIKKPYDGPK----VLQDEHSLYQPRPPSLPKPMGLGMGGKNLSFDE-KVGRRLRNSQ
Homo      SPALACSTPATPSGEDPPARAAPAPRPPARPL-----ERALSDDKGWRRRRFRGSQ
Mus       NPMPPFSIPAKTSNQNPQTKANLITPQQPIRPKL-----ERTLSDDKGWRRRRFRGSQ
                .   . *          .   *:* * *      : *:* : * *:* **

Danio      ESLTDPGETGSSSTDSLKDVASANGQTLASRRPLDLQHMEMPFRIRTGSLS-----
Homo      EDLEARNGTSPSRGVSQSEGPGAPAHSCSPCLSTSLQEI PKSRGVLSSSERGSPSSGGNP
Mus       EDLTVQNGASPCRGS LQDSVAQSPAYSRPLPCLSTSLQEI PKSRATGSEGGSPSLWSDC
                * * . . . * : : .      * . . * : * * . *

Danio      --ETDVSPHDLCDPNKERMKPSRIVLSPLQPTGTYPLENSTASASLRTTNRIDRCDLDY
Homo      LSGVASSSPNLPHRDA-AVAGSSPRLP SLLP RPPPALSLDIASDLRTANKVSDLDADY
Mus       LSGMISTSLDLLHRDA-ASGGPPSRLASLHASHTPPAMDLSIASSSLRTANKVDPEHTDY
                : : * . :      * *          * : . . * * * * * : * : *

Danio      GVVRRRGRSERLHRNLSDRLLDTMVDNTSVHSMKSTYSVLNPIRPRDVRNRSFLEGSV
Homo      KLRAQ-PLLVAHSSLGPRPRSPPLACDDCSLRS AKSFSLLAPIRSKDVRSRSYLEGS
Mus       KLRMQ-TRLVRAHNSLGP SRPR SPLAGDDHSI HSA-RSFSLLAPIRTKDIRSRSYLEGS
                : :      * * . * . * . . : * : * * *      : * : * * * : * : * * * *

Danio      LGNGALLCAEELDRYFPERRLGIYIATWNMQGKGLPYNLDLPTDTPAODVYVIGV
Homo      LASGALLGADELARYFDDRNVALFVATWNMQGQKELPPSLDEFLLPAEADYAQDLYVIGV
Mus       LASGALLGAELARYFDDRNMALFVATWNMQGQKELPASLDEFLLPTEADYTQDLYVIGI
                * .. * * * * * : * * : : : : * * * * * : * * . * * : * : * * * * *

Danio      QEGCPDRREWETRLQETLGPYYVMLYAAAAGVLYLTVFVRDLIWFCEVEHATVTTTRII
Homo      QEGCSDRREWETRLQETLGPYVLLSSAAHGVLMSLFIRDLIWFCEVECSTVTTTRIV
Mus       QEGCSDRREWETRLQETLGPQYVLLSSAAHGVLMSLFIRDLIWFCEVEYSTVTTTRIV
                * * * * * * * * * * * * * * * * * * * * * * * * * * * * * * * * * * * *
                                ↓ *STOP

Danio      SQIKTKGAVGIGFTFFPGTSFLFVTSHFISGDSKVYERILDYNKIIEALALPRNLPDTPNY
Homo      SQIKTKGALGISFTFFPGTSFLFVTSHFISGDKVAERLLDYTRTVQALVLRNVPDTPNY
Mus       SQIKTKGALGVSTFFPGTSFLFVTSHFISGDKVAERLLDYSRTIQALALPRNVPDTPNY
                * * * * * * : . * * * * * * : * * * * * * * * : * * * * * * * *

Danio      RSTTSDVTTTRFDEVEVFGDFNFRLNKARGDVEAILNQGVGVDMSPLLQHDQLTEMKGS
Homo      RSSAADVTTTRFDEVEVFGDFNFRLLSGGRVVDALLCQGLVVDVPAQLLQHDQLIREMKGS
Mus       RSSAGDVTTTRFDEVEVFGDFNFRLLSGGRVVAEAFKQKPEVDVLLQHDQLTEMKGS
                * : : * * * * * * * * * * * . * * : * : * *      * * : * * * * * : * *

Danio      IFKGFQEASIHFPPTYKFDIGCDVYDTTKQRTPSYTDRIYRNRQADDIRVIKYSKSS
Homo      IFKGFQEPDIHFLPSYKFDIGKDYDSTSQRTPSYTDRIYRSRHKGDICPVSYSSCPG
Mus       IFRGFEEAEIHFLPSYKFDIGKDYDSTSQRTPSYTDRIYKSRHKGDICPMKYSSCPG
                * : * * : * . * * * * * * * * : * : * : * * * * * * * * * * : * * .

Danio      IXTSDRHPVIGMFQVKLRPGRDNIPLAGLFDRLSLEYEGIRRRITRELKREAVMKQNN
Homo      IXTSDRHPVYGLFRVKVRPGRDNIPLAGKFDRELYLGLIKRRISKEIQRQQA-LQSQNS
Mus       IXTSDRHPVYGLFQVKVRPGRDNIPLAGKFDRELYLIGIKRRISKEIQRQEA-LKSQSS
                * * * * * * * * * * * * * * * * * * * * * * * * * * * * * * .

Danio      STVCSIS
Homo      STICSVS
Mus       SAVCTVS
                * : * : * *

```

Figure 21. INPP5E in human, mouse and zebrafish.

Alignment of INPP5E amino acid sequence of zebrafish, mouse and human. The 5-phosphatase catalytic domain is highlighted in light blue, human mutations are in red, CAAX motif is in yellow. Blue boxes show two 5-phosphatase consensus motifs. Green arrow indicates truncation of INPP5E that is present in inpp5e zebrafish mutant studied in my work.

4.2.2.1 Kidney cysts are accompanied by kidney cilia defect in the *inpp5e*^{-/-} mutant

Morphologically, *Inpp5e*^{-/-} zebrafish larvae display upward body curvature (Figure 22 B-B'). Kidney cysts are observed as early as 3 dpf. I used immunofluorescence staining of larvae at 5 dpf to check cilia morphology. No obvious difference was observed in cilia from ear cristae and olfactory neurons of *Inpp5e*^{-/-} compared to control siblings (Figure 22G-H'). Cilia in the pronephic duct were absent in *Inpp5e*^{-/-} whereas normal cilia were observed in control siblings. To evaluate photoreceptor development, I applied histology methods. Retina cryosections showed photoreceptor defects at 3 and 5 dpf in *Inpp5e*^{-/-} larvae. Occasionally, cell death was also observed as early as 3 dpf in the photoreceptor cell layer (Figure 22 C-F')

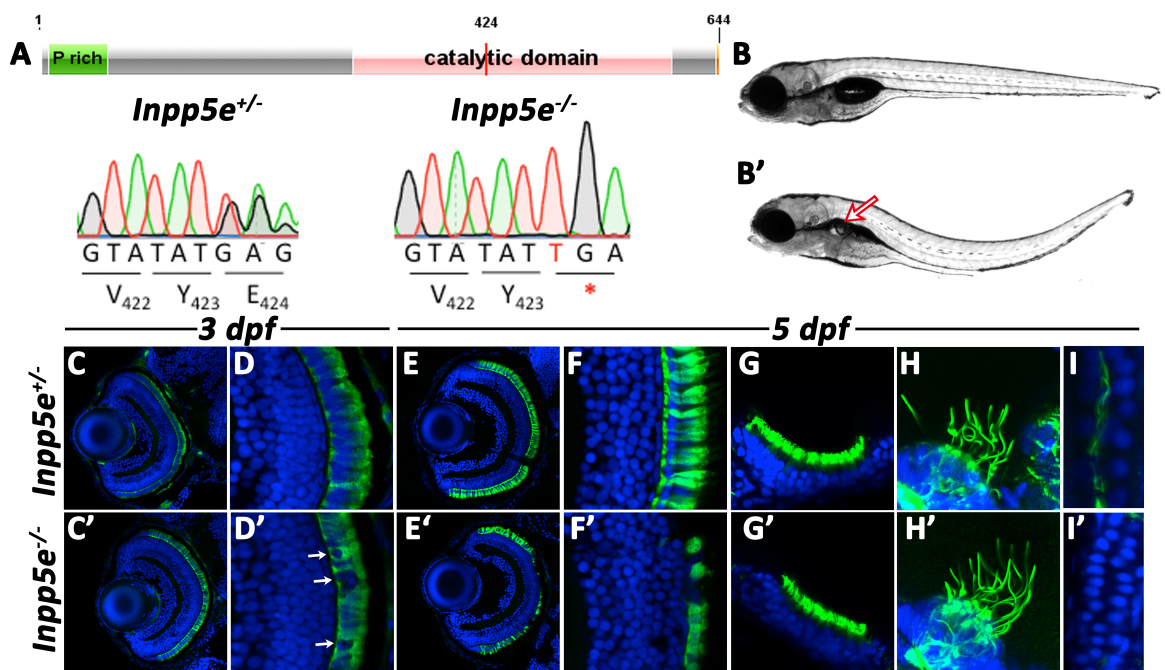


Figure 22. Phenotypes of *inpp5e* zebrafish mutants.

(A) A schematic representation of the *inpp5e* gene and sequencing data for the *inpp5e*^{sh509} mutant allele. *Inpp5e*^{sh509} involves a single base pair insertion that introduces a premature stop codon at position 424 of the open reading

frame causing by a frame shift.

(B-B') Lateral view of 5 dpf zebrafish larvae. Homozygous *inpp5e* allele mutant larvae (B') but not their wild-type siblings (B) display upward body curvature and kidney cysts (arrow).

(C-F') Confocal images of cyrosections through retinæ of *inpp5e* mutants and their control siblings stained to visualize double cones (green) and counterstained with DAPI (blue). (C-D') Control and mutant retinæ at 3 dpf. No obvious morphological changes are found in the *inpp5e* mutant retina (C' and D'), compared to control (C and D). (D, D') Enlargements of images in (C, C'). A closer inspection reveals photoreceptor abnormalities, most likely cell death, in the mutant photoreceptor cell layer (D', white arrows). (E-F') Control and mutant retinæ at 5 dpf. Pronounced photoreceptor cell loss is seen in mutant retinæ (E' and F') compared to the control (E and F). (F, F') Enlargements of images in (E, E').

(G-I') Confocal images of wholemount *inpp5e* mutant larvae and their wild-type siblings stained with anti-acetylated tubulin antibody to visualize cilia (green) and counterstained with DAPI (blue). (G-H') No obvious difference is seen in the nasal pit (G') and ear cristae (H') of *inpp5e*^{-/-} mutants, compared to their control siblings (G, H). (I, I') Cilia are absent in the kidney tube of *inpp5e*^{-/-} mutants (I') but not in sibling controls (I).

4.2.2.2 Lumen formation defects in *inpp5e*^{-/-} mutants

Morphological abnormalities were also observed in the ear and liver. There was a significant size decrease in the ear of *inpp5e*^{-/-} larvae compared to sibling controls. No otolith defect or obvious ear cilia defect was observed. Moreover, enlarged livers were found in mutant larvae but not in control siblings. The size of the liver and ear were both quantified and P values are listed in figure 23 legend.

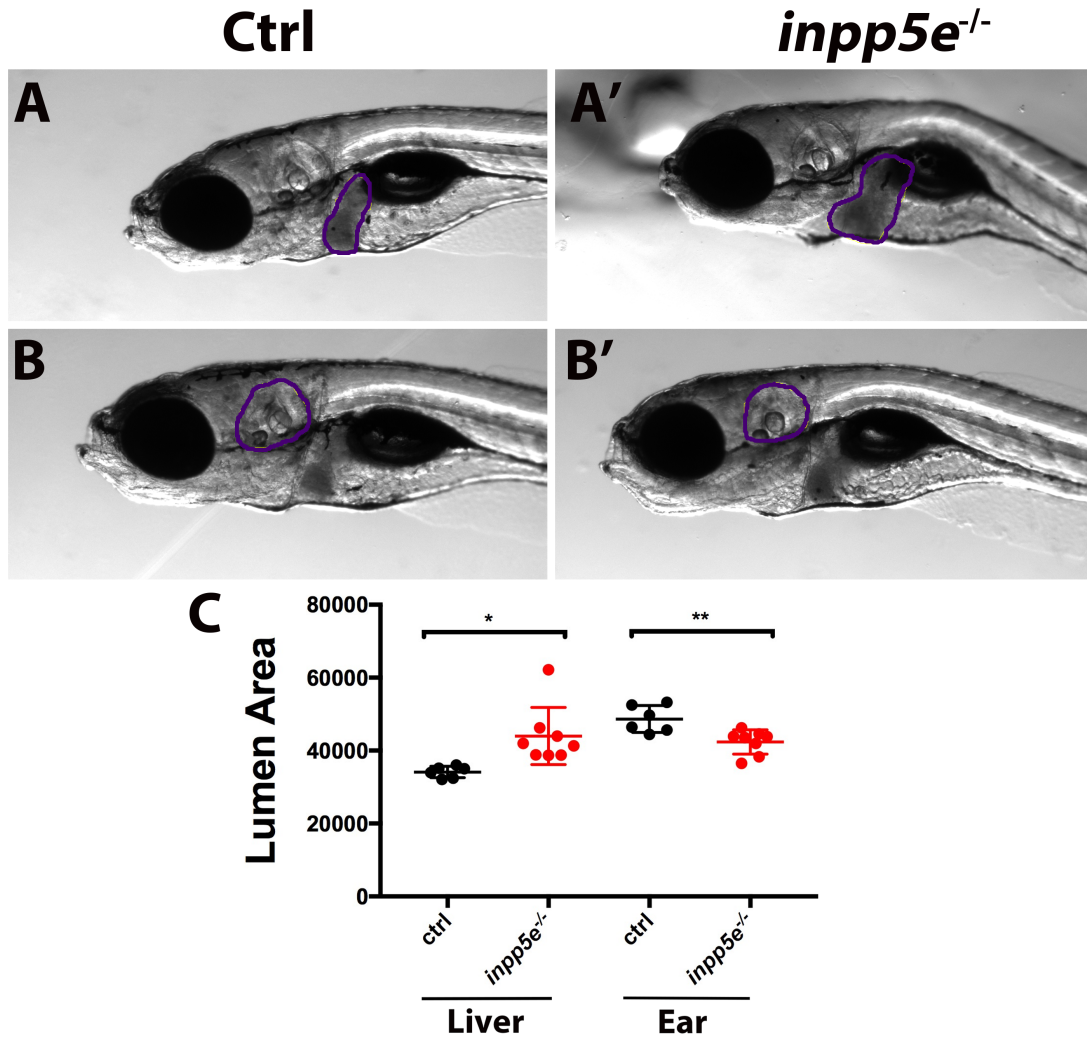


Figure 23. Ear and liver defects resulting from *INPP5E* dysfunction.

(A-B') Representative images of the lateral view of control sibling (A and B) and *inpp5e*^{-/-} (A' and B') zebrafish larvae at 7dpf. (A-A') An enlarged liver was observed in *inpp5e*^{-/-} mutants (A') but not control siblings (A). (B-B') The size of the ear decreased in *inpp5e*^{-/-} mutants (B') compared to sibling controls (B). (C) Quantification of the size of the liver and ear. $P_{liver} = 0.0109$, $P_{ear} = 0.0057$. Mean and SD are indicated. The area measured is shown in purple.

4.2.2.3 Photoreceptor degeneration in *inpp5e*^{-/-} mutant retina

Following-up on the photoreceptor defects observed on cryosections, I took a closer look at *inpp5e* mutant retina using electron microscopy. At 5 dpf, regular outer segments were observed in control siblings (Figure 24A) but not

the mutant retina (Figure 24B). In fact, in *inpp5e* mutant, regular cell structure was not observed in the area of the photoreceptor cell layer. The TEM result confirmed the degeneration of photoreceptor cells in the *inpp5e* zebrafish mutant.

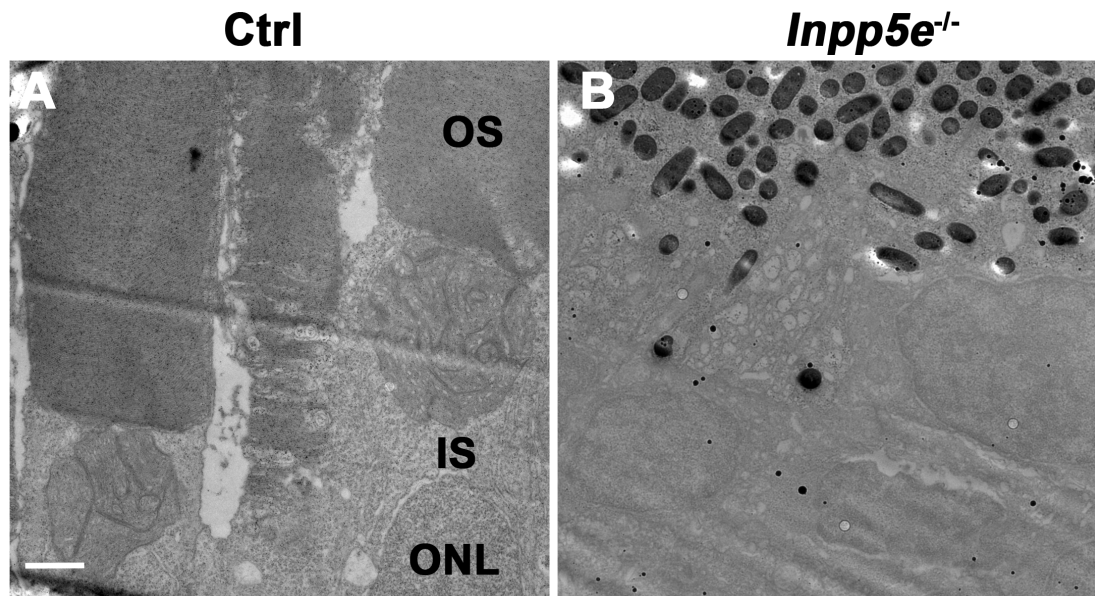


Figure 24. Photoreceptor degeneration in *inpp5e*^{-/-} zebrafish larvae

Transmission electron microscopy images of photoreceptors from control sibling (A) and an *inpp5e*^{-/-} mutant larva (B) retina at 5 dpf. Outer segments are missing in the mutant. Scale bar, 1 μ m. OS, outer segment; IS, inner segment; ONL, outer nuclear layer.

4.2.3 A novel genetic system to monitor Opsin transport in zebrafish

As photoreceptor defects are fairly insignificant at 3 dpf and become obvious only at 5 dpf, it is likely that INPP5E is not required for ciliogenesis but instead for ciliary function and maintenance in photoreceptors. To investigate the mechanism behind *inpp5e*^{-/-} photoreceptor degeneration, I constructed a genetic system to monitor opsin transport in zebrafish photoreceptors.

Opsin is one of the main protein components of photoreceptor cilia. In

addition to detecting light, its presence is essential for cilia morphogenesis (Pugh and Lamb, 2000). Mislocalization of opsin is a major cause of photoreceptor cell death, which has been demonstrated in a variety of ciliary mutants including *oval/ift88* (TsujiKawa and Malicki, 2004) and Kif3a mutants (Lopes et al., 2010b). The experiments revealed that it is the accumulation of the mislocalized opsin resulting in photoreceptor cell death.

Opsin transport assay, can be carried out by using antibody staining against opsin, or more informatively, by analysing the transport of opsin fused with a fluorescent protein in living animals. In *Xenopus*, the 44 amino C-terminal amino acids of opsin are sufficient to mediate outer segment transport (Tam et al., 2000). Transient expression of opsinCT44-GFP fusions was also applied to monitor opsin transport deficiency in zebrafish ciliary morphants (Zhao and Malicki, 2011).

To monitor the dynamics of opsin transport *in vivo*, I generated transgenic animals that express EGFP-opsin fusion specifically in rod photoreceptors from an inducible promoter. This system provides both spatial and temporal control of opsin expression. It consists of two transgenic lines: 1. A line that specifically expresses Cre recombinase in photoreceptors from rhodopsin promoter, and 2. a temperature-inducible line that conditionally expresses EGFP-opsinCT44 (EGFP fused with S-peptide and the 44 C-terminal residues of *Xenopus* rod opsin) from the heatshock promoter (Figure 25). A lox-mCherry-STOP-lox cassette is inserted upstream of EGFP-opsinCT44 in this line. In addition, a TEV cleavage site is inserted between the GFP sequence and the S-peptide. This makes it possible to use this line in tandem affinity purification experiments. When these two lines are mated together, the resulting progeny contains two transgenes and expresses EGFP-opsin44CT44 specifically in photoreceptors (Figure 25A). When heatshock is applied, embryos express mCherry ubiquitously and EGFP-opsinCT44 specifically in rods (Figure 25 E-E'). EGFP-opsinCT44

fusion localizes to photoreceptor outer segments in these animals. In a control line, which contains 44 random amino acids in place of 44 amino acids from rhodopsin C-terminus, the EGFP signal is no longer enriched in the outer segment and instead is present throughout the entire photoreceptor cell body (Figure 25 F-F').

To test the utility of the double transgenic system for opsin transport analysis, I first applied it to the *bbs9* mutant (Figure 26). This is a suitable strategy because Bardet-Biedl genes are required for GPCR transport (Berbari et al., 2008). However, *bbs9* mutant is not well characterized (Veleri et al., 2012). Using antibody staining against rhodopsin at the *bbs9*^{-/-} retina, strong opsin signal was observed in the cell body of photoreceptors (Data not shown, staining performed by Dr. E. Leventea, Malicki Lab)

Using this genetic system, as expected, mislocalized opsin was observed in photoreceptor cells of *bbs9*^{-/-} but not control siblings. This illustrates that my opsin transport monitoring system is capable to detect opsin transport defects in a mutant background in a precise way.

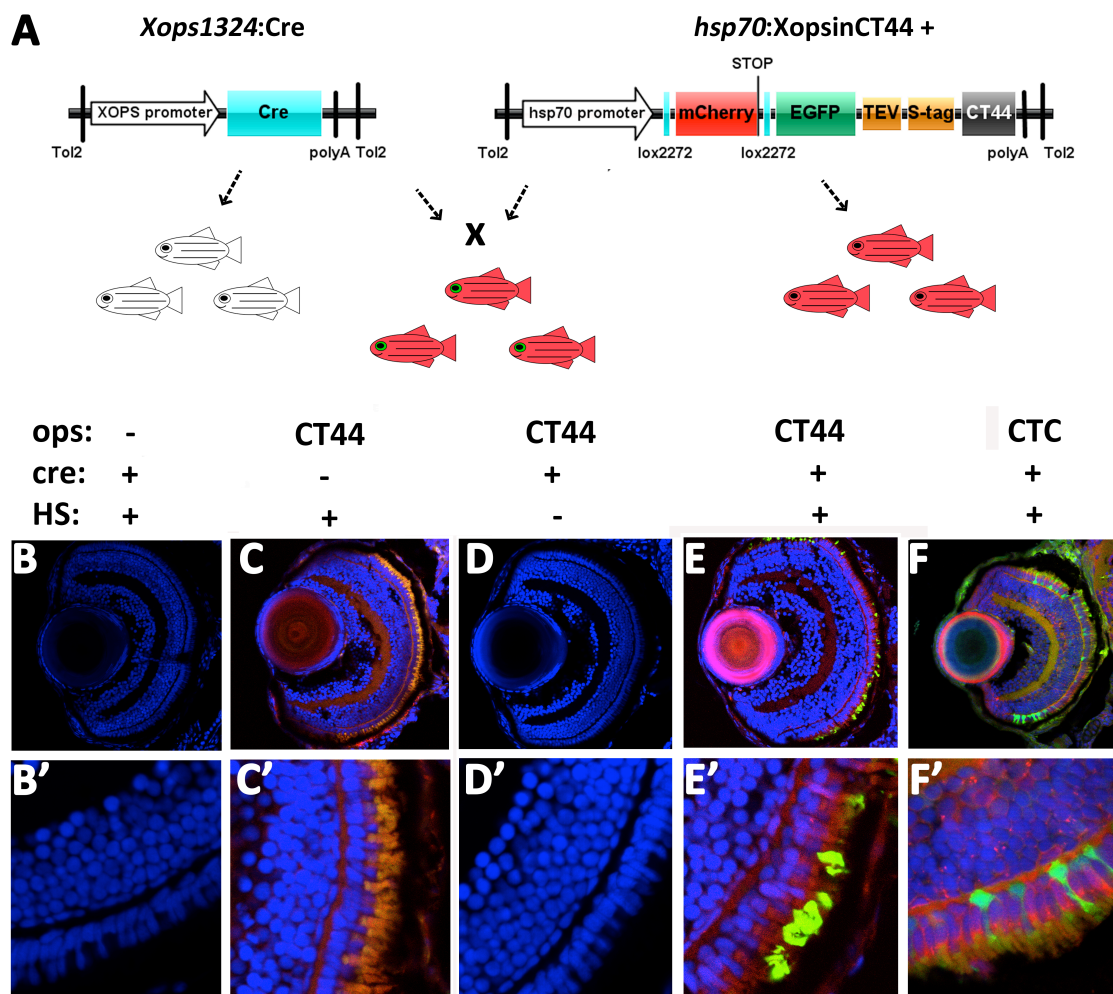


Figure 25. The opsin transport assay system

(A) Schematic of transgenes used to obtain temporal control of expression for EGFP-opsinCT44 specifically in zebrafish rods. (B-F') Confocal images of cryosections through retinæ of transgenic zebrafish larvae at 5 dpf. Genotypes are indicated image panels above. No fluorescent signal is observed in the Cre line even when heatshock is applied (B-B'). mcherry but not GFP expression is present when heatshock is applied to the *Tg(hsp70:lox2272-mCherry-lox2272-EGFP-TEV-Speptide-CT44)* transgenic line (C-C'). No signal is observed in the double transgenic line without applying heatshock (D-D'). EGFP is expressed in photoreceptors but not in other retinal cells when heatshock is applied to the double transgenic line (E, E'). EGFP signal localizes to the outer segment in this line (E'). In contrast,

EGFP signal is not targeted to the outer segment in a double transgenic line that contains a control EGFP construct in which CT44 cilia targeting signal was replaced with a random peptide (F-F').

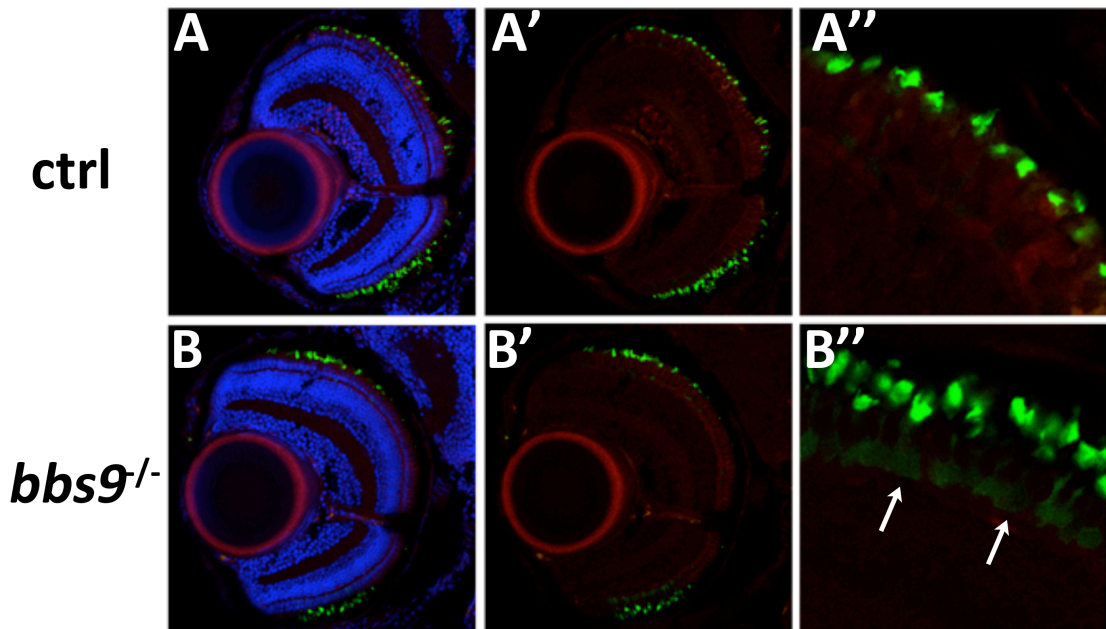


Figure 26. Opsin transport assay system applied to *bbs9* mutants

*The opsin-Cre double transgene system was applied to *bbs9* mutant. GFP labelled opsin-CT44 exclusively localized to the outer segment of photoreceptors 24 hours post-heatshock in a control sibling (A-A'') but mislocalized to the cell body and synapse of photoreceptors of the *bbs9* mutant (white arrows) (B-B''). The whole retina expresses mcherry (red) whereas Cre expressed in rod photoreceptor cells induces EGFP-opsinCT44 fusion (green) expression in place of mcherry. Nuclei were counterstained with DAPI in blue.*

4.3 Discussion

4.3.1 Upward body curvature in *inpp5e*^{-/-} mutant

Abnormal body curvature is one of the typical morphological phenotypes, which makes cilia mutants particularly easy to be identified in the zebrafish model (Zaghloul and Katsanis, 2011). Apart from kidney cysts and photo-

receptor degeneration, *inpp5e*^{-/-} mutant display unusual upward body curvature, which is different from the curly down phenotype that is well known from studies of IFT and ciliary Kinesin mutants (Omori et al., 2008; Pooranachandran and Malicki, 2016).

The mechanism, which controls zebrafish body axis morphology, is unclear. Work from Pierre-Luc Bardet *et al.* revealed that the Reissner's fiber and motile cilia control body axis development in zebrafish (unpublished data, a talk from the 10th of European zebrafish meeting, Budapest 2017). Their Reissner's fiber protein mutant zebrafish showed curly down body curvature, same as IFT mutant. Consistent with that, in classic IFT-B mutants *elipsa* and *ovl*, both of which display curly down body axis, the Reissner's fiber was damaged. Mutants with upward body curvature were not tested.

To my knowledge, there are two types of mutants that display body axis curly up phenotype in zebrafish, the Notch mutant (Hsu et al., 2015) and the Pkd2 mutant (Schottenfeld et al., 2007). It is unclear that what causes upward body curvature. The interaction, if there is any, between INPP5E and PKD2 or between INPP5E and Notch pathway would be also interesting to study.

4.3.2 Rapid photoreceptor degeneration shows the importance of INPP5E in photoreceptor cilia

Rapid photoreceptor degeneration was observed in the *inpp5e* mutant. At 3 dpf, few cell death morphology defects were observed. By 5 dpf, nearly all photoreceptors have degenerated. First, it suggests that loss of INPP5E does not affect ciliogenesis but cilia maintenance maybe. Second, the degeneration occurred very quickly compared to IFT-A mutants (Boubakri et al., 2016) and almost at the same speed as IFT-B mutants or ciliary Kinesin motor mutants (Pooranachandran and Malicki, 2016). This fast degeneration indicates, firstly, the importance of INPP5E during photoreceptor differentiation,

and in addition, shows that INPP5E may function upstream of the IFT-A complex, which is thought to mediate retrograde transport.

4.4 Summary

To further understand the role of PI, I utilized loss of function studies of a ciliary phosphatase in the zebrafish model. An *inpp5e* null mutant was generated using the CRISPR/Cas9 method and cilia specific phenotypes were observed including upward body curvature, kidney cysts and photoreceptor degeneration. To further study the mechanism of photoreceptor degeneration, a genetic opsin-transport monitoring system was established and tested in Bardet-Biedl gene mutant background. Mislocalized GFP-opsin fusion indicated an opsin transport defect and the capability of the monitoring system.

Chapter 5

Chapter 5

Discussion and Future Plans

5.1 The use of transgenic lines

Transgenic lines are effective tools for cell and developmental biology studies. Using transgenic zebrafish lines to express ciliary proteins fused with fluorescent proteins is widely used for cilia morphology analysis. Numerous transgenic lines have been made over the past 25 years. However, as a genetic tool, this approach faces some technical difficulties such as position effects, silencing of transgene expression and inconsistent expression.

Position effects occur as the result of the expression of transgene being affected by endogenous elements (such as the promoter or enhancer) near transgene integration site in the genome. Having several alleles of a single transgene can be used to control for position effects. The overall similarity of transgene expression patterns in multiple integration sites is very unlikely to be influenced by integration sites. In addition, position effects can be in some cases limited by the use of a strong promoter (Stuart et al., 1990).

Another aspect of position effects is that the integration site of a transgene may be flanked by essential genes. The insertion of a transgene may lead to misexpression of proteins that function during development or are essential for cellular housekeeping. To eliminate the possibility of the position effect, phenotype analysis was carried out on at least two alleles in Arl13b-EGFP fused effector transgenic lines. For the inactive control effector line, one line was examined as long as it showed normal cilia morphology compared to other controls or the Tg(β act:Arl13b-EGFP) line.

PH sensors are well characterized in cell culture. Subcellular localization

data from cell culture can be used to evaluate whether a transgenic PH sensor functions properly. The subcellular localization pattern of each transgenic sensor line that I used in this analysis is consistent with tissue culture data (for details see Chapter 2).

Silencing and inconsistent expression are another complication associated with transgene use. *Arl13b* has been widely used for cilia labelling. In zebrafish, *Tg(β act:Arl13b-EGFP)* line was previously published and is available in our lab (Borovina et al., 2010). However, its expression was silenced in some tissues after several generations. As constitutive overexpression is likely to cause stress in the long term, it is not surprising that the organism gradually shuts down the expression for self-protection. *Arl13* expression is, in fact, known to cause some changes in cilia morphology in zebrafish (Lu et al., 2015).

In our studies, an inducible promoter was used to overcome the silencing effect on transgene expression. As the transgene is only activated for a short period of time, relatively low toxicity and biological stress is produced, compared to constitutive expression, in which case, artefacts are less likely to occur. In this project, promoter from *hsp70* heatshock gene was used for both PH domain-based sensor lines and all effector and control lines. In heat shock-induced transgenic lines, all cilia appeared to be visualized consistent with antibody staining data. This contrasts with the *Tg(β act:Arl13b-EGFP)* line maintained in our lab in which some cilia did not display fluorescence, presumably due to silencing.

5.2 The use of Heatshock promoter

Two major factors are important while evaluating usefulness of an inducible promoter: basal level of expression prior to induction and degree of inducibility. Without induction, the activity of the promoter has to be as low as possible to

prevent side effects. Naturally inducible promoters such as *hsp70* were first used to induce gene expression in *Drosophila* during embryonic development (D'Avino and Thummel, 1999). Some leakage of expression has always been a shortcoming for heatshock promoters.

In zebrafish, heatshock protein is an endogenous product with specific cellular function during development (Basu et al., 2002). The gene products, which are generated in response to the heat stress, are usually also crucial for housekeeping. The fundamental role of *hsp70* may explain why some expression is seen even without heat shock. Because heat stress response plays a role during development (Basu et al., 2002), genes driven by *hsp70* may be expressed at low level regardless of artificial heat induction.

Nonetheless, the use of heatshock promoter has many advantages. It can be used to adjust the timing of expression according to research interests and, moreover, the amount of expressed protein can also be adjusted by varying the heatshock duration so that the lowest effective amount is used. This reduces the possibility of side effects due to continuous PI binding by sensor proteins.

5.3 Identification of Ciliary PIs

What do we know about PI composition in the ciliary membrane?

Membrane identity of cellular organelles is not only determined by specialized proteins but also by membrane lipid content. The first indication that ciliary PIs differ from these in the rest of the cell body came from TLC analysis of lipids extracted from deciliated *Paramecium* (Andrews and Nelson, 1979). Additional data came from the ciliary localization of PI-interacting proteins. PI phosphatases INPP5E and OCRL both localize to and function in cilia. Mutations in *inpp5e* and *ocrl* genes result in ciliopathies such as the Joubert syndrome and Lowe syndrome (Bielas et al., 2009; Luo et al., 2014).

Similarly, mutations in *C. elegans*, PI 5-phosphatase CIL-1, also cause cilia defects (Bae et al., 2009). CIL-1 regulates the localization of ciliary receptors and the transient receptor potential polycystin (TRPP) complex. Moreover, products of *tubby* and *tubby-like* genes bind phosphoinositides. Tubby protein family member, TULP3 (Tubby-like protein 3), for example, bridges the IFT-A complex and membrane PIs to mediate GPCR transport into cilia in mammalian cell culture (Mukhopadhyay et al., 2010).

In addition to indirect information regarding ciliary PIP content mentioned above, direct evidence from multiple models has been generated in the last several years. Work from Chávez *et al.* revealed that PI(4)P is the major ciliary PI whereas PI(4,5)P₂ was not detectable in primary cilia from neural stem cells using lipid antibody staining (Chávez et al., 2015). In a parallel study, Garcia-Gonzalo *et al.* confirmed that PI(4)P is enriched in the ciliary but also found that PI(4,5)P₂ localizes to the proximal end of cilia in NIH 3T3 and MEF cell culture (Garcia-Gonzalo et al., 2015). In addition, both studies demonstrated that INPP5E mediated PI(4)P enrichment is required to restrict TULP3 and Gpr161 function, both of which are negative regulators of Shh signalling. How to interpret the presence of both PI(4,5)P₂ and INPP5E at the proximal end of cilia at the same time? A possible answer to this question was provided by Xu *et al.* who showed that PIPKIγ, a centrosomal PI(4)P 5-kinase, counteracts INPP5E to create a PI(4,5)P₂ enriched environment which is crucial for ciliogenesis (Xu et al., 2016). The presence of PI(4,5)P₂ in the proximal end of cilia was also demonstrated in *C. elegans* (Jensen et al., 2015) and *T. brucei* (Demmel et al., 2014). More recently, PI(3,4,5)P₃, together with PI(4,5)P₂, were identified in the ciliary transition zone by Dyson *et al.* using mouse genetics (Dyson et al., 2017). All these studies demonstrated that similar to other organelles, the ciliary membrane also features characteristic PI content.

In Chapter 2, I tried to identify ciliary PIs using PH domain based sensors, which recognize PI(3,4)P₂, PI(4,5)P₂ and PI(3,4,5)P₃ respectively. I focused on PI(4,5)P₂ and PI(3,4,5)P₃ mainly because PI(4,5)P₂ binding proteins were shown to localize in cilia. Among all the PIs that were tested, I found that PI(4,5)P₂ is enriched the most in primary cilia of muscle cells. The degree of enrichment appears, however, to be relatively low. PI(3,4,5)P₃ was also identified with low frequency in cilia in my studies. The ciliary PI(3,4,5)P₃ content revealed in my experiments appears, however, much lower compared to what Dyson *et al.* showed. Overall, my data are nonetheless consistent with published studies.

How to interpret the differences between my results and published data?

First, PI(4,5)P₂ was more frequently found in muscle cilia than in epithelial cilia according to my data. The differences between studies may thus be due to different cell types examined. Specifically, epithelial cells are polarized but muscle cells are not. It is therefore important to note that all published papers regarding PI(4,5)P₂ ciliary content, were based on the analysis of non-polarised cells such as NIH 3T3 and MEFs. Second, in my work, PI detection experiments were carried out using *in vivo* live imaging in a developing organism, while the published work was done in mammalian cell culture. The PI composition is likely to depend on developmental stage, which is another possible reason for differences between my data and published work. At 2dpf, which is the time point that I focused on, zebrafish embryos are still undergoing multiple developmental transformations and cell proliferation and differentiation processes are highly active. In many embryonic tissues (epithelia and muscle cells for example), there is still a substantial portion of cells, which continue to proliferate. By contrast, in tissue culture after serum starvation, cells do not divide and cilia are differentiated to a similar degree. Possibly then in my studies, PI(4,5)P₂ was visualized only in quiescent or differentiated cells.

5.4 PI function in cilia

What role do ciliary PIs play in ciliogenesis and later in cilia function? As the absence of cilia usually results in embryonic lethality, human ciliopathies are most often caused by mild cilia dysfunction such as defects in ciliary protein transport or signal transduction. The transport of transmembrane signalling proteins to cilia, such as Opsin (a GPCR), or Polycystin (a TRP channel), requires a series of closely inter-related steps: first vesicle transport to the base of cilia, then crossing the selective diffusion barrier at the transition zone, and finally intraflagellar transport along the ciliary axoneme. These transport steps are selectively enhanced by a number of mechanisms, including microtubule and membrane modifications (Schou et al., 2015). Membrane phospholipids in particular are likely to function at each step of ciliary transport mechanisms.

My sensor experiments did not detect high levels of PIs in cilia, suggesting that ciliary PIs function at low concentration. If so, the PI depletion by the effectors would generate ciliary phenotypes that could give important clues into the function of PIs in ciliary transport and ciliary signal transduction.

5.4.1 The role of PI(4,5)P₂

The depletion of PI(4,5)P₂ by Inp54p expression resulted in a bulge forming at the cilia tip. At least two scenarios can account for this phenotype.

Hypothesis A: Since the phenotype observed in Tg(*hsp70*: Arl13b-EGFP-Inp54p) embryos is similar to that described in IFT-A mutants (Boubakri et al., 2016; Liem et al., 2012), bulge formation at cilia tip may be due to interruption of retrograde transport. As reported previously, PI(4,5)P₂ interacts with the IFT-A complex via TULP3 (Mukhopadhyay et al., 2010). Therefore the depletion of PI(4,5)P₂ may affect retrograde transport due to

IFT-A dysfunction. The IFT-A complex can be affected in at least two ways: 1. PI(4,5)P₂ may play a role in the assembly of the IFT-A and IFT-B complex at the base of cilia. Consequently, the depletion of PI(4,5)P₂ results in the absence of the IFT-A complex from IFT trains; 2. At the cilia tip, PI(4,5)P₂ may function as a signal for the IFT train, which switches from the IFT-B kinesin transport mode to the IFT-A dynein mode (Ishikawa and Marshall, 2011). The absence of PI(4,5)P₂ from the tip would cause accumulation of IFT-trains and their cargo at cilia tips, which would result in retrograde transport defects. To test these hypotheses, IFT particle accumulation should be examined using antibody staining for the IFT-A and IFT-B complex.

Hypothesis B: In the ciliary tip, there is a low amount of PI(4,5)P₂, which may function as a regulator of the ciliary architecture. Kinesin-4 family protein Kif7 is one of the well-studied ciliary tip complex components, which is also an evolutionarily conserved regulator of shh signalling pathway. In *Kif7*^{-/-} mutant mice, neural tube cilia are longer, twisted and display multiple tip-like structures (He et al., 2014). In Chávez *et al.* paper, PI(4,5)P₂ was not detected in wild-type cells. It was, however, highly enriched in cilia of *inpp5e*-deficient cells, especially at the tip. It is therefore possible that a low amount of PI(4,5)P₂ naturally occurs at the cilia tip and regulates the tip complex function. If this is the case, the depletion of the PI(4,5)P₂ may cause structural abnormalities of the ciliary tip.

5.4.2 PI(3,4,5)P₃ function

PI(3,4,5)P₃ regulates the formation of the basolateral plasma membrane in epithelial cells (Gassama-Diagne et al., 2006). In polarized epithelial cells, PI(3,4,5)P₃ is localized at the basolateral plasma membrane in a stable manner but is excluded from the apical plasma membrane. The ectopic overexpression of PI3K increases the amount of PI(3,4,5)P₃ at the apical surface (Hirono et al., 2004). As a consequence, cilia from the spinal canal

may disappear or differentiate in an abnormal way. This may be due to the ectopic PI(3,4,5)P₃ that affects the cell cycle or basal body docking. The spinal cord is one of the fast-developing organs, which may make it very sensitive to defects in centriole localization or function. In an alternative scenario, the ciliary expression of PI3K generates higher level of PI(3,4,5)P₃ in the ciliary shaft, which acts as an activator of signalling pathways. Misregulation of signalling pathways could result in cilia disassembly.

5.4.3 PI(4)P

What is the role of PI(4)P enrichment in the ciliary membrane? Despite recent advances, the understanding of how cilia acquire a unique lipid composition still remains largely unclear. For example, the ciliary role of OCRL remains undefined. The biological significance of PI(4)P enrichment in the ciliary membrane is poorly understood. In non-ciliated cells, one *in vitro* experiment demonstrated that the binding between PI(4)P and CEP164 inhibits the interaction between CEP164 and Ttbk2 (Xu et al., 2016). This would most likely inhibit ciliogenesis. In ciliated cells, PI(4)P function and its binding partners remain to be identified. Moreover, the Golgi complex is another PI(4)P membrane enriched organelle (Godi et al., 2004). It is likely that the Golgi complex contributes to ciliogenesis by supporting vesicle transport. It thus appears that PI(4)P may function at multiple stages of ciliogenesis either as an inhibitor or as a pro-ciliogenic factor.

5.5 Potential clinical benefits of this work

The *inpp5e* mutant, transgenic PI sensors and effectors generated in this work could be a very effective tool for studying INPP5E-related Joubert syndrome. First, combining a collection of PI sensors with mutant background allows us to study the possible pathology of INPP5E-related Joubert syndrome. For example, by crossing the PH-PLC and PH-BTK line respectively with *inpp5e*^{+/-},

I am able to have *Tg(hsp70:PH-PLC-mcherry);inpp5e^{+/-}* and *Tg(hsp70:PH-BTK-mcherry);inpp5e^{+/-}*. By examining the PH-PLC and/or PH-BTK sensor intensity in the mutant and control background, it allows us to distinguish the substrates of INPP5E *in vivo*. It is possible that in some organs or types of cells, INPP5E selectively dephosphorylates PI(4,5)P₂ but PI(3,4,5)P₃. It is also possible that different symptoms have different underlying molecular mechanisms. For example, the polycystic kidney might be associated with the up-regulated PI(3,4,5)P₃ level whereas retina degeneration could be due to PI(4,5)P₂ accumulation. Second, using a collection of effector lines, it allows us to test if rescue can be achieved by targeting a replacement enzyme, which can functionally mimic INPP5E. For example, the overexpression of *Ptena* could rescue the polycystic kidney phenotype by reducing or abolishing cysts in the kidney, or, the overexpression of *Inp54p* would help outer segment regeneration in the mutant photoreceptor. Moreover, by inducing enzyme expression at different time points and quantifying the phenotype rescue level, we are able to reveal at which developmental stages unbalanced PI levels initiate Joubert syndrome. These studies do not only improve the understanding of the role of ciliary PIs during vertebrate development but also will suggest new potential therapeutic methods for INPP5E-related Joubert syndrome patients.

5.6 Future plans

5.6.1 Additional controls

Studies presented in this thesis will have to be supplemented with additional experiments. One possibility is that some of the ciliary phenotypes observed in effector overexpression experiments are not due to PI function in the cilium but to low level of effector expression in the cytoplasm. The kinase or phosphatase overexpression may globally change the PI environment in the

cytoplasm. It is therefore possible that some cilia phenotypes that I observed are not due to a disruption of ciliary PI content but are a consequence of cytoplasmic effects. To distinguish cilia intrinsic phenotypes from cytoplasm effect phenotypes, I generated non-cilia targeted effector transgenic lines, which can be used as a control in these studies.

5.6.2 Determination of ciliary PI composition in zebrafish model of human ciliopathies

PH domain based sensor lines and PI effector lines can provide tools to analyse the PI defects in wild-type and mutant backgrounds, especially in mutants with mutations related to human ciliopathies.

As the first step, I will apply PH domain based sensor to test PI composition change in human ciliopathy zebrafish mutants with mutation on Joubert syndrome gene *inpp5e* and Lowe syndrome gene *ocrl*. I will cross PH domain based sensors into *ocrl* and *inpp5e* zebrafish mutants. *Ocrl* mutant is available in our lab and *inpp5e* mutant will be generated by the CRISPR/CAS9 technique. For the *inpp5e* mutant, I hypothesize that INPP5E dephosphorylates different substrates depending on different organs, tissues or cell types. In addition, I would like to distinguish which phosphorylation event is controlled by OCRL and INPP5E in cilia. This can be examined by imaging the ciliary localization of PH-BTK and PH-PLC sensors in mutant background.

As the second step, rescue experiments will be carried out once I determine the PI composition changes occurring in ciliopathy mutants. I will manipulate PI content in the ciliary and periciliary membrane to minimize the mutant phenotypes by inducing the effector expression. To test this strategy, I will first use the *inpp5e* mutant. PI(4,5)P₂-5 biphosphate Inp54p overpression in cilia should decrease the PI(4,5)P₂ concentration, and PTEN overpression should decrease PI(3,4,5)P₃ in cilia. I hope this manipulation will rescue or

partially rescue the mutant phenotype. If it is successful in the long run, this strategy may be useful as a treatment for ciliopathy patients.

5.6.3 Further studies on effector lines

It is likely that my studies performed thus far identified only a small subset of PI-related ciliary phenotypes. To identify additional functions of ciliary PIs, multiple heatshocks will be applied to deplete PI(3,4,5)P₃ or PI(4,5)P₂ in cilia from early stage. This may cause ciliopathy-related phenotypes, such as cystic kidneys, photoreceptor degeneration, anosmia, metabolic defects and hedgehog-related phenotypes. I will apply standard histology methods to evaluate photoreceptor loss. To test for more subtle changes in photoreceptors, opsin transport will be monitored using the opsin-GFP assay that was mentioned in chapter 4. In the kidney, I will evaluate morphology and cell proliferation rates. In addition, I could use behavioural assays to test olfaction, which also depends on GPCR signalling and is defective in ciliopathies. Finally I will also inspect cilia motility. These analyses may also reveal unexpected results, such as left-right asymmetry defects, planar cell polarity abnormalities or behavioural anomalies, which would point to unidentified functions of PI(3,4,5)P₃ or PI(4,5)P₂ in cilia.

Overall, these studies developed a method that is generally applicable to the manipulation of ciliary content of PIs using various enzymes. This approach, combined with genetic studies, will provide fundamental insights into the role of PIs and PI-related disease loci in cilia.

Chapter 6

Chapter 6

Materials and methods

6.1 Zebrafish maintenance

Zebrafish husbandry was performed in the aquarium of the University of Sheffield and conformed to UK Home Office requirements. Adult fish were maintained on a 14 hour light/10 hour dark cycle at 28 °C and fed with live artemia or dry food once/twice a day. Breeding and experiments were performed under the project licence 40/3624 held by Jarema Malicki. All experiments conformed to UK Home Office regulations.

Zebrafish (*Danio Rerio*) wild-type lines used in this study were AB and LWT (London Wild Type). Fish were pair mated and embryos were sorted and placed in 90mm diameter Petri dishes containing fresh E3 media (5mM NaCl, 0.17mM KCl, 0.33mM CaCl₂ 0.33mM MgCl₂, PH7.2) with addition of methylene blue.

6.2 Generation of transgenic lines

6.2.1 Engineering of DNA Constructs

6.2.1.1 Entry clones

For sensor lines, PH-PLC delta, PH-BTK and PH-TAPP1, all the entry clones were made through BP reactions and followed by LR reactions for the final vectors. For the effector lines, Arl13b-EGFP-Ptena, Arl13b-EGFP-INP54, were inserted to pME-MCS through Xho I/BamH I for entry clones and followed by LR reactions for the final vectors. Arl13b-EGFP-PI3K was inserted to pME-MCS through Xho I/Not I and the following steps were the same.

6.2.1.2 BP reaction

Gateway BP Clonase II Enzyme Mix (11789-020) was used to carry out BP reactions. The following components were added to a PCR tube at room temperature and mixed: *attB*-PCR product (150ng), pDONR221 (150ng) and TE buffer (PH 8.0) to 8µl. One microliter of BP Clonase II enzyme was added and sample was incubated at 25°C overnight. One microliter of Proteinase K was added and incubated for one hour the next day and transformation was followed.

6.2.1.3 LR reaction

Gateway LR Clonase II Plus Enzyme Mix was used for three-fragment vector recombination. Three entry clones were p5E-hsp70, pME-target fragment and p3E-polyA. The destination vector was pDestTol2-CG2, which included the *cmIc2:eGFP* as a fluorescent marker. The following components were added to a PCR tube at room temperature and mixed: p5E-hsp70 (10 fmoles), pME-target fragment (10 fmoles), p3E-polyA (10 fmoles), pDestTol2-CG2 (20 fmoles), dH₂O or TE buffer (PH 8.0) to 8µl. One microliter of LR Gateway reaction enzyme was added and sample was incubated at 25°C overnight. In the next step, 1µl of Proteinase K was added and the reaction was incubated for an additional one hour at 37°C. The transformation was followed afterwards.

6.2.1.4 Transformation after BP or LR reaction

For transformation, NEB-beta 10 competent cells (C3019H, New England Biolabs) were used. A tube of NEB-beta 10 competent cells were thawed on ice and 25 µl was taken for transformation. 10 µl of LR reaction (see above) was added into an eppendorf with 25µl of competent cell and kept on ice for 30 minutes. Cells were heat-shocked by incubation at 42°C for 30 seconds and

immediately tubes with cells were placed on ice for 3-5 minutes. 250µl of SOC medium was added and cells were further incubated at 37°C for one hour with shaking at 225 rpm. The liquid culture was sprayed on the agar plate with relative antibiotic.

6.2.1.5 Primers and templates

- **PH-PLC**

Template: GFP-C1-PLCdelta-PH (Addgene plasmid #21179)

PH-PLC BP reaction F: GGGGACAAGTTTGTACAAAAAAGCAGGCTTCGCC
ACCATGGACTCGGGCCGGGACTTCC

PH-PLC BP reaction R: GGGGACCACTTTGTACAAGAAAGCTGGGTCCTG
GATGTTGAGCTCCTTCAGG

PLC^{K30LK32LR40L}-F: TTGGTGTTCAGCTCATGGAGGAGAGAGCTGTTCT
A CAAGTTGCAGGAGGAC

PLC^{K30LK32LR40L}-R: CAGCTCTCTCCTCCATGAGCTGGACAACACCAACAGG
AGCTGGCTGCCCTTC

- **PH-Btk**

Template: pRSetb-PH-BTK (Wonhua Cho's lab, University of Illinois at Chicago, Chicago)

Sequence:

ATGGCCGCAGTGATTCTGGAGAGCATCTTTCTGAAGCGATCCCAACAGA
AAAAGAAAACATCACCTCTAACTTCAAGAAGCGCCTGTTTCTCTTGACC
GTGCACAACTCTCCTACTATGAGTATGACTTTGAACGTGGGAGAAGAG
GCAGTAAGAAGGGTTCAATAGATGTTGAGAAGATCACTTGTGTTGAAACA
GTGGTTCCTGAAAAAATCCTCCTCCAGAAAGACAGATTCCGAGAAGAG
GTGAAGAGTCCAGTGAAATGGAGCAAATTTCAATCATTGAAAGGTTCCCT
TATCCCTTCCAGGTTGTATATGATGAAGGGCCTCTCTACGTCTTCTCCCC
AACTGAAGAACTAAGGAAGCGGTGGATTCACCAGCTCAAAAACGTAATC
CGGTACAACAGTGATCTGGTTCAGAAATATCACCTTGCTTCTGGATCGA

TGGGCAGTATCTCTGCTGCTCTCAGACAGCCAAAAATGCTATGGGCTGC
CAAATTTTGGAGAAC

PH-Btk BP reaction F: GGGGACAAGTTTGTACAAAAAAGCAGGCTTCGCC
ACCATGGCCGCAGTGATTCTGGAGAGC

PH-Btk BP reaction R: GGGGACCACTTTGTACAAGAAAGCTGGGTTCGTTCC
TCCAAAATTTGGCAGCCCATAG

- **PH-TAPP1**

Template: C1-TAPP1 (pEYFP) Dario Alessi (University of Dundee)

Sequence:

ATGTTTACTCCTAAACCACCTCAAGATAGTGCGGTTATCAAAGCTGGATA
TTGTGTAAAACAAGGAGCAGTGATGAAAACTGGAAGAGAAGATATTTTC
AATTGGATGAAAACACAATAGGCTACTTCAAATCTGAACTGGAAAAGGAA
CCTCTTCGCGTAATACCACTTAAAGAGGTTCATAAAGTCCAGGAATGTAA
GCAAAGCGACATAATGATGAGGGACAACCTCTTTGAAATTGTAACAACGT
CTCGAACTTTCTATGTGCAGGCTGATAGCCCTGAAGAGATGCACAGTTG
GATTAAGCAGTCTCTGGCGCCATTGTAGCACAGCGGGGTCCCGGCAG
ATCTGCGTCTTCTGAGCATCCC

PH-TAPP1 BP reaction F: GGGGACAAGTTTGTACAAAAAAGCAGGCTTCG
CCACCATGTTTACTCCTAAACCACCTCAA

PH-TAPP1 BP reaction R: GGGGACCACTTTGTACAAGAAAGCTGGGTTCGG
GATGCTCAGAAGACGCAGATCTG

- **PH-AKT**

PH-AKT (pME-MCS) was a gift from Xingang Wang (P. Ingham Lab in Singapore)

- **Arl13b (Danio Rerio)**

NCBI reference sequence: NM_173272.1

Template: pCS S10 vector, gift from Dr. Zhaoxiao Sun (Yale University)

Arl13b-XhoI-F: ATTCTCGAGGCCACCATGTTCAATCTGATGGCGAACTGTT

GCAAC

Arl13b-HindIII R: AATAAGCTTGGAAATGACATCATGAGTATCGCTGTTC

Arl13b(1-307)-HindIII R: AATAAGCTTTTCATCTTCCTCTTCTTCCTC

- **EGFP**

Template: plasmid from Malicki Lab

EGFP HindIII F: AATAAGCTTATGGTGAGCAAGGGCGAGGAGCTG

EGFP EcoRI R: AATGAATTCCTTGTACAGCTCGTCCATGCCGAGAG

- **Ptena454 (Danio Rerio)**

Template: Ptena454 in pT7TS vector (gift from Greg Kelly, University of Western Ontario)

Sequence Ontology ID: SO:0000704

Ptena454 EcoRI F: GGCGAATTCATGGCAATGACTGCTAAACTAAAAG

Ptena454 BamHI R: ATTGGATCCGACTTTTGTAACTGTGCGTG

Ptena454^{C124GG129E}-F:

GGCAAGGCAGGCAAAGAGCGCACAGGTGTCATGATATG

Ptena454^{C124GG129E}-R:

CTCTTTGCCTGCCTTGCCGTGGATGGCAGCCACATGG

- **PI3K**

Template: pSD64-p110^{K227E}CAAX (gift from Dr. Yasushi Okamura, Osaka University. Originally from Dr. Thomas Franke, New York University)

NCBI Reference Sequence: NP_006209.2

PI3K BamHI F: ATTGGATCCCCTCCAAGACCATCATCAGGTGAACTGTGG

PI3K NotI R:

ATTCTTGTGTCAGCGGCCGCTCAGTTCAAAGCATGCTGCTTAATTGTG

PI3K (K802R)-F2: CATCTTTCGAAATGGGGATGATTTACGGCAAG

PI3K (K802R)-R2: CCCATTTTCGAAAGATGATCTCATTGTTC

- **Inp54p and Inp54p^{D281A} (*S. cerevisiae* (budding yeast))**

Template: plasmids from Addgene #20155 and #20156

Inp54-EcoRI-F: GCCGAATTCATGAACAAAACGAATTGGAAGGTATC

Inp54-BamHI-331-R:

ATTGGATCCTCACGGCACTGGCGTCCCTGTAGACCTTG

- **Rhodopsin CT44 (*Xenopus*)**

Template: plasmid from Malicki Lab

Sequence:

AAACAGTTCCGTAAGTCTGCTTGCACACCCTGTGCTGTGGAAAGAATCC

ATTCGGTGATGAAGATGGCTCCTCTGCAGCCACCTCCAAGACAGAAGCT

TCTTCTGTCTCTTCCAGCCAGGTGTCTCCTGCA

Opsin-sv40-F: CACATGGACAGCAAACAGTTCCGTAAGTCTGC

Opsin-R: ATGTCTGGATCTTATGCAGGAGACACCTGGCTG

- **XOPS**

Template: XOPS-EGFP-N1 (Malicki Lab stock, gift from Jim Fadool)

Sequence: GenBank U23808.2

XOPS-508-F: ATTCTCGAGCTGCAGCCCCTAGGCCATG

XOPS-R: ATCGGATCCCTAGAAGCCTGTGATC

XOPS-1324-F: GCTCTCGAGAGATCTTTATACATTGCTC

- **Other vectors or plasmids**

pDONR211, pDestTol2-CG2, pDestTol2-PA2, pME-MCS, p5E-MCS, p3E-mcherry-PA, p3E-PA, pME-Cre, pDestTol2-hsp70-lox2272-mcherry-lox2272-TEV-S-peptide-EGFP-opsinCT44ctrl are all achieved from Malicki Lab stock.

6.2.1.6 Preparation of competent cells

A single colony of *E. coli* was inoculated into 3ml LB in a 15 ml falcon tube and grown overnight at 37°C. Further growth was accomplished by inoculating 1ml of the above culture into 100ml LB in 250 ml bottle. OD value was

monitored to keep it lower than 0.4. Ice was used to keep the cell cool for about 10 min. Cells were collected by centrifugation for 5 min. at 4000 rpm. The supernatant was discarded and the pellet was re-suspended using 10ml of pre-cooled 0.1M CaCl₂ in a gentle way. Resuspended cells were kept on ice for 20 min. and centrifuged for 5 min. at 4000 rpm. The supernatant was discarded again and the pellet was resuspended using 5ml of ice cold 0.1 M CaCl₂/15% Glycerol. 100 ul aliquots was prepared and stored in -80°C.

6.2.1.7 Bacterial cultures, plasmid isolation and restriction digests

Plasmid DNA can easily be propagated and amplified in bacteria such as New England Biolabs' 10-beta *E. coli* strain. The transformation of plasmids into 10-beta cells was performed according to supplier's (Posor et al.) specifications. Bacterial colonies were selected on plates with 10µg/ml kanamycin, 10µg/ml ampicillin depending on plasmid antibiotic-resistance gene. For most subsequent applications, the plasmid DNA was amplified further in bacteria. For small bacterial cultures (up to 10 ml) this was done using the isolate II plasmid mini kit (BIO52056, Bioline) according to the manufacturer's manual. For larger cultures up to 100 ml the NucleoBond Xtra Midi Kit (Macherey-Nagel/Germany) was employed according to manufacturer's instruction for high-copy plasmid purification protocol.

Restriction enzymes digests were performed with New England BioLabs (USA) enzymes according to manufacturer's instructions.

6.2.1.8 DNA purification

Purification was generally applied to the DNA amplification products after PCR reactions or restriction enzyme digestions to clean the salts and residual nucleotides for further applications. DNA was purified using EZNA gel

extraction kit (v-spin) (OMEGA, D2500-01) following manufacturer's instructions.

6.2.1.9 Colony PCR and restriction digestion

Colony PCR and restriction digestion were applied to select the correct clone. Bacteria from individual colonies were lysed in a PCR tube with 10µl fresh milliQ water. 5µl of the lysis was used as the template for PCR reactions, which were carried out using Reddy MIX (Thermo, AB0575DCLDB). Primers applied were either from the insert sequence or from the vector. Amplified DNA was run on the gel to identify correct clones.

Two to three correct clones were chosen to inoculate liquid culture. Plasmids were purified from liquid culture using the Isolate II plasmid mini kit (BIO52056, Bioline) as mentioned above on the following day and restriction enzyme digestion was used to further confirm that recombination proceeded correctly.

6.2.2 Preparation of capped Tol2 transposase mRNA for injections

pCS2 transposase vector was linearized to completion through NotI digestion and purified using the Qiagen PCR purification Kit. Ambion mMessage mMachine SP6 kit was used for the transcription as described in the manufacturer's instructions (3ul of 400ng/ul DNA, 5ul of NTP CAP mix, 1ul of 10x buffer, 1ul of enzyme mix). Transcribed mRNA clean up was carried out using Qiagen RNeasy MinElute (Qiagen, Cat. #74204) kit elute with 14ul of fresh milliQ water. mRNA concentration of about 1 ug/ul was obtained.

6.2.3 Microinjection of embryos with a mix of transposon DNA and transposase mRNA

The injection mix contained the following components: 25ng/ul of DNA, 25 ng/ul of transposase, 1ul of phenol red (P0290, Sigma) and dH₂O added to obtain the final volume of 10 ul. After the RNA or DNA was back loaded into the needle (GC100TF-10, Harvard Apparatus), the needle tip was broken to make a small opening. Injection volume was adjusted to about one tenth of yolk size using microinjector settings. Injection was performed no later than the one-cell stage for both mutant generation and transient expression assays.

6.2.4 Selections of transgenics

G0s were selected for raising on the basis of *cmlc*:GFP expression in the heart or heat-shock induced fluorescent signal. Specifically, all sensor lines, as well as the effector lines PTENA and PTENA^{C124GG129E}, were constructed using the pDestTol2-pA2 destination vector, which does not contain the *cmlc*:GFP maker. To identify transgenics of these lines, heatshock was required. For the rest of effector lines, however, the pDestTol2-CG2 was used, which contains the *cmlc*:GFP heart marker. As the *cmlc*:GFP cassette is independent from the heat-shock promoter, the individual embryos that express transgene can be identified on the basis of green fluorescence in the heart without the use of heat-shocking.

To generate stable lines, three months after injection, the G0s were out crossed to wild-type fish and the positive F1 embryos were selected to raise by fluorescent markers as above. Another three months later, the best lines were selected by observing transgene expression in F2 embryos. Confocal microscope was applied to collect images of cilia expression in multiple organs, in selected transgenic lines.

6.2.5 Heatshock procedure

For embryos from 6-60 hpf, PCR machine was used. Up to 3 embryos were

placed in each well of a PCR plate. A 96 well PCR plate was used when a large number of embryos were needed. The plate was sealed with a sealing tape Polyolefin Film 100 (Starlab). A small hole was made with a probe in the sealing tape to facilitate air circulation. The PCR machine was programmed as follows: 23°C for 5 min, 39°C for 30 min. and 28.5°C incubation after that. Subsequently, embryos were removed from the PCR machine and placed in E3 medium.

Older embryos or larvae were heat shocked in a heating block in a 15 ml falcon tube. Before heatshock, petri dishes with embryos were moved out from the incubator and kept at room temperature for at least 15 mins to cool down. 3 mls of fresh E3 medium was preheated for each 15 ml falcon tube to 39°C. Embryos or larvae were then transferred into falcon tubes with preheated E3 medium with as little cold medium as possible and incubated in a heating block at 39°C for half an hour. Afterwards, all larvae were moved to petri dishes with fresh 28.5°C E3 medium and kept in in an incubator at 28.5°C.

6.3. Generation, selection and identification of *inpp5e* mutants

6.3.1 Using CRISPR/Cas9 system to generate *inpp5e* mutants

To generate mutant strains, Cas9 and guide RNAs were prepared and injected. The final concentrations of 2.4 µg/µl gRNA with 0.5 µg/µl of Cas9 mRNA were used. RNA was injected into one-cell stage embryos. The fish larvae with no obvious morphology defects were selected and raised to adulthood.

In total, 5 gRNAs were designed and sequences are indicated below. The fifth gRNA (CR5) worked according to T7 assay results and were used for mutant generation.

● **CRISPR- INPP5E**

GenBank: BX001023.12

(<http://www.ncbi.nlm.nih.gov/nuccore/BX001023?report=GenBank>)

GTCTGGCGTTGCTAAGGAAGTCAAGTAAGTTTTCTTCATCTGCGAACTGG
AGGTAACAAACATCAATTTTCAGCTTAAATATGCGTCATTTAGTTATTCACA
CCAATGTATCGTAATATAGCTTTTAGTTCAATTTTATGGATTATATTTTACA
AAAAGGAAAATGCTAGGTTTGAAGTGTAGCCAGCAAACGCCTGACATCA
GTGAATATATCATCGCTGTGAGAGACAGAGATTTTCAGTCAACTGTAAACA
ATTTATTTATCACTATACATGGCTTTTAATTATATTTGGTTAAGTGTTAGTT
AACATCTAATACCAAACATTTCGCTCGGAGGAAACGCCATTATATTTTACTA
ATGATAATAATAACGGTTTGCTTGTTTTTCATGGTAATGTTGTTTAATTCGT
CGATTACCATATAATAATCTAATTGTTTATAATGCGTTATAAATACAGTATG
TTTGATTGAGATAAACGGTCTTGATTGAGGTAAGCTATCTTTATATTTG
CACATTCGCCAGTGACAGCTAGTGACATGCTCACTAACGTTATATTATT
TACCATGGTAACGTTACGTTACTTTGAATATTCGGTCTGAAATCACAAACA
AGTATGACTTCAAACAACATTATCACTGTTAATTCGACTGAAACATTTTG
GACTTTGATAGTCACTGGCTGCTGATATGATTTTCAGATATGATTTCAAATT
TAGAATTGGCAAGGAATACTTTTATGAAATTATATTATTAAGAAGAAAGTC
TGAATCTGTGAATATAAACTGAATATAATATAAATATAAATAAAGTTTACCT
CAGTCATTATTGTTGGGCAATTACCATTCAATTTTTTAATAACTTTTTCCA
TTAAATAATATTGAAAAATATGTTACTTAGAATGTTGCAATGCAGGATTCC
AGAGGTTTTTAAAGCTATATATATATATATATATAGCTTATATATATACA
GTTGAAGTCAGAATTATCAGCCCCCTGAATTATTAGTGCCCCCTGTTTAT
TTTTTCCCAATTTCTGTTTAATGGAGGGGAGATTCTTTCAGCACATTTCT
AAGCATAATAGTTTTAATAACTAATTTCTAATAACTGATTTATTTTATTTTTC
CCATGATGACAGTAATTAATATTTTACTTAATATTTTTCAAGACACTTCTAT
ACAGCTTAAAGTGACATTTAAAGGCTTAACTAGGTTAGTTAGGTGAACTT
TGCAGGTTAGGGTAATTAGGCAAGTTATTGTATAACAATGGTTTGTCTG
TAGACTATCGAAAAAAAAAATTAGCTTTTTAAAGGGCTAATAATTTTGTCCC
AAAAATGGTTTGTAAAAATTAATAACTGTTTTTATTCTAGCCGAAGTAAA
GAAAATAAGACTTTTTCCAGAAGAAAAAAAAACACAAATTTAAACATAATTT
GGGAAATATTGCAAAAAGAAGAAAAAAGTCAAAGGGGGCAAATAATTCT
GACTTCAACTGTGTGTGTGTGTGTGTGTGTGTGTGTGTGTATATACACAC
ACA
CACACACACACACACACACACACAGTTGCAATCAGAATTATTAACCCT
GAATTTTTAGCCCCATTTATTTTTCCCTCTAATTTCTGTTTAACAGAGAG
AAGATTTTTCAACACATTTCTAATCATAATAGTTTTAATAACTAATTTCTA
AAAATTTATTTATTTAACTTTGCCATGATGACAGTAAATAATTTGACTAG
TTTTCAAGACACTTCTATAAAGCATTAAAGGCTTAAATTGGGTAACTAGG
CAGGTTAGGGTAATTAGGCAAGTTCATGTATAACAATGGTTTGTCTGTA
GACTATAAAAAAATGCTTAAAGGGGCTAATAATTTTGTACCTTAAATGCTTT
TTTTTTTTCTTTTTTTTTCTTTTAATTAAACTGCTTTATTCTAGCCGAAAT
ACACAAAAAAGAAAACCATTATTTTTACAGACTCTAAATCTTGCCCTCAA

CATATGGAATCTTAAAAGAGTGATCATCCCTTGATTGAAAATATTTAACTC
AAGTTCACCACCTACAAAACAAATTTTACCATATCATTTTTTTGCTGGATAC
CAGGACATGCTGAACTTTCAGGGAATGAACGAGCGGATGCAGCTGCTAA
AGCCGCTCTAAAACAAGCTGTGAACAAATGTCAAACCTTCTCCGTCAGAGA
TGAGACCTTTTATTTACAATTACATTTTAAACAAGTGGCAAGAGGAGTGG
GATACTCTGGAAAACAATAAATTACATGAAATCCAGCCTGAAATTACACA
CAGAGGTATAAAAACATTTTAAAGAAACGAGCTGATCAAGTAATTTTTACCA
GATGTCGTATTGGACATACAGGATTAACACATAACTTTTTACTCAAAGATG
AAGAGCCTACCCAATGTTTGCCTGTAAAACCCCATGGACCGTAAAACC
CATTTTACTGGACTGCCCTGCTTTTAAATGACTTCAGAAAGACTTTTTGTGA
TGAGAACTCTCTTAAGGACATTTTGAACAAAGTGACACCAGAAAAAGTAT
TAGAATTTTTAACATGTATTAACGAGAAAAATCTTATTTAATCTGTATATTC
AATTATTTATTTTAACTGTTGATGTTTTTCAATTACTGAAATGCTCATGCC
ATGAAAATAGCTTTAGTAGCTGACATGGCAATACATAAATAAATAAATAA
AACCTGAGAATATTTTTAAATTAGCTTATTAATTATATGTAATATCATTAAA
AAAAGTAATTCAATGACTGATCATAAATAATCTCGTTGTCTCCACAGGAT
GTAATCAGCAGAGTACCATGGGGCTTGTTTACATCTAAAATCAAGCCCGC
CAATAGGATGAGTGAGCATGGAGACAGCATTGTCCCATTTAACCCACA
GATCTCAGGTCAGGAGAACCAGCCACCAAACGGACATCACTGTCCTGA
GTGTAGACCTGAGGACAGAGAAGAGCCACAATGAGGAGCTCAGAGACA
TTAAGAAGCCATACGATGGTCCTAAAGTACTTCAGGATGAGCATAGTCTC
TATCAGCCTCGACCTCCCTCTTCCGAAGCCCATGGGATTGGGAATGG
GGGTAAAACCTCTCGTTTGATGAAAAGGTGAGGGGAAGGAGATTGAG
GAACAGCCAGGAGAGTCTCACGGATCCGGGAGAGACGGGTTCTTCTAC
TGATTCTCTCAAAGATGTTGCCTCAGCAAACGGTCAAACCCTTGCATCTC
GACGTCCTCTCGATCTCCAGCACATGGAGATGCCACCGTTCAGGATTAG
GACCGGGAGCTTGTCCGAGACGGATGTGTCTCCTCATGACCTTTGTGAT
CCGAATAAAGAGCGCATGAAACCATCCAGAATCGTTCTGTCTCCTCTGCA
GCCACAGGCACGTATCCTCTTCTGGAGAACAGCACCCGCCTCTGCGTCT
TTAAGAACAATAATAGGATTGACAGGGATTGTTTGGATTACGGTGTGGT
GGGGAGAAGAGGGCGGTCCGAGAGGCTTCACAGGAATCTGAGCGATAG
CCGGCTGTTGGACACCATGGTGTCCGACAATACATCTGTCCATTCCATG
AAGTCCACATATAGCGTTCTGAACCCCATCAGACCTCGGGATGTGAGGA
ACAGGTGAGAAGCTTTTGTCTTTCTGTTTATAGTTTTCTGCTCTGC
AGATCTCCATGCTCCGCTTTAGGATCACATGTGCTGATGTGTCGTCTTGA
TTACCTCTTAAGAATCTGAAGCTGCGATACATTTGACCATTAGTTGACTTT
AAAGTTGACTCAGAAGTGTTCGACCATCTTAAAGGGATAGTTCACCCC
CAAAAAGACATTTTACTTACCTTCAGGTGGTTACAGACCTTTCTACGTTT
CTTTATTCTGTTAAACACTAAAAAGATGGTTTGAAAAAGCTGACCCATT
GACTTCGTAGGAAAAATGGAAGTCAATGGTTACAGGTTTTCACTTACTT
GAACTATCTTCTTTAGTGTTTAACAGAATAAAGAAAGTCATAAAGGTTTG
TAACCACTTACTTTATTCTGTTAAACACTAAACAAGATAGTTGAAAGAAAG
CTGACCTGTAACCATTGACTTCATAGTAGGAAAAATGGAAGTCAATAGT
TTCAGGTTTCCAGCATTCTTCAGATTATCTTCTTTTGTGTTCAACAGAATA

AATAAAGTCTAACAGGTTTGAACAAGTAAAGCATAATGAATGAATTTTAA
TTTGATCTCTTTAAGTGACATTCTAATGCCTAGGGAGCAAGTATGTTCACT
CTATAGCAAATAAGTGAGCATCGACATCACATGTAATATCAAAGATGTTTA
AATTA AAAAGTGGTCCTGAAGTTATTATAAGTATCGAGTTTATAATGTTAA
TTAACATTAAATCACACCTGTTTTGAGTTGTATTTGTCTGTTCAAAGGTAT
GAAATTAGCATGATTACTGTTAAAGGGATAGTTCACCCAAAAATCTGTAAT
CTTTGACTTTTTATATTGTTTTATTCTTCTATAGAAGTCAATGGTTACAGGTT
TTCAGCTTTTTTCAAACCTATGCTCTTTAGTGTTAACAGAATAAAGAAAGT
CATAAAGGTTTGTAACCACTTATTTTATTCTGTTAAACACTAAACAAGATA
GTTGAAAGAAAGCTGACCTGTAACCATTGACTTCCATAGTAGGAAAAATG
GAAGTCAATGGTTTCAGGTTTCCAGCATTCTTCAGATTATCTTCTTTTGTC
TTCAACAGAATAAATAAAGTCAAACAGGTTTGATACAAGTAAAGCATGAT
GACAGAATTTTAATTTTATCTCTTTAAGTGACAATGCCTAGGGAGCAAGT
ATGTTCACTCTATAGCAAATAAGTGAGCATCGATATACATCACATCAAATA
TCAAAGATGTTTGAATTAATAGTGGTCTTAAAGTTATTATTAAGTATCGA
GTTTATAATGTTAATTAACATTAAATCACACCTGTTTTGAGTTGTATTTGTC
TGTTCAAAGGTATGAAATTAGCATGATTACTGTTAAAGGGATAGTTCACC
CAAAAATCTGTAATCTTTGACTTTTGTTTTGTTTTATTCTTCTATAGAAGTC
AATGGTTACAGGTTTTCAGCTTTCTTCAAATATCTTCTTTTGTGTTCAAC
AGACGAAAGAAATATTGAGGAAATGTTCAATTTTAGGTGAACCGTCTTAA
ATAAGATTA AAAAAGATTTCACTTCAATTTAGTTTTATATTAATGCCACA
ACAAATGCCAAATTTGTCACCTCACTTTAGAGCTTTAAGTATGCTCTCATT
GAGCTGCACGATATTGAAAAAATCTAACATTACAATATATATTGCGATAT
GAATACAATTTCAACAAACGAGTTGAATAACCATTTAGAAAGAATTTTAAA
TTTATATATTGATTGGGATGATTCTGTATATTAGTGCAATAAACAATCTAC
AAGCATATGTAAAGTCAATAAAGAAAAAGTACAACCTTAAATTAACAGCCTT
TTATTGTTTTCTAAACTGTATTAAGGAATACATTAATTGAACATTCAAATGC
GCATAGTCTTTGTTTTATAACGATTCAATAAAATTAATCTCTTTTAAATGTG
TGAAATTTACAAATTGTA AATTTCTTAGACCTCATTGCTTTAAAAACCCA
CACACAGTTGCAAATGCTAAATTA AATCTAGACTCAACATTATACATCG
CGTATATATAACAATGTGACTATTGCAAATAATCACATTACGGTATCGATG
CTAAAACATATTGTGCAGGCTTAGCTCTTATATAAATAATAATTATTGCAT
TTCTTATATAAAAATGCTCATTGGCATATTAATAGTGTAATACAAGCCT
GATCTCAGGAGAAAATATAACTATTTTTTGATTTGGCAGAATAGAGACAG
ATTTTTGGTTCATTTTGTCTTCTGTGCATAAGTTCATGACATACCAAGCCA
ACAGCAAAGAACTGGAAGTCAAGAAATGTCTTGTTTGTGTTCCATAGA
TATATACACTATTGCATAGGGACCCTGAGCATGCGTCAATAGCGCCGCC
ACATTTGTACAGGGCTCCCAGGACAAACGTCATTTAACCGCACTATTCAA
GACTGTTACTACATGAAGATGCTGGACTTTAGCGCTGTCTATGGGTGTAG
TAACGAGCAAACAAAGAAAATAAGCTCAAAGGCAGAACGTTTCATAGGT
AAGGTTTAGTTTTTTACGTTTTTGTATGTTATGAACTTTTGTGCTAAACAG
GTAACATTATTGATTATAATACAGTCACTTACTGCATTCACCATAAGGCAA
AGCAGCAGCAACTCACACTAAACACTCGGCTTATGCTAGTTTTGTTGAAT
AAAATCAGCAAACAATGCAAAGAAATATGACAATGAGATGCCGCGGTG

GCTGAAACTTGAATTATTGTCTGTTAGTGAATGAGTCGTTCCATAACAGGG
ATTCATTAACAAACAAATCGCTCCCTCCGTCAGTGTGAGAAGTGAAAGCG
GGAGAGGAGATGTGTTTCAGGACACGGATTAGATCACTTTTAAACAGGGA
GGGTGGATAGTACATTTTCATACACACAAACACAAGCTTTTTGTGAGGAA
TTCCTGTGGGATCACTGATCCATCAATGTAGAAAAGTGATGTAAAATTAT
AATTTTCGTAATTTAAAAATTGCATACTGACCTTCGGGAAAACCTCTGATC
ATAGATATATGTGTATATCTCTGGCTCTGGATGGCCACAGTCCTCCACTG
CAGCTTGGTCCCACATTCATTTCAAAGAAGCGCACCCCTGTAATAAATGG
CGGCTCTATTGACGCATTCCTTCCAATAGACAACAACAGCGTAGGCGAC
ATCTAATGTATATATCTATGTGTTGTTTCATCTAATGCAGGCTGTCGGGTAT
TTTTATTTAAAGTCATCAGAATTATGATATTCAGCCCAATTTCTTGAGG
AAAGAATTGTACGTATAATATTGTCAAACCTCAAAGTCCTGTAACATTTGC
ACTCAAATCCTGATTTTTTTTTCAAAGTAGTTATTTGAAATATGCTGAATGA
ACTGAATTCTTGAGATTTTTTTGGGGGACAACCTTAATGGTTTTATATCAA
TCTACTTCAATTTGTTAAGTTAATGTAATCAATTTGTGTTGGGACAACATG
AATGAATTGTGTGGAGGCCAGCTAGTGTGTGCTGTTCCAGGTAAACCTCA
CTATGGCTATGGTCTTTAGCCTCCTTGGTAGAGCATCCGACTCCCATGC
GGAAGGTTGCCGGTTCGATACCAGCTCGGAGCGAGTTTGGTGGCGTAG
GACCGGCGGGGTTACATTGGTGCCGTGACCCGGATGGGAGTGAGGTTT
AGGGGGGTGAGTGTAAACGGAGGCCAGCTAGTGTGTGCTGTGCAGGTAA
ACCTCACTCCTCTGACCTCAAAGCTGCTCTAGCGCTAGACGCCATGGT
CTTTAGCCTCCTTGGTAGAGCATCCGACTCCCATGCGGAAGGTTGCCGG
TTCGATACCAGCTCGGAGCGAGTTTGGTGGAGTAGGACCAGCGGGGTT
ACATGTGGAACCCTGCATTTCCAGTGTGTGACCGGAATTTCTCTGTTT
GATGACGTTGCAAAGTCAATCCTCAACAGATATCCCGTGCTTAGGGAAC
AGTGAACACTGTGTAGGGACCCTGTAAAACAGAAGTATCAAGGCCTCCT
CTTAAGCAGAATGTGAATATATTTGTGTGATTGAGTTAATAACATGAATTG
TTTCATTATGAAGTGATGAATAATGTTCCCTGCAGGAGTGAGTACACTTGC
TGAGTTCTACAGAATCAGCTGTGATGTTAGACTGACTGTATAGAGAGAGG
GAGAGTGAAGCTGAGTGAATGTAAAGGAGATTATTGGATCAGTAGGATA
CTAGTTCAGCGACTGTCAAACCTGCATCAGGAGACCATTCAAGTTCT
GCTTAAAACGACAGGAGGGTTAAAGAGTGTATGGTCCAATAAGATTGA
GAAAGTCATTTTATGCAGAAAGTAAAGGAAAATGTCTACTTTAATGTTTTA
AAAAATCTACAAATAAAAATAAAAAGTCAAATAGCAATGTTCCAGTCATTC
GTCATTTATTTATGTAAAATAAAAAGCAGATGTTAAACTTCATGCATATTCT
GATCTGACTGTGATTAAGGATACAATGCAAGCGATTAACCTTAGTAAA
GCCTAATGGTATGTAGGATAGTGGTAAAGTAGATTTAAATTATGATTCAT
ATTTGTTTTGCATTGTGATCCTCAATATGTGATCAAATTATTGTTGGTCTA
AATATACCTTTTGGTGTATGGACTATTGTTATTTTGAATGAATTTTTCCGT
GTACGTGAAAATGTATATGGATTTTATATTTGAGATCAGCTAAAATGAT
GACTCATTTAAGTGTATCTGTAACACATAGTATCTAAAATGTAAAATATTG
TACAGTCTCACTTTACAATAAGGTTTTATTAGTTTATGTATTTACTAATTAT
GAGCTATACTTGTACATCATTTGGTAATCATAGTTCAACATTTGCTAATGC
ATTATTAACATCCAATTAATGCTTGTTAAAATTATTGCACTGAGTTTAAAT

GAATTACCAACAAACAACACTGTATTTTTATTAACCTTGCATTAAAGAACATAA
ACAACATAATGTAATATATGTATTGTTGAAATTAGTAAATGCGTAAATGCCT
TAACTAATACAACCTTATTGTTAAGTGTACCTAATGTACTCTAATTTTAAA
GGCTTAAAAATGACTTTTAATGGAGTGTACAAAGACAGCAAAGGTAATTC
ACATCAACAAAAATCTATGAATGAACAGAAATAAAAAATCTATAAAGACTG
CTACATAAAATTGCCAGTACAAAAAAATGAAAATTATTTATATATATATAT
AT
ATATGT
GTGTGTATACATACAGAAAAAAATAAAATGATATATATATATATATATATA
TATATATATATATATATATATACACACAGAAAAAAATTATATATATATATA
TTTAATTA
TATATATATATATATAATTTTTTTTTCTGTGATATTGGCTCATAAATGAT
GTGGTGCAGATTTATAAATAATTATGTCACCACCTGGACAGATTTAAATGT
ATTTATATATTTAAAAAATGCTTTATTTGCTTAATTTTTTTATTATGGGCATA
GAGACAATATTTTTAGCCATAAAAAAACTAAAATACTTAATCCATAAAATT
AAATAATTTGTTATCGGTCAGTCTAATGTAGGTGACAGTTTACCCACCC
TCATGCAAAAAATGTTACAAAAGCAAGGGATTAATGATTGATAAATATTAG
GCACATCAATTCATAAATATAAGAGAAAAAAATCCGTAATAATAACTAAA
CATTTAGTCATTTAACAGAACTTTTGGTCAAAGCGACCTACAATTGAGG
AGACGCTTAGAGATTCAACAAGAATAATTGTTAATTTACAAAGCAACTGT
TTGTGCTCAGATAATTTAGTGCTAGAGTAAGGAGAGGCGAGTTTTTTTGA
GCTTCTACAGGTGGTTTGTCAAGCCCACTCACCTGTGTGAAGCTCGCTT
CATAAACGCAGTGTTTTTTTTAAACAGAGTTATTGTAACAATTAGTCTGG
TGCAGTTGTGCAAATAAACTGGTGCACACATTGGTTAAAGTGTTAAAGA
GATGAAAGAGCGTGTTTTTACAGGTGGTTTGTCAAGCCCACTCACTTGT
TTGAGGCACACTCAGAATTAATGATTTTTGGGGGATGCTACAATATTTCA
TGAAAAATATCTAATTGTA AAAATGATTTGGATTCCATGATGATGTTAAAC
ACATTAATTCTTCAGGAGCTTTCTGGAGGGCAGTGTTTTGGGCAACGGC
GCCTTGCTGGGTGCAGAAGAGCTTGACCGTACTTCCCAGAGAGACGTC
TCGGCATCTACATCGCCACATGGAACATGCAGGGAGAGAAGGTGTGAAC
CAATACTGTCATTCCTAATTATTTTATTTGCATAGGAGTTGTCACCTAAGC
TCTCTTTCTTGCTCTCAGGGCCTTCCATACAATTTAGATGATCTGCTGCT
GCCAACTGACACTGACTTTGCACAGGACGTCTATGTTATAGGGGTTTCAG
GAGGGCTGTCCTGATAGGTGAGATGTTGCTTTCTTGCAGCGTTTAAATGT
CCTTCTTGATACTCATTTTCTTGGGCTTCATGTTTGTCCACAGGAGGGAG
TGGGAGATCCGTCTGCAGGAACTCTTGGGCCATATTACGTGATGCTGT
ATGCAGCAGCCCATGGAGTGCTCTATCTCACTGTATTTGTCAGGAGAGA
CCTCATATGGTTTTGTTCAAGGTAAATCGTTTCTTTAGAATGAAATAGTAGG
GCGGCATGGTGGCTCAGTGGTTAGCACTGTCATCTCACAGCAAGAAGGT
CGCAGGTTTCGAGTCCTGGCTGGCATTCTGTGTGGAGTTTGCATGTTCT
CCCCATGTTGGCGTAGGTTTCTCCGTAGTCCAAAGACATGCTCTATAAG
TGAATTAATAAACTAAATTGGTCATAGTGTATGAATGTGTGTAATGTGA
GAGTGTATGGGTCTTTTCCAGTATTAGGTTGCTGCTGGAAGGGCATGTG
CTGCGTAAAACATATGCCAGAATAGTTGGCGGTTTCATTCCGCTGTGGCG

ACCTCTGATAAATAAGGGACTAAGCTGAAGGAAAACAAATAACTGAATGA
ATAATATAGTATCTTCTCTTCTTTTTCTTTGGCCTTAGTCCCGTATGGTTG
CGGGGTCAGCTCCATTTAGACTTGTCCATATGATAACGACTTTTTAAAATT
TTTTAAAATTTTTTTTTATTTTCATTTTTTTTATACATATTCCGGCCAGCCTGT
CGTCTGGGCCTGTCACCCTCATACTCATACTACGGACAATTTAGCC
TACCCAATTCACCTGTACTGCATGTCTTTGGACTGTGGAGCACCGGAGC
AAACCCACGCGAACGCAGGGAGAACATGCAAACACTCACAGAAATGCC
AACTGAGCCGAGGTTCTGAACCAGCAATCTTCTTGCTGTGAGGCGACAGC
ACTACCTACTGCGCCACTGCTTCGCCCAATGAATATTATGGTATAATAAAA
ATGATAAAAGCATTCAATGTAAAATAATAAATGGTAAAATACATATTTAAAA
ATGATGTATATAAATTTAAAATACATTGAAAAAATTAATAACATTAAACATA
ATACAATATAAATAAAAAAACACACTGAACTGTTAATATAGATAAGTTTAC
AATTACAATAAATTAACATAAAATTACAATTACAATAAAAATTACAATTTA
AAGCAAATGTTTTCAATTCATTAGATTTCTAAATGCAATTTATTCCTGCCAA
TTTTTCAGCAGCTGTTATTCCAGTTTTAAGTGTACATGATTGTTCAATAA
TGACAGAACAATAAGAAAACAGTTATTTAAAATTGTAGTAATAATTCAA
AAACATAACTGTATTGTTATTATTATTTTTTATTAATATAATTTTATAATT
ATTATTAATGTTATTATTATTTTTTAAGTGGTATTTTATAAACAAATTCAG
GAGAAGCACGATCAGTTTTGATGAGGCTAATTCATTATCAACAATCATT
TATTATGCAATCATCTTAAGACCAAACCACCAAAAATAGTCAAACATGTCA
TACCTCTATTTTCTGTTGATTTTAGTATCCCTCCACCACCCCAACTCCACA
CTATTAACATGATACCTACATAAATCTGAGGGGGGAGGGTTCTAGAGC
CGGTCTAGACACTGGCTCAGACTCTGTCCTGATAAGGGGAATAACACAA
GTTAGGGTGTCTTTCTGAGCTCAGAGCCTTTTCCCCGGACAGTGTGCCA
AATACGCCTATTCTATTAGTCTAATATCTGTGAGTGTGAACTCGTTAATT
CAGCCTTGGTGCACAGAATACTTTTGAAAATATTTAAGAACCTACTGAT
TCCATAATTTCTAGTGTAAAGTGTATGTATGTTTATATGTAAATGAACATTAT
GTAATTTGATTTTGGATAAACGTTTTCTACCCAGTGCATTAATGTAATAAT
AATATAATATAATATAATATAATATAATATAATATAATATAATATAATATAAT
ATAATATAATATAATATAATATAATATAATATAATATAATATAATATAATATA
ATATAATATAATATAAAAATATAATAAATAATATAATATAAAAATAAAAATGT
TATAATAATATAATATTATGTAATATAAAAATATTATAAAAATAATATAATATA
ATGTAATATAAAAATAAAAATGTTATAAAAATAACAATAAAAATATAAACTAATA
ATATAATATAATATGTGTCTTTTTCTGACATTACAGAGGTGGAACATGCTA
CAGTCACAACCAGAATTATATCTCAGATTAAGACTAAAGGAGCAGTGGGC
ATCGGCTTCACCTTCTTCGGGACGTCCTTCTCTTTGTCACTTCCCATT
CACCTGTAAGTAGAATATCTCAGAAATTTAAACAAGGGTTCAACAACCCC
AGTTACATGTTACAAAGTCACGATGGCGTTAAATGTATGCTCGATTAATA
ATAAATCCAACCAAACTGACTTTGTGTTTGTTCAGCTGGAGATTCCAAA
GTATATGAGAGGATCTTGGACTATAACAAGATCATCGAAGCTTTGGCTCT
TCCTAGAAACCTTCTGATACAAACCCTTACCGCTCTACGACCTGTGAGT
TTTCTGTGTTTGTGATATGGACAATGCTCAATGGACTGTGCAATACCAA
TATCACTGTTAACATTATCATAACAGTAGACTGTTAATACTTATAACATAG
GGGACTCTGCTATGTACATTTACTTCCAGGGTAATATATAAAAATATATGAC

CCTGTTAGGGTAATATTCATTCATTCGTTTCATTCATTCATTCATTCATTCAT
TTATTCATTCATTCATTCATTAATGTTTATATAACACTAAAAATCTTATTTAA
TTGATGTATTCATTTGTTTGTGATTTGTAATTGTATATTTATTATTGAAAT
GTTCTGCCATGAAAATAGCCTTGGTTGCTAACATGGCATTAAATAAAAA
ATACACTACATTACTIONTTTGTATATTTAAAATAATTCTGATCCTAATTCTG
ATCTCGTTTACCCACAGCTGATGTCACGACCCGTTTTGATGAAGTCTTCT
GGTTTGGAGATTTCAACTTCCGCCTGAATAAAGCCAGAGGAGACGTGGA
GGCATTTTAAATCAGGGCGTTGGCGTTGATATGAGCCCGTTATTACAAC
ATGATCAGCTGACGAGAGAGATGAAGGAAGGCCGAGTTAAGACACAAATG
CAGAGTGATGCCAAATTAAGTCTTACGCAGTATGGTGTTCCTCTGG
GGGAAATGTTTATTCTGTGTACGTTTGATTAACAGGATAAATCTGTTTGG
GTTTTTGCAGGATCCATTTTTAAAGGCTTTCAGGAAGCATCAATTCCTTC
CCTCCGACTTACAAGTTCGACATTGGTTGTGATGTTTATGACACCACGAC
AAAACAAAGAACACCTTCATACACCGTAAGCTTTCTTACTCATTTTTATTG
AATACATTGCTGTATACAGTTCCAGTACATGTTAGTCGACCCTAACATAT
TTTGTCAGAATATCCCTTCCCTTTTATGTAAATAATAATTGACTCTGGGCC
ATTGAATTTTTTTTTCTAATAATTCCGCTTAGGCTGAGATTTACTTATTAGTT
TTTTTTGTGGGACTCATTCTTGAGCATATAATTCAAAGGCTTTTTGTTTTGT
TTTGATAGGTTTTTTTTTTTTTTTTTTTTGGTTTGGTTTTACTGTTGTAGACA
GCAAATAGCTTAAATTGTCCAGCATGGCCATATGGAGCTATAATGTAGT
CAAGACCTGGCTAAACTACTTTTGTGTGTGTTTATCTGAAACTAATCGC
ACACCTCATTGCACACCCCAAATGTTTCATCAGCCAATCAGAAACAAGCTT
TCAAACCCCTGCTGTATAAAATGAGATATTTTATGCAAATCTGGTTTATT
GGGTTTACATTAGATTAGTCAGTACCAAAGCCAAAACAGGAAGTAACTAA
TCAAATAAATAAAAGTAAAAAATGAGTTCATAAATTAATGTTAGGAGA
GCATTTAAAAAAAATCTAGCCCAACATAATGTTGCAAATTTTTTATAAATC
ATATTATATTTTCAGTTAAATTTTATATGTTATTTTTATAAATTCTATCTTTTTA
AATAATTTTTAATAACTGTTAAATAAACTGTATTGGAAAAAATGACCAAT
AAATATTGTCCAACCATATATATATATATATATATATATATATATATATAT
AT
TGTGTGTGTGTGTGTGTATGTATGTATGTATGTATATATACGTGTATATAT
ATGTGTATATATATATATATATATTCACTTATAAAATAATTAATTTTTAAAAG
GGATGTACTTTATGCTGGGCCTCTGTAATAATGTTGTATACTTTTCCTCAT
GTGTCAACAGGATCGTATTCTTTATCGAAACAGACAAGCAGATGACATAA
GAGTGATAAAGTACACGTCTTGCTCGTCCATTAAGACGTCAGATCACCG
GCCAGTCATTGGCATGTTTCAGGTCAAACACTACGTCCGGGTAGAGACAAG
TAAGCATTTGATTTTACATGTACGGGGCTGGTGCAGGGCAGGGCCGATT
AGTTCACCTAGAAACAGTACTGCGTTCAAATTTAGAAATGTATCAAGAA
CAAACATTACATGTTAAAAAGTGTGTGTGTGTGCGTGCGTGTGCATATA
TA
TATATATATATATATATATACATACATGCATACAGTTTAAATTATGCATAAG
TCAAATTTATTAGCCCCTCTTTGAATTTTTGTATTCTTTTTAAATATTTATTA
ATTATGTTTAAACAGAGCAAAGAAATTTACACAGTATGTCTGATAGTATTTT
TTCTTCTGGAAAAAGTCTTATTTGTTTTATTTCCGGCTAGAATAAAAGCAGT

TTTTAATTTTTTAAAAACATTTTCAAGTCAAATTATCAGCCCCTTTTACC
TATATATTTTTATATTTTATATATATTTATATATTTTACTTTATCCTGGCAA
GATAAAATAAATCAGTTATTAGAAACAAGTTATTAAACTATTACGTTAAT
TCTGTCTGATTGCAACTGTATATATGGTCTCAAAAACTAATTTAATTGGA
CAACATTACAGCCAACATGGCCTTCATGAGCTAAAGTGGCAGTGTGCCA
AATTTGTTTCTTTATTTTCTGTAATGTTTGGCTTGATCGAGCTCCTGCCTT
TAAGATTTTTTCCAGATGTGCACACACTGATGTTTTATCCCAGTGGTCCA
ATTAATATGTTATAAATATTATATGGTCAAATATTGTTATGAAGCTACGATC
ATTATTTTGTGGCTGAATAAAAACTACTGAAATAAATAACGACATCTTTGT
GCTTAGTTCATTGGCACTGTGTGTGTTTGTCTGCTGTTGAAGTGTACTT
TGGAGGACGCAACAATGTTGTTAGTACCTGTCTGGGTTTTGAATGTTTCA
TCTGTCTATGGAGGGTCCGAGAGCTCAAGGATTTCTTCAAAAATCAATTC
TATTGTGGTCTAGCGATGATTGTAGGTCTCAAGTCCCATTTCAGATTGCAT
TTTCTTTTCTTTGATTTTTGCTTGACGTTGGGTTTTGTAGAGATAAGTCATT
GATAAATGGTCATCCAGACATAATATTCAATTGTGTTATTCTTCTCGTGTA
GTGTGGCATAGTTCACAACGTGTCGAAGCCATATTTACGTCAATAAAGCCA
GCAATAAAAATCTTGTAGGAGCTTTATGGGTTTGTAAAGGAAATGAGTGTG
AATAATTAAGATCTCGTGAAGTGCTTTGAAATGTGCTTTTTTTATTGGAT
GTTTGATGTAATCTCAACTGAAACAAGAAGAGAGGGTGAACATAGTGTA
GCAAAAAAAGCAGCCAATAGCGTTTTATTTTCATCACAGCTCTGCCAGTGA
GAGCAGTTGAGCTCAAGCGCATCAAATGAAAAGCAAATATGAAACGTTTT
GAAGGGGGAGGGGCTTTTTAGACACTAGAGAGCATTGATTGGTCAAGA
TTTGATGAGAACTGATGTATGAGGTGACGTCGAAAAAATTATTGACCC
ATTTAAGCGGAAGTGATCAACTGCAAGCTTTACAGGTTTCTATCAGTTGT
ATATCTTTTTATAAGCAAATTTTGTCACTGTTTTGGAGCGCACTAGCTCAT
AGATATCTAAAAAACTAACAATACTGATACTAACATATAAAAATACTTTATTT
TAATTTCAATTGGACCTTTAATGACAATTAATTTAAGTAAAATAACCCTTT
AAAAAGCATTAGTAAAGAGATGACTTCTTATCACCGTATACACTGAGCAA
TGTAACGTTCTGCTCAATTTATATTTTTTTTTTCGTCAGTTGAAGTGAAT
GTAATGTTTTGACTTTGTGTTTACATTTGATGGGATGTTATTTCGTGCATTT
TAATAAACCACTAACTCAAGTGTGGTCCTTCCCAGCATTCTCTGGGCGC
TGGCCTTTTCGACAGGAGTCTGTACCTCGAAGGAATCCGACGGAGAATC
ACCAGAGAGCTGAAAAAGAGAGAGGCGGTCATGAAAAACCAGAACAACA
GCACAGTCTGCTCCATATCCTGATCCGGGACCAGTGTGCGACAGCCATA
AGGTGCTAAAACCTGATCATTTTCAAACACGCCTGGTACTCGGAAAGCT
GGACTTTACAGGACCGAGGGATAACTCGGTTTACTGTCACTTAAGTGAC
AGCCCGCGGACCAAAGCACTACAGCTGGTGTGGATTAATATATAAAAA
CATGACTTTATTCCTATGATTTAATCTTTAAATTATACTGACCAGAGTAAA
GGAAGTTAACAGTACTGTACATTCATTCCTAATGCGTTTCTTTGTTTT
ACTTCATTTAACTTGCAAGCTGAAACAGTCTGTGCTGTGTATGGTTTTCAAT
GTATAGCATCTCATGGCCTTGTTAAAGGGACAGCACACCCAAATATGAAA
ATCGTTTACTCATCCTCTCATTACTCAGTTTCTCTCTTCTTGTTTTTGTTT
AACAGAAGAAAGAAATTGATTGAAACGACTTGAGTTTGAAGTAAAACAGTG
TGAGAATTTTCATTTTTGTACACGCCGTCCCTTTAAATGATTACACTACCT

TACAGTTGTAAGAGCAACAAATAATAGCTTCACTTCTAGTTGATCATTGG
AAAAGTGGCAGAGGGTCAATTTTTGTTCAATACTGACCTATTAACCTTG
CATGGACCCAAAATTCTCAGAGTAATCAGTCAAGTTTGGTGAGGGAAAAA
TCCTGGTTTGGGGTTATATTCAGTATAGGGGTATGTGAGAGAT

CRISPRs (CRs) design

CR1: AACCCACAGATCTCAGGTC exon1

CR1-F: CATCTAAAATCAAGCCCGCCA

CR1-R: AGCTCCTCATTGTGGCTCTT

CR2: AAGGAGATTGAGGAACAGCC exon1

CR2-F: GACCTCCCTCTCTTCCGAAG

CR2-R: ATGTGCTGGAGATCGAGAGG

CR3: GAACAATAATAGGATTGAC exon1

CR3-F: AAGAGCGCATGAAACCATCC

CR3-R: TTCCTGTGAAGCCTCTCCG

CR4: GGAGTGGGAGATCCGTCTGC exon 4

CR4-F: GGTGAGATGTTGCTTTCTTGC

CR4-R: ACCATGCCGCCCTACTATTT

CR5: GAGATTCCAAAGTATATGAG/CTCATATACTTTGGAATCTC exon 6

CR5-F: TGGCGTTAAATGTATGCTCGA

CR5-R: CACAGGAAAACCTCACAGGTCTG

6.3.2 DNA extraction from fin clips

DNA extraction from fin clipped tissue was used to identify carriers of recessive mutations. I used this method to genotype INPP5E mutant animals. Fin clips were performed following Home Office recommendations and fin tissue was transferred directly to 50 µl of fresh base solution (50 mM NaOH in MilliQ H₂O) in a 96-well plate and incubated for 30 minutes at 98°C. Following that, the plate was vortexed for 5 seconds on a benchtop. Subsequently, 5.5 µl of neutralization buffer (1 M TrisHCl in MilliQ H₂O) were added to each sample and the plate was vortexed again for 10 seconds. 1.5 µl of the resulting mixture was used per PCR reaction.

6.3.3 T7 assay

T7 assay is used for genotyping CRISPR-generated mutants that do not have a restriction site. In a reannealed mixture of wild-type and mutant DNA strands, the T7 endonuclease will cleave mismatches. In wild-type DNA, there should not be any mismatches so no additional bands are generated. First, PCR product of interest was generated. Second, PCR product was denatured at 95°C for 5 min and cooled in PCR machine to 85°C at a rate of 2°C per second. Upon reaching 85°C, the product was further cooled at a rate of 0.1°C per second to 25°C. Such slow re-annealing results in the appearance mismatches, which were then cleaved by T7 endonuclease I (NEB, M0302S). The product after T7 digestion was checked by checked through electrophoresis on a 2-2.5% agarose gel to resolve any small differences between DNA molecules.

6.4. Histological analysis

6.4.1 Cryosectioning

Zebrafish embryos or larvae were fixed in 4% paraformaldehyde/PBS 4°C overnight, and placed in 30% sucrose at 4°C overnight. When incubated in sucrose, embryos gradually sink to the bottom of tubes. Embedding moulds were prepared from 3 ml plastic transfer pipettes (Falcon, Corning 357524). The middle section of the plastic pipette was cut into 0.5 cm tall cylinders which were then placed vertically onto glass slides and filled with OCT compound (VWR, cat no. 361603E). This was performed gently to avoid bubble formation in the embedding compound. Embryo specimen was transferred from an eppendorf tube into the OCT compound with gentle stirring to dilute the sucrose transferred along with the embryos in OCT. Specimen was then transferred in OCT-filled embedding moulds. Embryos were

submerged in the OCT with blunt probes or tweezers, and positioned vertically in a way that their heads were directed towards the bottom and their body axis was positioned at the 90° angle relative to the slide. Afterwards, embedding moulds with embryos were carefully placed in -80°C freezer or on dry ice.

A Cryostat (Leica) was set to -20°C. A razor blade was used to trim away the plastic embedding mould and expose the specimen block. This procedure was performed on dry ice. A large drop of OCT compound was placed on the centre of a pre-cooled cryostat specimen holder. The specimen block was then carefully positioned in the OCT in such a way that heads of embedded larvae were directed away from the specimen holder. The holder with a specimen block were then left at -20°C in the cryostat chamber so that the block became firmly embedded in frozen OCT. More OCT was added around the specimen block if necessary.

The section thickness was set to 20 micrometres on the cryostat. The block was trimmed by sectioning until the zebrafish head tissues became visible on sections. Sections were collected from the cryostat blade to microscope slides (10149870, Thermo Scientific) by gently placing a slide (kept at room temperature) next to cryosection. To avoid sectioning past the area of interest, sections were checked using a basic dissecting microscope (Zeiss Stemi 1000). Slides with sections were left at the room temperature for at least 2 hours to dry prior to immunostaining or imaging.

6.4.2 Antibody staining

6.4.2.1 Whole-mount zebrafish embryos staining

Embryos were dechorinated if necessary, and treated with Tricaine until they stopped moving. Embryos or larvae were fixed in 4% paraformaldehyde/PBS at 4°C overnight or at room temperature for 4 hours in eppendorf tubes. A

quick wash with PBST (PBS + 0.1% Tween) was applied after fixation. Samples were transferred to 1% Triton X-100 in PBST and incubated at room temperature for 8-24 hours for permeabilisation. Embryos/larvae were placed in the blocking buffer (0.5% Triton, 10% normal goat serum in PBST) at room temperature for 2 hours. Subsequently, the blocking buffer was removed and replaced with fresh blocking buffer containing the primary antibody (for example, monoclonal anti-acetylated tubulin mouse IgG at 1:500 dilution). Specimen was incubated in this solution at 4°C overnight. Embryos or larvae were then washed in PBST three times, 30 min. each, on a rotator and incubated in secondary antibody (for example, goat anti-mouse Alexa 488 at 1:500 - 1:800 dilution) in the blocking buffer for 4 hours at room temperature. Embryos were washed with PBST 3 times, 10 min. each and then incubated in DAPI (40 ng/ml in PBS) one hour. For imaging, embryos were mounted on the surface of 1% agarose gel in a 35 mm petri dish in 1.5% low melting agarose (Sigma, cat no. A9414).

6.4.2.2 Staining of Sections

Once dried, slides with sections were covered with PBS for 5 min. Blocking buffer (0.5% Triton, 2% normal goat serum in PBST) was placed on top of slides. Slides were incubated at room temperature for 45 min. in a humidified chamber made from a slide box. The blocking buffer was removed and replaced with the primary antibody solution (for example, monoclonal anti-acetylated tubulin mouse IgG at 1:500 dilution in the blocking buffer). Slides were then incubated at 4°C overnight or at room temperature for 3 hours. PBST was used to wash slides three times, 10 min. each. Secondary antibody was applied as above at room temperature for 2 hours and again slides were washed with PBST three times, 10 min each. DAPI (40 ng/ml) was applied for one hour, as above. Cover slips were placed on slides and sealed with nail polish.

The following primary antibodies were applied: anti-acetylated α -tubulin (1:500; Sigma), zpr3 (1:500; Zebrafish International Resource Center), zpr1 (1:500; Zebrafish International Resource Centre), anti-IFT88 (1:200; gift from Brain Perkins). Alexa Fluor 488-conjugated secondary antibody was used for all staining procedures. Images of cryosections were collected using the Olympus FV1000 confocal microscope with the 40x oil lens. Live images or images of immunostained whole mount embryos were collected using the Olympus FV1000 confocal microscope equipped with a 60x water-dipping lens.

6.4.3 Electron microscopy

6.4.3.1 Sample preparation

Zebrafish embryos from 3 dpf and 5 dpf were fixed in Modified Karnovsky's fixative (2.5% glutaraldehyde, 2% paraformaldehyde, 0.1M Cacodylate buffer and 2.5 mM CaCl_2). Embryos were kept still to avoid fixation artefacts. Fixation was applied at 4°C for 5 hours up to overnight. Embryos were rinsed in 100 mM cacodylate buffer 3 times, 10 min. each. Specimens can be kept in 100 mM cacodylate buffer at 4°C indefinitely. Embryos were transferred into a glass vial (plastic top) and the cacodylate buffer was removed as much of as possible. 2% OsO_4 was added for 1.5 hour at room temperature. During this step, embryos or larvae were placed in a glass vial on the rotator. Specimen were transferred into 2% Uranyl acetate for 30 min, and dehydrated as follows: 5 min. in water; 5 min in 25% EtOH; 7 min. in 50% EtOH; 10 min in 70% EtOH; 5 min in 95% EtOH; 10 min in 95% EtOH; 5 min in 100% EtOH; 10 min in 100% EtOH; 15 min in 100% EtOH; 5 min in Propylene oxide and 10 min in Propylene oxide.

The following Epon formula was used: Agar 100 epoxy resin 20 ml (24g), DDSA (EM grade) 22ml (22g), MNA (EM grade) 5ml (6g) and BDMA (c. 3%) 1.4 ml (1.5g). Samples were transferred to 1:2 of Epon / Propylene oxide mix

for 3 hours at room temperature and following that to 2:1 mix overnight. The next day, samples were transferred to 100% Epon for 6 hours. Embryos were then removed with a pipette tip drained from Epon as much as possible. Embryos were then transferred into a mould containing freshly made Epon and arranged with their heads directed toward the narrow end of the mould. Molds with embryos were placed in a 60°C oven for at least 2 days.

6.4.3.2 Semi thin sections

Solidified blocks with embryos were mounted on the microtome and gently shaved with a razor blade until the target tissue appeared. Glass knives, made by knife maker LKB78000, were mounted on the microtome (Reichert-Jung Ultracut E ultramicrotome) and applied for polishing the surface of the sample and cutting semi thin sections.

When analysing the retina, semi thin sections were collected until the central region of the eye was reached. A staining with toluidine blue was applied (one drop of toluidine blue was placed on sections for 30 seconds on a hot plate and then washed out with dH₂O) to make sure that the sectioned region was correct and the quality of the semi thin sections was good enough for the preparation of ultra thin sections. Sections from the center of the eye were collected to eliminate the risk of variation due to the location or the sectioning angle.

6.4.3.3 Ultra thin sections

85nm thick ultra thin sections were prepared using a diamond knife. 400 or 200 nm mesh copper grids were used to collect ultra sections.

6.4.3.4 Image and analysis

Images were collected on the FEI Tecnai G2 microscope using a Gatan Orius

SC1000B camera and analysed with Gatan Digital Micrograph Software.

6.4.4 Scanning Electron microscopy

Embryos were collected at 33 hpf and fixed at 4°C overnight in fixation buffer (2.5% glutaraldehyde, 2% paraformaldehyde, 0.1M cacodylate buffer and 25 mg /100ml of CaCl₂) and placed in 0.1 M cacodylate buffer wash with 3% sucrose (PH 7.4) at least 3 times, 5 min each. Post-fixation was performed for 0.5 hour with 2% OsO₄ in dH₂O. After 2 washes, 5 min each, with sterile water embryos/ larvae were transferred to fresh tubes and three further washes in dH₂O followed. Embryos were then dehydrated in increasing ethanol concentrations (10%, 20%, 30%, 40%, 50%, 60%, 70%, 80%, 90% and 100% (3 times) for 10 min each and critical point-dried in liquid nitrogen. Embryos were sputtered with gold and analysed with Philips XL-20 SEM.

References

- Adoutte, A., Ramanathan, R., Lewis, R.M., Dute, R.R., Ling, K.-Y., Kung, C., Nelson, D.L., 1980. Biochemical studies of the excitable membrane of *Paramecium tetraurelia*. III. Proteins of cilia and ciliary membranes. *The Journal of cell biology* 84, 717-738.
- Andrews, D., Nelson, D.L., 1979. Biochemical studies of the excitable membrane of *Paramecium tetraurelia*. II. Phospholipids of ciliary and other membranes. *Biochimica et Biophysica Acta (BBA)-Biomembranes* 550, 174-187.
- Bae, Y.-K., Kim, E., L'Hernault, S.W., Barr, M.M., 2009. The CIL-1 PI 5-phosphatase localizes TRP Polycystins to cilia and activates sperm in *C. elegans*. *Current Biology* 19, 1599-1607.
- Balla, T., 2005. Inositol-lipid binding motifs: signal integrators through protein-lipid and protein-protein interactions. *Journal of cell science* 118, 2093-2104.
- Balla, T., 2010. Putting G protein-coupled receptor-mediated activation of phospholipase C in the limelight. *The Journal of general physiology* 135, 77-80.
- Basu, N., Todgham, A., Ackerman, P., Bibeau, M., Nakano, K., Schulte, P., Iwama, G.K., 2002. Heat shock protein genes and their functional significance in fish. *Gene* 295, 173-183.
- Berbari, N.F., Lewis, J.S., Bishop, G.A., Askwith, C.C., Mykytyn, K., 2008. Bardet-Biedl syndrome proteins are required for the localization of G protein-coupled receptors to primary cilia. *Proceedings of the National Academy of Sciences* 105, 4242-4246.
- Bielas, S.L., Silhavy, J.L., Brancati, F., Kisseleva, M.V., Al-Gazali, L., Sztriha, L., Bayoumi, R.A., Zaki, M.S., Abdel-Aleem, A., Rosti, R.O., 2009. Mutations in INPP5E, encoding inositol polyphosphate-5-phosphatase E, link phosphatidyl inositol signaling to the ciliopathies. *Nature genetics* 41, 1032-1036.
- Bloodgood, R.A., 2009. From central to rudimentary to primary: the history of an underappreciated organelle whose time has come. *The primary cilium. Methods in cell biology* 94, 2-52.
- Borovina, A., Superina, S., Voskas, D., Ciruna, B., 2010. Vangl2 directs the posterior tilting and asymmetric localization of motile primary cilia. *Nature*

cell biology 12, 407-412.

- Boubakri, M., Chaya, T., Hirata, H., Kajimura, N., Kuwahara, R., Ueno, A., Malicki, J., Furukawa, T., Omori, Y., 2016. Loss of ift122, a Retrograde Intraflagellar Transport (IFT) Complex Component, Leads to Slow, Progressive Photoreceptor Degeneration Due to Inefficient Opsin Transport. *Journal of Biological Chemistry* 291, 24465-24474.
- Brockerhoff, S.E., 2011. Phosphoinositides and photoreceptors. *Molecular neurobiology* 44, 420-425.
- Chalhoub, N., Baker, S.J., 2009. PTEN and the PI3-kinase pathway in cancer. *Annual Review of Pathological Mechanical Disease* 4, 127-150.
- Chávez, M., Ena, S., Van Sande, J., de Kerchove d'Exaerde, A., Schurmans, S., Schiffmann, S.N., 2015. Modulation of ciliary phosphoinositide content regulates trafficking and Sonic hedgehog signaling output. *Developmental cell*.
- Chuang, J.-Z., Zhao, Y., Sung, C.-H., 2007. SARA-regulated vesicular targeting underlies formation of the light-sensing organelle in mammalian rods. *Cell* 130, 535-547.
- Corbit, K.C., Aanstad, P., Singla, V., Norman, A.R., 2005. Vertebrate Smoothed functions at the primary cilium. *Nature* 437, 1018.
- Corbit, K.C., Shyer, A.E., Dowdle, W.E., Gauden, J., Singla, V., Reiter, J.F., 2008. Kif3a constrains [beta]-catenin-dependent Wnt signalling through dual ciliary and non-ciliary mechanisms. *Nature cell biology* 10, 70.
- Cremona, O., Di Paolo, G., Wenk, M.R., Lüthi, A., Kim, W.T., Takei, K., Daniell, L., Nemoto, Y., Shears, S.B., Flavell, R.A., 1999. Essential role of phosphoinositide metabolism in synaptic vesicle recycling. *Cell* 99, 179-188.
- Czech, M.P., 2000. PIP2 and PIP3: complex roles at the cell surface. *Cell* 100, 603-606.
- D'Avino, P.P., Thummel, C.S., 1999. [7] Ectopic expression systems in *Drosophila*. *Methods in enzymology* 306, 129-142.
- Davey, M., James, J., Paton, I., Burt, D., Tickle, C., 2007. Analysis of talpid 3 and wild-type chicken embryos reveals roles for Hedgehog signalling in development of the limb bud vasculature. *Developmental biology* 301, 155-165.
- Daza, D.O., Sundström, G., Bergqvist, C.A., Larhammar, D., 2012. The

evolution of vertebrate somatostatin receptors and their gene regions involves extensive chromosomal rearrangements. *BMC evolutionary biology* 12, 1.

Delling, M., Indzhykulian, A., Liu, X., Li, Y., Xie, T., Corey, D., Clapham, D., 2016. Primary cilia are not calcium-responsive mechanosensors. *Nature* 531, 656-660.

Delous, M., Baala, L., Salomon, R., Laclef, C., Vierkotten, J., Tory, K., Golzio, C., Lacoste, T., Besse, L., Ozilou, C., 2007. The ciliary gene RPGRIP1L is mutated in cerebello-oculo-renal syndrome (Joubert syndrome type B) and Meckel syndrome. *Nature genetics* 39, 875.

Demmel, L., Schmidt, K., Lucast, L., Havlicek, K., Zankel, A., Koestler, T., Reithofer, V., de Camilli, P., Warren, G., 2014. The endocytic activity of the flagellar pocket in *Trypanosoma brucei* is regulated by an adjacent phosphatidylinositol phosphate kinase. *J Cell Sci* 127, 2351-2364.

Deng, Q., Yoo, S.K., Cavnar, P.J., Green, J.M., Huttenlocher, A., 2011. Dual roles for Rac2 in neutrophil motility and active retention in zebrafish hematopoietic tissue. *Developmental cell* 21, 735-745.

Di Paolo, G., De Camilli, P., 2006. Phosphoinositides in cell regulation and membrane dynamics. *Nature* 443, 651-657.

Duldulao, N.A., Lee, S., Sun, Z., 2009. Cilia localization is essential for in vivo functions of the Joubert syndrome protein Arl13b/Scorpion. *Development* 136, 4033-4042.

Dyson, J.M., Conduit, S.E., Feeney, S.J., Hakim, S., DiTommaso, T., Fulcher, A.J., Sriratana, A., Ramm, G., Horan, K.A., Gurung, R., 2017. INPP5E regulates phosphoinositide-dependent cilia transition zone function. *J Cell Biol* 216, 247-263.

Eley, L., Yates, L.M., Goodship, J.A., 2005. Cilia and disease. *Current opinion in genetics & development* 15, 308-314.

Erickson, K., Baron, I.S., Fantie, B.D., 2001. Neuropsychological functioning in early hydrocephalus: Review from a developmental perspective. *Child Neuropsychology* 7, 199-229.

Essner, J.J., Amack, J.D., Nyholm, M.K., Harris, E.B., Yost, H.J., 2005. Kupffer's vesicle is a ciliated organ of asymmetry in the zebrafish embryo that initiates left-right development of the brain, heart and gut. *Development* 132, 1247-1260.

Ezratty, E.J., Stokes, N., Chai, S., Shah, A.S., Williams, S.E., Fuchs, E., 2011.

- A role for the primary cilium in Notch signaling and epidermal differentiation during skin development. *Cell* 145, 1129-1141.
- Falkenburger, B.H., Jensen, J.B., Dickson, E.J., Suh, B.C., Hille, B., 2010. Phosphoinositides: lipid regulators of membrane proteins. *J Physiol* 588, 3179-3185.
- Faucherre, A., Taylor, G., Overvoorde, J., Dixon, J., den Hertog, J., 2007. Zebrafish pten genes have overlapping and non-redundant functions in tumorigenesis and embryonic development. *Oncogene* 27, 1079-1086.
- Faucherre, A., Taylor, G., Overvoorde, J., Dixon, J., Den Hertog, J., 2008. Zebrafish pten genes have overlapping and non-redundant functions in tumorigenesis and embryonic development. *Oncogene* 27, 1079.
- Ferguson, K.M., Kavran, J.M., Sankaran, V.G., Fournier, E., Isakoff, S.J., Skolnik, E.Y., Lemmon, M.A., 2000. Structural basis for discrimination of 3-phosphoinositides by pleckstrin homology domains. *Molecular cell* 6, 373-384.
- Ferguson, K.M., Lemmon, M.A., Schlessinger, J., Sigler, P.B., 1995a. Structure of the high affinity complex of inositol trisphosphate with a phospholipase C pleckstrin homology domain. *Cell* 83, 1037-1046.
- Ferguson, K.M., Lemmon, M.A., Sigler, P.B., Schlessinger, J., 1995b. Scratching the surface with the PH domain. *Nature structural biology* 2, 715.
- Ferrante, M.I., Zullo, A., Barra, A., Bimonte, S., Messaddeq, N., Studer, M., Dollé, P., Franco, B., 2006. Oral-facial-digital type I protein is required for primary cilia formation and left-right axis specification. *Nature genetics* 38, 112.
- Fliegauf, M., Benzing, T., Omran, H., 2007. When cilia go bad: cilia defects and ciliopathies. *Nature Reviews Molecular Cell Biology* 8, 880-893.
- Foerster, P., Daclin, M., Asm, S., Faucourt, M., Boletta, A., Genovesio, A., Spassky, N., 2017. mTORC1 signaling and primary cilia are required for brain ventricle morphogenesis. *Development* 144, 201-210.
- Frew, I.J., Thoma, C.R., Georgiev, S., Minola, A., Hitz, M., Montani, M., Moch, H., Krek, W., 2008. pVHL and PTEN tumour suppressor proteins cooperatively suppress kidney cyst formation. *The EMBO Journal* 27, 1747-1757.
- Fruman, D.A., Chiu, H., Hopkins, B.D., Bagrodia, S., Cantley, L.C., Abraham, R.T., 2017. The PI3K Pathway in Human Disease. *Cell* 170, 605-635.

- Furnari, F.B., Huang, H.S., Cavenee, W.K., 1998. The phosphoinositol phosphatase activity of PTEN mediates a serum-sensitive G1 growth arrest in glioma cells. *Cancer Research* 58, 5002-5008.
- Gamper, N., Shapiro, M.S., 2007. Regulation of ion transport proteins by membrane phosphoinositides. *Nature Reviews Neuroscience* 8, 921-934.
- Garcia-Gonzalo, F.R., Phua, S.C., Roberson, E.C., Garcia, G., Abedin, M., Schurmans, S., Inoue, T., Reiter, J.F., 2015. Phosphoinositides Regulate Ciliary Protein Trafficking to Modulate Hedgehog Signaling. *Developmental cell* 34, 400-409.
- Gassama-Diagne, A., Yu, W., ter Beest, M., Martin-Belmonte, F., Kierbel, A., Engel, J., Mostov, K., 2006. Phosphatidylinositol-3, 4, 5-trisphosphate regulates the formation of the basolateral plasma membrane in epithelial cells. *Nature cell biology* 8, 963-970.
- Godi, A., Di Campli, A., Konstantakopoulos, A., Di Tullio, G., Alessi, D.R., Kular, G.S., Daniele, T., Marra, P., Lucocq, J.M., De Matteis, M.A., 2004. FAPPs control Golgi-to-cell-surface membrane traffic by binding to ARF and PtdIns (4) P. *Nature cell biology* 6, 393-404.
- Grunwald, D.J., Eisen, J.S., 2002. Headwaters of the zebrafish--emergence of a new model vertebrate. *Nature reviews. Genetics* 3, 717.
- Hammond, G., Schiavo, G., Irvine, R., 2009. Immunocytochemical techniques reveal multiple, distinct cellular pools of PtdIns4P and PtdIns (4, 5) P2. *Biochem. J* 422, 23-35.
- Hammond, G.R., Fischer, M.J., Anderson, K.E., Holdich, J., Koteci, A., Balla, T., Irvine, R.F., 2012. PI4P and PI (4, 5) P2 are essential but independent lipid determinants of membrane identity. *Science* 337, 727-730.
- Hampshire, D.J., Ayub, M., Springell, K., Roberts, E., Jafri, H., Rashid, Y., Bond, J., Riley, J.H., Woods, C.G., 2006. MORM syndrome (mental retardation, truncal obesity, retinal dystrophy and micropenis), a new autosomal recessive disorder, links to 9q34. *European journal of human genetics* 14, 543-548.
- Han, S.-J., Cho, Y.L., Nam, G.H., Kim, C.K., Seo, J.-S., Ahn, W.S., 2003a. cDNA microarray analysis of gene expression profiles associated with cervical cancer. *Cancer Research and Treatment* 35, 451-459.
- Han, Y.-G., Kwok, B.H., Kernan, M.J., 2003b. Intraflagellar transport is required in *Drosophila* to differentiate sensory cilia but not sperm. *Current Biology* 13, 1679-1686.

- Harlan, J.E., Hajduk, P.J., Yoon, H.S., Fesik, S.W., 1994. Pleckstrin homology domains bind to phosphatidylinositol-4, 5-bisphosphate. *Nature* 371, 168.
- Hasegawa, J., Iwamoto, R., Otomo, T., Nezu, A., Hamasaki, M., Yoshimori, T., 2016. Autophagosome–lysosome fusion in neurons requires INPP5E, a protein associated with Joubert syndrome. *The EMBO Journal*, e201593148.
- Haycraft, C.J., Banizs, B., Aydin-Son, Y., Zhang, Q., Michaud, E.J., Yoder, B.K., 2005. Gli2 and Gli3 localize to cilia and require the intraflagellar transport protein polaris for processing and function. *PLoS genetics* 1, e53.
- He, M., Subramanian, R., Bangs, F., Omelchenko, T., Liem Jr, K.F., Kapoor, T.M., Anderson, K.V., 2014. The kinesin-4 protein KIF7 regulates mammalian Hedgehog signaling by organizing the cilia tip compartment. *Nature cell biology* 16, 663.
- Hildebrandt, F., Benzing, T., Katsanis, N., 2011. Ciliopathies. *New England Journal of Medicine* 364, 1533-1543.
- Hille, B., Dickson, E.J., Kruse, M., Vivas, O., Suh, B.-C., 2015. Phosphoinositides regulate ion channels. *Biochimica Et Biophysica Acta (BBA)-Molecular and Cell Biology of Lipids* 1851, 844-856.
- Hirono, M., Denis, C.S., Richardson, G.P., Gillespie, P.G., 2004. Hair cells require phosphatidylinositol 4, 5-bisphosphate for mechanical transduction and adaptation. *Neuron* 44, 309-320.
- Hokin, L.E., 1985. Receptors and phosphoinositide-generated second messengers. *Annual review of biochemistry* 54, 205-235.
- Hokin, L.E., Hokin, M.R., 1955. Effects of acetylcholine on phosphate turnover in phospholipides of brain cortex in vitro. *Biochimica et biophysica acta* 16, 229-237.
- Hong, S.-K., Dawid, I.B., 2009. FGF-dependent left–right asymmetry patterning in zebrafish is mediated by *lrr2* and *Fibp1*. *Proceedings of the National Academy of Sciences* 106, 2230-2235.
- Hsu, C.-H., Lin, J.-S., Lai, K.P., Li, J.-W., Chan, T.-F., You, M.-S., Tse, W.K.F., Jiang, Y.-J., 2015. A new *mib* allele with a chromosomal deletion covering *foxc1a* exhibits anterior somite specification defect. *Scientific reports* 5, 10673.
- Huang, P., Schier, A.F., 2009. Dampened Hedgehog signaling but normal Wnt signaling in zebrafish without cilia. *Development* 136, 3089-3098.

- Huangfu, D., Liu, A., Rakeman, A.S., Murcia, N.S., Niswander, L., Anderson, K.V., 2003. Hedgehog signalling in the mouse requires intraflagellar transport proteins. *Nature* 426, 83-87.
- Humbert, M.C., Weihbrecht, K., Searby, C.C., Li, Y., Pope, R.M., Sheffield, V.C., Seo, S., 2012. ARL13B, PDE6D, and CEP164 form a functional network for INPP5E ciliary targeting. *Proceedings of the National Academy of Sciences* 109, 19691-19696.
- Idevall-Hagren, O., De Camilli, P., 2015. Detection and manipulation of phosphoinositides. *Biochimica et Biophysica Acta (BBA)-Molecular and Cell Biology of Lipids* 1851, 736-745.
- Ishikawa, H., Marshall, W.F., 2011. Ciliogenesis: building the cell's antenna. *Nature reviews. Molecular cell biology* 12, 222.
- Itoh, T., Takenawa, T., 2002. Phosphoinositide-binding domains: functional units for temporal and spatial regulation of intracellular signalling. *Cellular signalling* 14, 733-743.
- Jacoby, M., Cox, J.J., Gayral, S., Hampshire, D.J., Ayub, M., Blockmans, M., Pernot, E., Kisseleva, M.V., Compère, P., Schiffmann, S.N., 2009. INPP5E mutations cause primary cilium signaling defects, ciliary instability and ciliopathies in human and mouse. *Nature genetics* 41, 1027-1031.
- Jensen, V.L., Li, C., Bowie, R.V., Clarke, L., Mohan, S., Blacque, O.E., Leroux, M.R., 2015. Formation of the transition zone by Mks5/Rpgrip1L establishes a ciliary zone of exclusion (CIZE) that compartmentalises ciliary signalling proteins and controls PIP2 ciliary abundance. *The EMBO journal* 34, 2537-2556.
- Jin, H., White, S.R., Shida, T., Schulz, S., Aguiar, M., Gygi, S.P., Bazan, J.F., Nachury, M.V., 2010. The conserved Bardet-Biedl syndrome proteins assemble a coat that traffics membrane proteins to cilia. *Cell* 141, 1208-1219.
- Jones, C., Roper, V.C., Foucher, I., Qian, D., Banizs, B., Petit, C., Yoder, B.K., Chen, P., 2008. Ciliary proteins link basal body polarization to planar cell polarity regulation. *Nature genetics* 40, 69-77.
- Joubert, M., Eisenring, J.-J., Preston, J., Andermann, F., 1969. Familial agenesis of the cerebellar vermis A syndrome of episodic hyperpnea, abnormal eye movements, ataxia, and retardation. *Neurology* 19, 813-813.
- Kaneshiro, E., 1987. Lipids of Paramecium. *Journal of lipid research* 28, 1241-1258.

- Katso, R., Okkenhaug, K., Ahmadi, K., White, S., Timms, J., Waterfield, M.D., 2001. Cellular function of phosphoinositide 3-kinases: implications for development, immunity, homeostasis, and cancer. *Annual review of cell and developmental biology* 17, 615-675.
- Kee, H.L., Dishinger, J.F., Blasius, T.L., Liu, C.-J., Margolis, B., Verhey, K.J., 2012. A size-exclusion permeability barrier and nucleoporins characterize a ciliary pore complex that regulates transport into cilia. *Nature cell biology* 14, 431-437.
- Kennedy, B., Malicki, J., 2009. What drives cell morphogenesis: a look inside the vertebrate photoreceptor. *Developmental Dynamics* 238, 2115-2138.
- Kim, B., Bang, S., Lee, S., Kim, S., Jung, Y., Lee, C., Choi, K., Lee, S.-G., Lee, K., Lee, Y., 2003. Expression profiling and subtype-specific expression of stomach cancer. *Cancer research* 63, 8248-8255.
- Kisseleva, M.V., Cao, L., Majerus, P.W., 2002. Phosphoinositide-specific inositol polyphosphate 5-phosphatase IV inhibits Akt/protein kinase B phosphorylation and leads to apoptotic cell death. *Journal of Biological Chemistry* 277, 6266-6272.
- Kisseleva, M.V., Wilson, M.P., Majerus, P.W., 2000. The isolation and characterization of a cDNA encoding phospholipid-specific inositol polyphosphate 5-phosphatase. *Journal of Biological Chemistry* 275, 20110-20116.
- Klaus, A., Birchmeier, W., 2008. Wnt signalling and its impact on development and cancer. *Nature reviews. Cancer* 8, 387.
- Kodani, A., Timothy, W.Y., Johnson, J.R., Jayaraman, D., Johnson, T.L., Al-Gazali, L., Sztriha, L., Partlow, J.N., Kim, H., Krup, A.L., 2015. Centriolar satellites assemble centrosomal microcephaly proteins to recruit CDK2 and promote centriole duplication. *Elife* 4, e07519.
- Kong, A.M., Speed, C.J., O'Malley, C.J., Layton, M.J., Meehan, T., Loveland, K.L., Cheema, S., Ooms, L.M., Mitchell, C.A., 2000. Cloning and characterization of a 72-kDa inositol-polyphosphate 5-phosphatase localized to the Golgi network. *Journal of Biological Chemistry* 275, 24052-24064.
- KozMINSKI, K.G., Johnson, K.A., Forscher, P., Rosenbaum, J.L., 1993. A motility in the eukaryotic flagellum unrelated to flagellar beating. *Proceedings of the National Academy of Sciences* 90, 5519-5523.
- Kramer-Zucker, A.G., Olale, F., Haycraft, C.J., Yoder, B.K., Schier, A.F., Drummond, I.A., 2005. Cilia-driven fluid flow in the zebrafish pronephros,

brain and Kupffer's vesicle is required for normal organogenesis. *Development* 132, 1907-1921.

- Kurokawa, T., Takasuga, S., Sakata, S., Yamaguchi, S., Horie, S., Homma, K.J., Sasaki, T., Okamura, Y., 2012. 3' Phosphatase activity toward phosphatidylinositol 3, 4-bisphosphate [PI (3, 4) P₂] by voltage-sensing phosphatase (VSP). *Proceedings of the National Academy of Sciences* 109, 10089-10094.
- Lemmon, M., Ferguson, K., 2000. Signal-dependent membrane targeting by pleckstrin homology (PH) domains. *Biochem. J* 350, 1-18.
- Lemmon, M.A., 2003. Phosphoinositide recognition domains. *Traffic* 4, 201-213.
- Lemmon, M.A., 2008. Membrane recognition by phospholipid-binding domains. *Nature reviews Molecular cell biology* 9, 99-111.
- Lemmon, M.A., Ferguson, K.M., Schlessinger, J., 1996. PH domains: diverse sequences with a common fold recruit signaling molecules to the cell surface. *Cell* 85, 621-624.
- Liem, K.F., Ashe, A., He, M., Satir, P., Moran, J., Beier, D., Wicking, C., Anderson, K.V., 2012. The IFT-A complex regulates Shh signaling through cilia structure and membrane protein trafficking. *J Cell Biol* 197, 789-800.
- Link, B.A., Megason, S.G., 2008. Zebrafish as a model for development. *Sourcebook of Models for Biomedical Research*, 103-112.
- Liu, F., Wagner, S., Campbell, R.B., Nickerson, J.A., Schiffer, C.A., Ross, A.H., 2005. PTEN enters the nucleus by diffusion. *Journal of cellular biochemistry* 96, 221-234.
- Lopes, S.S., Lourenço, R., Pacheco, L., Moreno, N., Kreiling, J., 2010a. Notch signalling regulates left-right asymmetry through ciliary length control. *Development* 137, 3625-3632.
- Lopes, V.S., Jimeno, D., Khanobdee, K., Song, X., Chen, B., Nusinowitz, S., Williams, D.S., 2010b. Dysfunction of heterotrimeric kinesin-2 in rod photoreceptor cells and the role of opsin mislocalization in rapid cell death. *Molecular biology of the cell* 21, 4076-4088.
- Lu, H., Toh, M.T., Narasimhan, V., Thamilselvam, S.K., Choksi, S.P., Roy, S., 2015. A function for the Joubert syndrome protein Arl13b in ciliary membrane extension and ciliary length regulation. *Developmental biology* 397, 225-236.

- Lunt, S.C., Haynes, T., Perkins, B.D., 2009. Zebrafish *ift57*, *ift88*, and *ift172* intraflagellar transport mutants disrupt cilia but do not affect hedgehog signaling. *Developmental Dynamics* 238, 1744-1759.
- Luo, N., Conwell, M.D., Chen, X., Kettenhofen, C.I., Westlake, C.J., Cantor, L.B., Wells, C.D., Weinreb, R.N., Corson, T.W., Spandau, D.F., 2014. Primary cilia signaling mediates intraocular pressure sensation. *Proceedings of the National Academy of Sciences* 111, 12871-12876.
- Luo, N., Kumar, A., Conwell, M., Weinreb, R.N., Anderson, R., Sun, Y., 2013. Compensatory role of inositol 5-phosphatase INPP5B to OCRL in primary cilia formation in oculocerebrorenal syndrome of Lowe. *PloS one* 8, e66727.
- Majerus, P.W., Kisseleva, M.V., Norris, F.A., 1999. The role of phosphatases in inositol signaling reactions. *Journal of Biological Chemistry* 274, 10669-10672.
- Majerus, P.W., York, J.D., 2009. Phosphoinositide phosphatases and disease. *Journal of lipid research* 50, S249-S254.
- Malicki, J., Neuhauss, S., Schier, A.F., Solnica-Krezel, L., Stemple, D.L., Stainier, D., Abdelilah, S., Zwartkuis, F., Rangini, Z., Driever, W., 1996. Mutations affecting development of the zebrafish retina. *Development* 123, 263-273.
- Malicki, J.J., Johnson, C.A., 2017. The cilium: cellular antenna and central processing unit. *Trends in cell biology* 27, 126-140.
- Manna, D., Albanese, A., Park, W.S., Cho, W., 2007. Mechanistic basis of differential cellular responses of phosphatidylinositol 3, 4-bisphosphate-and phosphatidylinositol 3, 4, 5-trisphosphate-binding pleckstrin homology domains. *Journal of Biological Chemistry* 282, 32093-32105.
- Mao, Y., Balkin, D.M., Zoncu, R., Erdmann, K.S., Tomasini, L., Hu, F., Jin, M.M., Hodsdon, M.E., De Camilli, P., 2009. A PH domain within OCRL bridges clathrin-mediated membrane trafficking to phosphoinositide metabolism. *The EMBO Journal* 28, 1831-1842.
- Martin, C.-A., Ahmad, I., Klingseisen, A., Hussain, M.S., Bicknell, L.S., Leitch, A., Nürnberg, G., Toliat, M.R., Murray, J.E., Hunt, D., 2014. Mutations in *PLK4*, encoding a master regulator of centriole biogenesis, cause microcephaly, growth failure and retinopathy. *Nature genetics* 46, 1283-1292.
- Mayer, B.J., Ren, R., Clark, K.L., Baltimore, D., 1993. A putative modular

domain present in diverse signaling proteins. *Cell* 73, 629-630.

- Mayinger, P., 2012. Phosphoinositides and vesicular membrane traffic. *Biochimica et Biophysica Acta (BBA)-Molecular and Cell Biology of Lipids* 1821, 1104-1113.
- McCrea, H.J., De Camilli, P., 2009. Mutations in phosphoinositide metabolizing enzymes and human disease. *Physiology (Bethesda, Md.)* 24, 8.
- Mukhopadhyay, S., Wen, X., Chih, B., Nelson, C.D., Lane, W.S., Scales, S.J., Jackson, P.K., 2010. TULP3 bridges the IFT-A complex and membrane phosphoinositides to promote trafficking of G protein-coupled receptors into primary cilia. *Genes & development* 24, 2180-2193.
- Nauli, S.M., Alenghat, F.J., Luo, Y., Williams, E., Vassilev, P., Li, X., Elia, A.E., Lu, W., Brown, E.M., Quinn, S.J., 2003. Polycystins 1 and 2 mediate mechanosensation in the primary cilium of kidney cells. *Nature genetics* 33, 129.
- Neugebauer, J.M., Amack, J.D., Peterson, A.G., Bisgrove, B.W., Yost, H.J., 2009. FGF signaling during embryo development regulates cilia length in diverse epithelia. *Nature* 458, 651.
- Nigg, E.A., Raff, J.W., 2009. Centrioles, centrosomes, and cilia in health and disease. *Cell* 139, 663-678.
- Ocbina, P.J.R., Anderson, K.V., 2008. Intraflagellar transport, cilia, and mammalian Hedgehog signaling: analysis in mouse embryonic fibroblasts. *Developmental dynamics* 237, 2030-2038.
- Okkenhaug, K., 2013. Signalling by the phosphoinositide 3-kinase family in immune cells. *Annual review of immunology* 31, 675.
- Omori, Y., Zhao, C., Saras, A., Mukhopadhyay, S., Kim, W., Furukawa, T., Sengupta, P., Veraksa, A., Malicki, J., 2008. Elipsa is an early determinant of ciliogenesis that links the IFT particle to membrane-associated small GTPase Rab8. *Nature cell biology* 10, 437.
- Orešković, D., Klarica, M., 2011. Development of hydrocephalus and classical hypothesis of cerebrospinal fluid hydrodynamics: facts and illusions. *Progress in neurobiology* 94, 238-258.
- Otto, E.A., Hurd, T.W., Airik, R., Chaki, M., Zhou, W., Stoetzel, C., Patil, S.B., Levy, S., Ghosh, A.K., Murga-Zamalloa, C.A., 2010. Candidate exome capture identifies mutation of SDCCAG8 as the cause of a retinal-renal ciliopathy. *Nature genetics* 42, 840-850.

- Otto, E.A., Schermer, B., Obara, T., O'Toole, J.F., Hiller, K.S., Mueller, A.M., Ruf, R.G., Hoefele, J., Beekmann, F., Landau, D., 2003. Mutations in INVS encoding inversin cause nephronophthisis type 2, linking renal cystic disease to the function of primary cilia and left-right axis determination. *Nature genetics* 34, 413.
- Pazour, G.J., Bloodgood, R.A., 2008. Targeting proteins to the ciliary membrane. *Current topics in developmental biology* 85, 115-149.
- Pazour, G.J., Rosenbaum, J.L., 2002. Intraflagellar transport and cilia-dependent diseases. *Trends in cell biology* 12, 551-555.
- Pazour, G.J., San Agustin, J.T., Follit, J.A., Rosenbaum, J.L., Witman, G.B., 2002. Polycystin-2 localizes to kidney cilia and the ciliary level is elevated in orpk mice with polycystic kidney disease. *Current Biology* 12, R378-R380.
- Pedersen, L.B., Rosenbaum, J.L., 2008. Chapter two intraflagellar transport (IFT): role in ciliary assembly, resorption and signalling. *Current topics in developmental biology* 85, 23-61.
- Plotnikova, O.V., Pugacheva, E.N., Golemis, E.A., 2009. Primary cilia and the cell cycle. *Methods in cell biology* 94, 137-160.
- Pooranachandran, N., Malicki, J.J., 2016. Unexpected roles for ciliary kinesins and intraflagellar transport proteins. *Genetics* 203, 771-785.
- Posor, Y., Eichhorn-Gruenig, M., Puchkov, D., Schöneberg, J., Ullrich, A., Lampe, A., Müller, R., Zerbakhsh, S., Gulluni, F., Hirsch, E., 2013. Spatiotemporal control of endocytosis by phosphatidylinositol-3, 4-bisphosphate. *Nature* 499, 233-237.
- Pugh, E.N., Lamb, T.D., 2000. Phototransduction in vertebrate rods and cones: molecular mechanisms of amplification, recovery and light adaptation. *Handbook of biological physics* 3, 183-255.
- Quade, B.J., Wang, T.Y., Sornberger, K., Cin, P.D., Mutter, G.L., Morton, C.C., 2004. Molecular pathogenesis of uterine smooth muscle tumors from transcriptional profiling. *Genes, Chromosomes and Cancer* 40, 97-108.
- Rajala, R.V., Rajala, A., Morris, A.J., Anderson, R.E., 2014. Phosphoinositides: minor lipids make a major impact on photoreceptor cell functions. *Scientific reports* 4.
- Rauch, A., Thiel, C.T., Schindler, D., Wick, U., Crow, Y.J., Ekici, A.B., van Essen, A.J., Goecke, T.O., Al-Gazali, L., Chrzanowska, K.H., 2008. Mutations in the pericentrin (PCNT) gene cause primordial dwarfism.

Science 319, 816-819.

- Raucher, D., Stauffer, T., Chen, W., Shen, K., Guo, S., York, J.D., Sheetz, M.P., Meyer, T., 2000. Phosphatidylinositol 4, 5-bisphosphate functions as a second messenger that regulates cytoskeleton–plasma membrane adhesion. *Cell* 100, 221-228.
- Reiter, J.F., Blacque, O.E., Leroux, M.R., 2012. The base of the cilium: roles for transition fibres and the transition zone in ciliary formation, maintenance and compartmentalization. *EMBO reports* 13, 608-618.
- Rodieck, R.W., 1973. The vertebrate retina: principles of structure and function.
- Rohatgi, R., Milenkovic, L., Scott, M.P., 2007. Patched1 regulates hedgehog signaling at the primary cilium. *Science* 317, 372-376.
- Rosenbaum JL1, W.G., 2002. Intraflagellar transport. *Nat Rev Mol Cell Biol*, 813-825.
- Saburi, S., Hester, I., Fischer, E., Pontoglio, M., Eremina, V., Gessler, M., Quaggin, S.E., Harrison, R., Mount, R., McNeill, H., 2008. Loss of Fat4 disrupts PCP signaling and oriented cell division and leads to cystic kidney disease. *Nature genetics* 40, 1010-1015.
- Salinas, R.Y., Pearing, J.N., Ding, J.-D., Spencer, W.J., Hao, Y., Arshavsky, V.Y., 2017. Photoreceptor discs form through peripherin-dependent suppression of ciliary ectosome release. *J Cell Biol*, jcb. 201608081.
- Satir, P., Christensen, S.T., 2007. Overview of structure and function of mammalian cilia. *Annu. Rev. Physiol.* 69, 377-400.
- Sato, M., Ueda, Y., Takagi, T., Umezawa, Y., 2003. Production of PtdInsP3 at endomembranes is triggered by receptor endocytosis. *Nature cell biology* 5, 1016-1022.
- Schier, A.F., Neuhauss, S., Harvey, M., Malicki, J., Solnica-Krezel, L., Stainier, D., Zwartkuis, F., Abdelilah, S., Stemple, D.L., Rangini, Z., 1996. Mutations affecting the development of the embryonic zebrafish brain. *Development* 123, 165-178.
- Schottenfeld, J., Sullivan-Brown, J., Burdine, R.D., 2007. Zebrafish curly up encodes a Pkd2 ortholog that restricts left-side-specific expression of southpaw. *Development* 134, 1605-1615.
- Schou, K.B., Pedersen, L.B., Christensen, S.T., 2015. Ins and outs of GPCR signaling in primary cilia. *EMBO reports*, e201540530.

- Shiba, D., Yamaoka, Y., Hagiwara, H., Takamatsu, T., Hamada, H., Yokoyama, T., 2009. Localization of Inv in a distinctive intraciliary compartment requires the C-terminal ninein-homolog-containing region. *Journal of cell science* 122, 44-54.
- Stauffer, T.P., Ahn, S., Meyer, T., 1998. Receptor-induced transient reduction in plasma membrane PtdIns (4, 5) P₂ concentration monitored in living cells. *Current biology* 8, 343-346.
- Steinberg, R.H., Fisher, S.K., Anderson, D.H., 1980. Disc morphogenesis in vertebrate photoreceptors. *Journal of Comparative Neurology* 190, 501-518.
- Stephens, L., Jackson, T., Hawkins, P., 1993. Agonist-stimulated synthesis of phosphatidylinositol (3, 4, 5)-trisphosphate: a new intracellular signalling system? *Biochimica et Biophysica Acta (BBA)-Molecular Cell Research* 1179, 27-75.
- Stuart, G., Vielkind, J., McMurray, J., Westerfield, M., 1990. Stable lines of transgenic zebrafish exhibit reproducible patterns of transgene expression. *Development* 109, 577-584.
- Suchy, S.F., Olivos-Glander, I.M., Nussbaum, R.L., 1995. Lowe Syndrome, a deficiency of a phosphatidyl-inositol 4, 5-bisphosphate 5-phosphatase in the Golgi apparatus. *Human molecular genetics* 4, 2245-2250.
- Suh, B.-C., Inoue, T., Meyer, T., Hille, B., 2006. Rapid chemically induced changes of PtdIns (4, 5) P₂ gate KCNQ ion channels. *Science* 314, 1454-1457.
- Sun, Z., Amsterdam, A., Pazour, G.J., Cole, D.G., Miller, M.S., Hopkins, N., 2004. A genetic screen in zebrafish identifies cilia genes as a principal cause of cystic kidney. *Development* 131, 4085-4093.
- Takenawa, T., Itoh, T., 2006. Membrane targeting and remodeling through phosphoinositide-binding domains. *IUBMB life* 58, 296-303.
- Tam, B.M., Moritz, O.L., Hurd, L.B., Papermaster, D.S., 2000. Identification of an outer segment targeting signal in the COOH terminus of rhodopsin using transgenic *Xenopus laevis*. *The Journal of cell biology* 151, 1369-1380.
- Taulman, P.D., Haycraft, C.J., Balkovetz, D.F., Yoder, B.K., 2001. Polaris, a protein involved in left-right axis patterning, localizes to basal bodies and cilia. *Molecular biology of the cell* 12, 589-599.
- Thisse, C., Zon, L.I., 2002. Organogenesis--heart and blood formation from the

zebrafish point of view. *Science* 295, 457-462.

Thornton, G.K., Woods, C.G., 2009. Primary microcephaly: do all roads lead to Rome? *Trends in Genetics* 25, 501-510.

Toftgård, R., 2009. Two sides to cilia in cancer. *Nature medicine* 15, 994-996.

Travaglini, L., Brancati, F., Silhavy, J., Iannicelli, M., Nickerson, E., Elkhartoufi, N., Scott, E., Spencer, E., Gabriel, S., Thomas, S., 2013. Phenotypic spectrum and prevalence of INPP5E mutations in Joubert syndrome and related disorders. *European Journal of Human Genetics* 21, 1074-1078.

Tsujikawa, M., Malicki, J., 2004. Intraflagellar transport genes are essential for differentiation and survival of vertebrate sensory neurons. *Neuron* 42, 703-716.

Tsujikawa, M., Omori, Y., Biyanwila, J., Malicki, J., 2007. Mechanism of positioning the cell nucleus in vertebrate photoreceptors. *Proceedings of the National Academy of Sciences* 104, 14819-14824.

Van Eeden, F., Granato, M., Schach, U., Brand, M., Furutani-Seiki, M., Haffter, P., Hammerschmidt, M., Heisenberg, C.-P., Jiang, Y.-J., Kane, D.A., 1996. Mutations affecting somite formation and patterning in the zebrafish, *Danio rerio*. *Development* 123, 153-164.

Van Leewenhoek, A., Observations, Communicated to the Publisher by Mr. Antony van Leewenhoek, in a Dutch Letter of the 9th of Octob. 1676. Here English'd: concerning Little Animals by Him Observed in Rain-Well-Sea. and Snow Water; as Also in Water Wherein Pepper Had Lain Infused. *Philosophical Transactions* (1665-1678) 12, 821-831.

Vanhaesebroeck, B., Guillermet-Guibert, J., Graupera, M., Bilanges, B., 2010. The emerging mechanisms of isoform-specific PI3K signalling. *Nature reviews. Molecular cell biology* 11, 329.

Várnai, P., Balla, T., 1998. Visualization of phosphoinositides that bind pleckstrin homology domains: calcium-and agonist-induced dynamic changes and relationship to myo-[³H] inositol-labeled phosphoinositide pools. *The Journal of cell biology* 143, 501-510.

Várnai, P., Lin, X., Lee, S.B., Tuymetova, G., Bondeva, T., Spät, A., Rhee, S.G., Hajnóczky, G., Balla, T., 2002. Inositol Lipid Binding and Membrane Localization of Isolated Pleckstrin Homology (PH) Domains STUDIES ON THE PH DOMAINS OF PHOSPHOLIPASE C δ1 AND p130. *Journal of Biological Chemistry* 277, 27412-27422.

Veleri, S., Bishop, K., Dalle Nogare, D.E., English, M.A., Foskett, T.J., Chitnis,

- A., Sood, R., Liu, P., Swaroop, A., 2012. Knockdown of Bardet-Biedl syndrome gene BBS9/PTHB1 leads to cilia defects. *PLoS One* 7, e34389.
- Veleri, S., Manjunath, S.H., Fariss, R.N., May-Simera, H., Brooks, M., Foskett, T.A., Gao, C., Longo, T.A., Liu, P., Nagashima, K., 2014. Ciliopathy-associated gene *Cc2d2a* promotes assembly of subdistal appendages on the mother centriole during cilia biogenesis. *Nature communications* 5.
- Vieira, O.V., Gaus, K., Verkade, P., Fullekrug, J., Vaz, W.L., Simons, K., 2006. FAPP2, cilium formation, and compartmentalization of the apical membrane in polarized Madin–Darby canine kidney (MDCK) cells. *Proceedings of the National Academy of Sciences* 103, 18556-18561.
- Whitfield, T.T., Granato, M., Van Eeden, F., Schach, U., Brand, M., Furutani-Seiki, M., Haffter, P., Hammerschmidt, M., Heisenberg, C.-P., Jiang, Y.-J., 1996. Mutations affecting development of the zebrafish inner ear and lateral line. *Development* 123, 241-254.
- Wiradjaja, F., Ooms, L.M., Whisstock, J.C., McColl, B., Helfenbaum, L., Sambrook, J.F., Gething, M.-J., Mitchell, C.A., 2001. The Yeast Inositol Polyphosphate 5-Phosphatase *Inp54p* Localizes to the Endoplasmic Reticulum via a C-terminal Hydrophobic Anchoring Tail REGULATION OF SECRETION FROM THE ENDOPLASMIC RETICULUM. *Journal of Biological Chemistry* 276, 7643-7653.
- Worby, C.A., Dixon, J.E., 2014. *Pten*. *Annual review of biochemistry* 83, 641-669.
- Xu, Q., Zhang, Y., Wei, Q., Huang, Y., Hu, J., Ling, K., 2016. Phosphatidylinositol phosphate kinase PIPKI [gamma] and phosphatase INPP5E coordinate initiation of ciliogenesis. *Nature communications* 7.
- Yang, J., Cron, P., Thompson, V., Good, V.M., Hess, D., Hemmings, B.A., Barford, D., 2002. Molecular mechanism for the regulation of protein kinase B/Akt by hydrophobic motif phosphorylation. *Molecular cell* 9, 1227-1240.
- Yoder, B.K., Hou, X., Guay-Woodford, L.M., 2002. The polycystic kidney disease proteins, polycystin-1, polycystin-2, polaris, and cystin, are co-localized in renal cilia. *Journal of the American Society of Nephrology* 13, 2508-2516.
- Yoo, S.K., Deng, Q., Cavnar, P.J., Wu, Y.I., Hahn, K.M., Huttenlocher, A., 2010. Differential regulation of protrusion and polarity by PI (3) K during neutrophil motility in live zebrafish. *Developmental cell* 18, 226-236.

- Yuan, S., Li, J., Diener, D.R., Choma, M.A., Rosenbaum, J.L., Sun, Z., 2012. Target-of-rapamycin complex 1 (Torc1) signaling modulates cilia size and function through protein synthesis regulation. *Proceedings of the National Academy of Sciences* 109, 2021-2026.
- Zaghloul, N.A., Katsanis, N., 2011. Zebrafish assays of ciliopathies. *Methods in cell biology* 105, 257.
- Zhao, C., Malicki, J., 2011. Nephrocystins and MKS proteins interact with IFT particle and facilitate transport of selected ciliary cargos. *The EMBO journal* 30, 2532-2544.